Portable microfluidic chip perfusion and heating solution for high-magnification optical microscopy

Vladimir Leshko

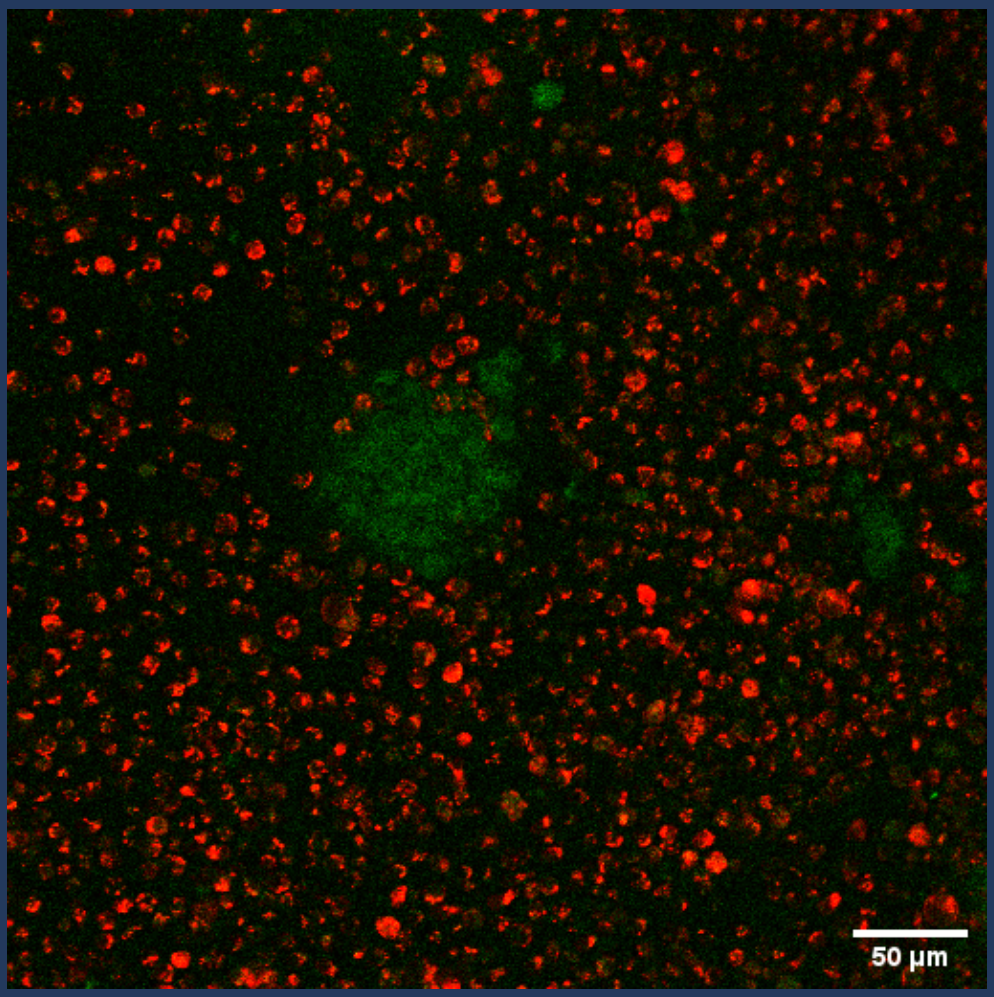

TU Delft

Portable microfluidic chip perfusion and heating solution for high-magnification optical microscopy

Thesis report

by

Vladimir Leshko

to obtain the degree of Master of Science
at the Delft University of Technology
to be defended publicly on August 22, 2023, at 10:00

Supervisors:	Dr. Murali Ghatkesar
	Dr. Massimo Mastrangeli
Daily supervisor:	Zhilin Wang
Erasmus MC supervisors:	Dr. Giorgia Zambito
	Dr. Laura Mezzanotte
Place:	3mE, Delft
Project Duration:	January, 2023 - August, 2023
Student number:	5278112

Faculty of Mechanical, Maritime and Materials Engineering · Delft University of Technology

Contents

1

Introduction

In developed countries like the Netherlands various kinds of cancer are the leading cause of death in the population [1]. That explains the growing interest in the development of novel techniques for studying tumour biology and investigating potential therapeutic interventions, e.g. delivery of drugs or immunotherapy (priming the specific types of immune cells in the body to kill the tumour cells). One of the immunotherapy types, adoptive T-cell therapy, was proven efficient against blood cancers (B-cell malignancies) but is quite inefficient against solid tumours such as sarcomas, carcinomas and lymphomas. Solid tumours account for around 90% of cancers in adults thus the search for effective treatments is an active branch of research [2].

This thesis project is aimed at developing and improving the quality of immunotherapy modelling in microfluidic chips. Mainly aiming at supplying chips with 3D models of tumours with perfusion and heating whilst also ensuring the ability to image the T-cell and tumour interactions with a state-of-the-art optical microscopy setup.

The final thesis report consists of a Literature Review and Preliminary Design Chapter where the existing solutions are examined and a design direction is determined. It's followed by the thesis itself structured as a scientific paper. Chapter 4 gives a brief analysis of the taken design path and provides recommendations for further development of the system. Chapter 5 is the author's reflection on the project. It's followed by Appendix containing additional information not included in the paper (CAD drawings, experimental results, images and videos of the setup).

2

Literature Review and Preliminary Design

2.1. Project description

2.1.1. Spheroids and T-cells

The research group from the Department of Radiology and Nuclear Medicine of Erasmus Medical Centre (EMC) is advancing the field by developing techniques to perform fluorescent and luminescent imaging of spheroid tumours or just ”spheroids”. A spheroid is an aggregation of tumour cells which have been cultivated in a specific way to form a spherical shape ranging from a hundred to several hundred µm in diameter, depending on the cultivation method and time.

The spheroids can either be free-floating (suspended in a solution) or encapsulated (immobilised inside a polymerised hydrogel structure). Hydrogel simulates the extracellular matrix (ECM) environment and immobilises the spheroid to allow for easier imaging.

Cytotoxic T-cells facing solid tumours have to overcome both the physical barriers and the immunosuppressive factors presented by the tumour microenvironment (TME). Mimicking TME invitro is a technological challenge. That’s where the Organ-on-a-Chip (OoC) technologies come in. OoC platforms provide cells with a regulated environment which is close to body conditions (in terms of temperature, nutrient supply, pH, oxygen concentration and other factors) and thus increase the accuracy and reproducibility of the experiments. Shang et el. conclude that microfluidic chips can allow capturing the essence of TME [3]. EMC group makes use of OoC technology by encapsulating a spheroid inside a hydrogel in a chamber of a microfluidic chip. The chip can be perfused with a medium containing nutrients and growth factors to keep the spheroid cells alive.

The cells used are murine colon adenocarcinoma (MC38) cells expressing NanoLuc luciferase and Green fluorescent protein (GFP). Nanoluc Luciferase is a luminescent enzyme derived from deep sea shrimp [4]. Cells expressing luciferase will emit weak green light (only detectable with a specialised microscopy setup) for around 20 minutes after contacting the luciferase substrate. The cells are cultured into spheroids using the ultra-low attachment plates technology, this process takes about 10 to 14 days in the incubator, and the resulting spheroids are about 100 µm in diameter.

It’s important to note that modification or alteration of the steps preceding the delivery of the spheroids into a microfluidic device is not a task of this thesis work.

The exact equipment and techniques utilised by EMC and the requirements which our collaboration is supposed to fulfil will be covered in the sections to follow.

2.1.2. Utilised chip

The lab currently uses a Polydimethylsiloxane (PDMS) chip attached to a glass coverslip. The chip is manufactured at the University of Twente. The size of the chip is 17 x 12 x 4 mm. The optical detection chamber has dimensions of 7.5 x 2 x 0.25 mm and a volume of 4.7 µl. The central channel is used to deliver the spheroids in the liquid hydrogel (fibrin) solution to the chamber. When the gel polymerises the central channel is sealed by the gel itself and is no longer used. The side channels are used to deliver nutrients and T-cells which diffuse into the hydrogel. The side channels are 100 x 100 microns. The side channels are separated from the optical detection chamber by an array of sixteen trapezium-shaped pillars. The inlets and outlets are 500 µm in diameter. The chip is plasma bonded to a glass coverslip measuring 24 x 50 mm and of 0.17 mm thickness. A maximum of two chips can be placed on one coverslip.

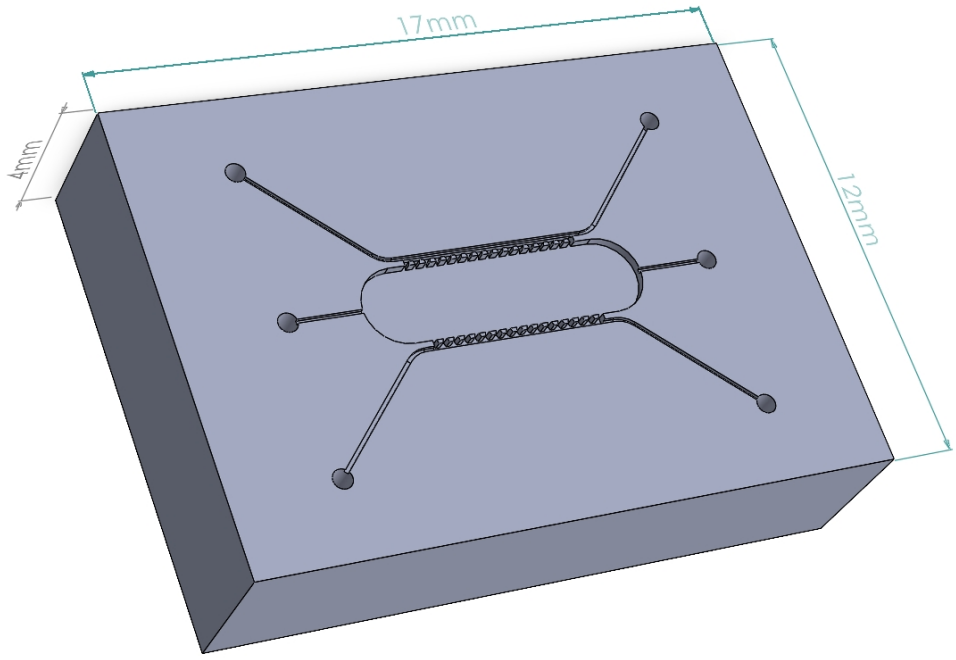

Figure 2.1: A SOLIDWORKS representation of the inside structure of the chip (glass coverslip is not shown)

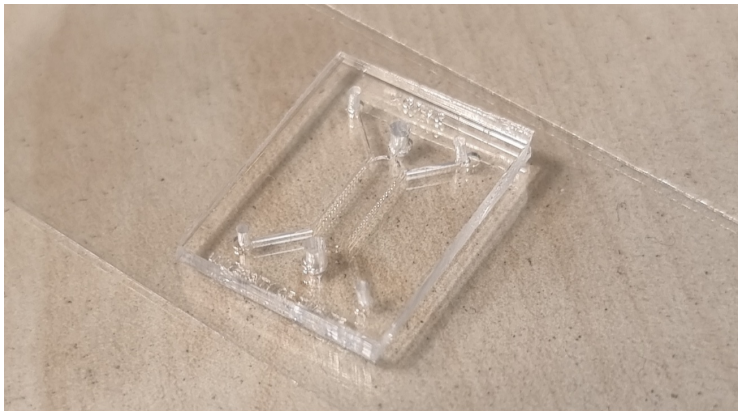

Figure 2.2: A photograph of the chip mounted on a coverslip

PDMS is a common material used to manufacture bio-compatible microfluidic chips. An important property of this material which has to be noted is gas permeability which, for example, can allow the CO^2 from the incubator to penetrate into the chamber [5]. Commercially available alternative options to the chip described above will be explored as a part of this literature review.

2.1.3. Chip preparation and imaging setup

The spheroids then are mixed with the fibrin hydrogel. Fibrin is a protein involved in blood clotting and is produced by platelets. The spheroids are mixed with the hydrogel solution and are immediately pipetted into the central chamber of the chip. The filled chips are placed in the incubator at 37 °C, the fibrin hydrogel will polymerise in one hour. To prevent drying out of the chip, the side channels are filled with cell growth medium, also the droplets are placed on the inlets and outlets.

Afterwards, the cytotoxic T-cells (specifically designed to target MC38 cells) are brought from the immunology lab and mixed with the cell growth medium. The mixture is pipetted into one of the side channels of the chip. The other channel is filled with Interleukin-2 (IL-2) dissolved in a medium. IL-2 is an inflammatory cytokine which enhances the activity of CTLs. Droplets of the medium are, once again, pipetted on the inlets and outlets of the chip to prevent drying out. The chip is placed in the incubator for 24 hours to give time for the T-cells to migrate to the centre of the central chamber.

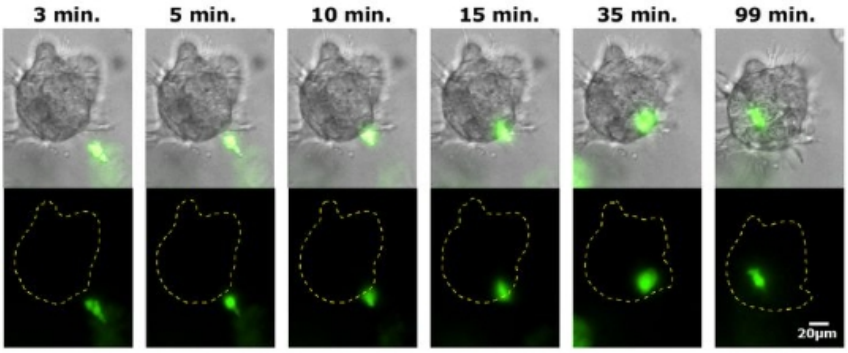

Figure 2.3: Time sequence of CTL (green) migrating and adhering to a spheroid inside hydrogel [6]

After the CTL diffusion is complete the chip is placed on the microscope stage and luminescence substrate is injected into one of the side channels. After that, the optical, luminescent and fluorescent images of the spheroids can be taken and the damage done by the CTLs can be evaluated. It's important to note, that this step doesn't have any temperature control since the chip cannot be positioned in the Tokai Hit stage top incubator connected to the microscope. The microscope used is ZEISS ELYRA PS1 (figure 2.4). This review won't focus on exploring alternative imaging solutions.

2.1.4. Requirements

It can be noted that during the experiment, the chip undergoes several transitions in and out of the incubator and to the microscope stage. Thus there are fluctuations in temperature in the central chamber and the imaging is even performed at room temperature. It's impossible to do prolonged imaging because there is no nutrient supply (or the medium needs to be constantly refreshed manually) and maintained body temperature. After the initial meetings with the EMC research group, the following requirements were collected:

1. The lab needs to perfuse the chip for up to two days before and during imaging.
2. The temperature in the central chamber should be between 36 and 37.5 °C at all times and at the same time the system should be incubator-free.
3. The flow rate used for perfusion is 10 µl/min.
4. The setup has to be portable and allow enough battery time to be able to carry to the microscope and back to the lab (under 30 minutes).
5. The distance from the objective to the bottom of the chamber should be under 1mm to allow the use of high-magnification objectives.
6. The system should be compatible with oil objectives (up to and including 40X).
7. Minimum of two chips should be used simultaneously.

Additional requirements were collected from the TU Delft supervisors:

1. The applicability of the TU Delft Portable Microfluidic Platform (PMP) to this project should be investigated. The platform was developed by Haoyu Zhu during his Master's thesis project at the PME department.

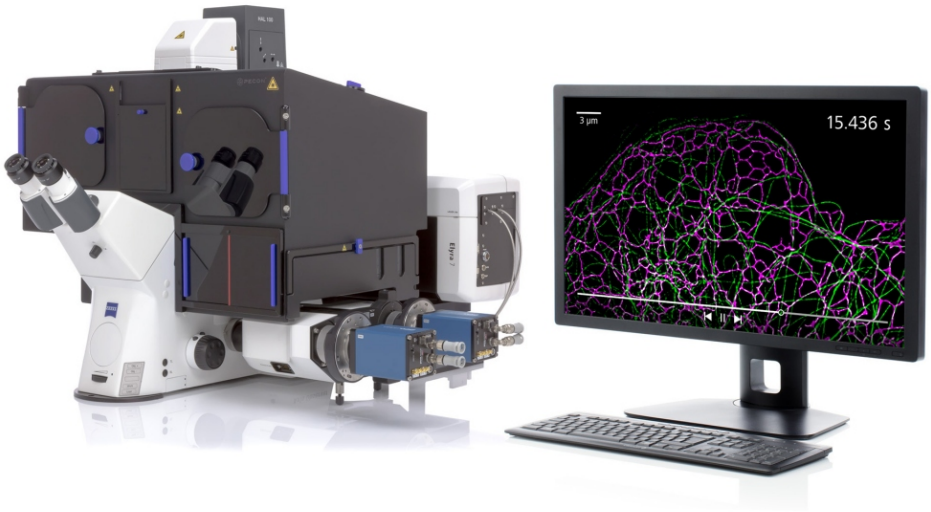

Figure 2.4: ZEISS ELYRA PS1 microscope. Image courtesy: zeiss.com

2. The system has to be compatible with multiple microfluidic chip types relevant to spheroid tumour growth (exact types have to be identified during the literature study).
3. The system has to be compatible or allow easy customisation with several inverted microscope types.
4. The system has to be assembled from off-the-shelf components.

2.1.5. Literature study contents

According to the above project description and requirements the literature study is to be conducted in order to cover the knowledge gaps and investigate the state-of-the-art approaches in the field in the directions stated below.

1. Latest advancements, setups and microfluidic chips for growing and experimenting on spheroid tumours.
2. Commercially available microfluidic platforms.
3. State-of-the-art solutions for heating microfluidic chips compatible with imaging.

Parts (2) and (3) are crucial in order to come up with system design, part (1) was added

because the EMC team suggested it would be a valuable addition to the project. In-depth research on other topics (e.g. immunotherapy studies in microfluidic chips) was not conducted because of the time restrictions of the project. The studied literature will allow me to formulate the research question for this project and the required specifications. Afterwards, the preliminary design will be proposed and the primary components will be selected (heating element and temperature sensor). The risks and mitigations of the proposed design will be discussed. The project planning and experiments plan will conclude this paper.

2.1.6. Methodology used

The review was conducted by searching papers on the scholar.google.com database using the relevant keywords and Boolean operators. An emphasis was put on the papers released in the last five years. This review has a lot of intersections with the work done by TU Delft MSc students Shieema Elhassan (design of a microfluidic heating device) and Haoyu Zhu (design of a portable microfluidic platform) so their reviews were also used as sources. When examining commercial microfluidic products, the search was also done through the conventional google.com engine.

2.2. Literature Review

2.2.1. Spheroid culturing

The development of drugs is a very slow and expensive process, especially when it concerns trials. We need models which more accurately, in fact, as close to the in-vivo conditions as possible, represent the complexity of the human body. Mice were and still are considered such a model, however, we can do faster, cheaper and more ethically acceptable than using mice. One of the most promising ways to go is 3D models like spheroids and organoids. To get a 3D model the cells are cultured under special conditions which makes them assemble in a sphere. The diameter of the sphere is usually between 100 and 500 µm. This leads to gene expression of the cells to more accurately resemble the clinical expression if you compare it with 2D models (e.g. a layer of cells on a glass surface) [7]. 3D models could serve as the main tool for drug selection to continue to human trials because many therapies become inefficient when tried out on a 3D model, compared to a 2D model [8, 9, 10]. 3D models allow for more cell-ECM interactions, lactate accumulation (and thus a low pH environment closer to the spheroid centre), varying glucose distribution, oxygen gradient, central necrosis and other characteristics of actual tumours [7].

The techniques for spheroid culturing include

1. Low-adhesion surfaces. Cells suspended in a medium are incubated at 37°C in cell-culture wells which don't allow the binding of the cells, making them aggregate instead. [11]
2. Hanging drop method. Cells are suspended in a drop hanging from a specially designed plate. The gravity makes the cells assemble in the lower part of the drop which promotes the formation of a spheroid [12]. The method is shown in figure 2.8. The important advantage of the hanging drop method compared to

the low-adhesion surface method is that it allows the production of spheroids of controlled and uniform size [13].

3. Rotating bioreactors that make the cells aggregate by employing gravitational and centrifugal forces [14].
4. Microfluidic methods which are mostly based on the methods stated above but offer generally better replication of the in-vivo environment [15].

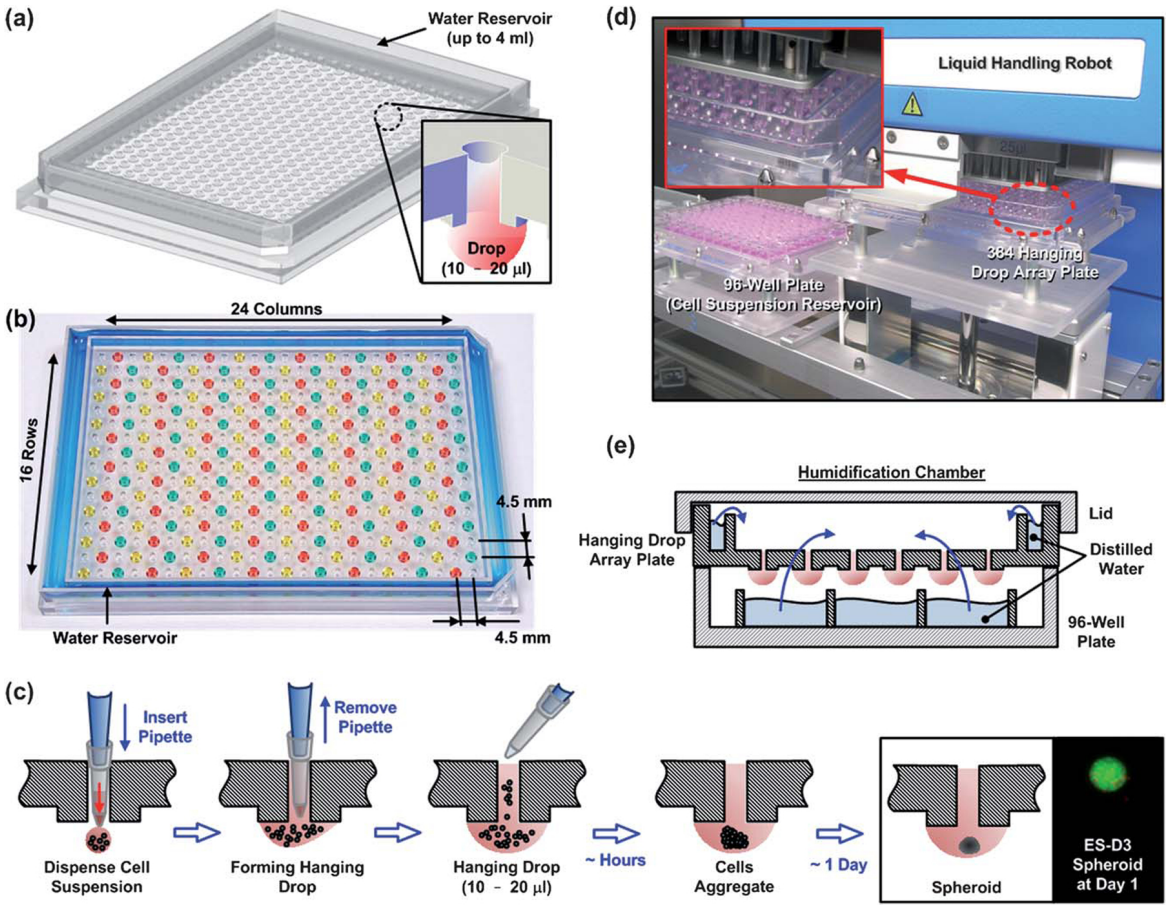

Figure 2.5: The step-by-step process of high-throughput hanging drop spheroid culturing [12]

2.2.2. Microwell approach

The latest advancements in microfluidic technology allow the incorporation of the whole process of culturing large numbers of spheroids in a single device. Sart et al. introduced a method called multiscale cytometry and cultured 500 spheroids with an average diameter of 73 µm on a single microfluidic chip. To achieve this they deliver droplets of agarose gel, containing cells via an inlet into a chamber containing 500 microwells. The droplet size is controlled to match the well volume. Droplets randomly fill in the wells and the ones which did not encounter a microwell exit the device. When all the wells are filled (on average 800 drops are required), the chip is incubated for 24 hours which was shown to be enough to let the spheroids assemble inside the agarose drops. Then the device is placed to a 4 °C chamber to solidify the agarose gel. Afterwards, the cell culture medium

can be flown through the same channel to deliver nutrients to the spheroids (the nutrients diffuse through the gel) [16]. The need to cool the chip to 4 °C and the complicated seeding procedure can be viewed as the shortcomings of this approach. Also, the quality of images can be affected by the thickness of the chip, in this case, the imaging was done through a thick layer of PDMS which did not allow for high-magnification pictures of the spheroids.

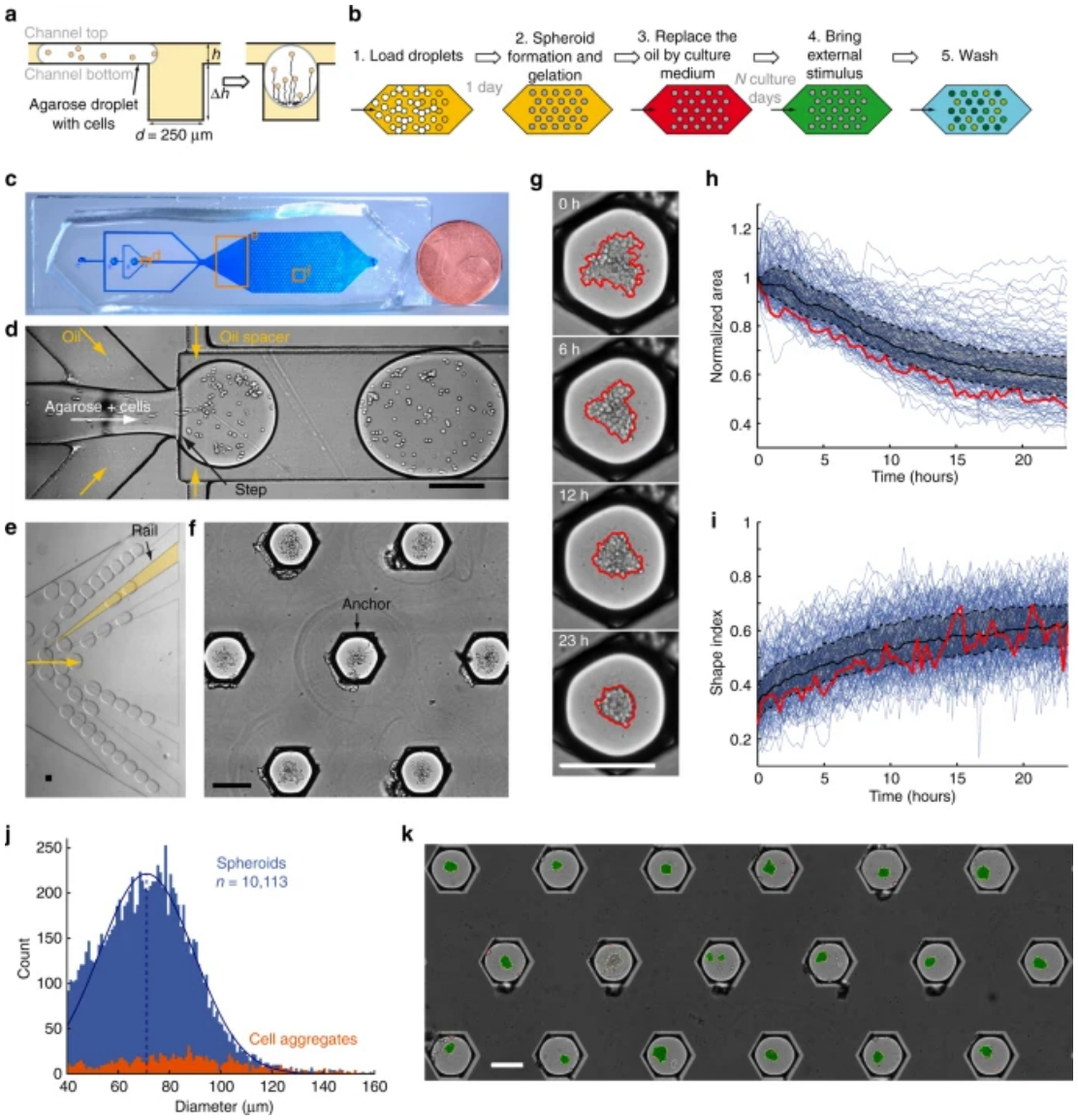

Figure 2.6: Multiscale cytometry: culturing 500 spheroids on a single microfluidic chip [16]

Rontiex et al. further expanded on the concept of multi-microwell chips to study Cytotoxic T-lymphocytes (CTLs) cooperation when killing a spheroid tumour. The chip was fabricated from PDMS on a standard glass slide which allowed for better image quality. Spheroids encapsulated in Matrigel were incubated in the chip for 24 hours inside the microwells and then fused with another droplet containing CTLs. After that, the interaction between CTLs and tumour cells could be observed by fluorescence microscope with a

×20 objective lens. The authors do not mention whether the temperature during imaging was controlled or not. The perfusion of nutrients was not performed, CTLs and tumour cells relied only on the nutrients present in the droplets [17].

Behroodi et al. came up with a flexible approach to fabricate multi-microwell microfluidic devices for large-scale spheroid culturing. The group 3D printed the mould for the central microwell part of the chip via a high-resolution PμSL 3D printer. The less-precise parts of the chip were produced from PDMS via CNC milling. The target was to examine how the depth and shape of the wells influence the diameter and formation of the spheroids. 300 μm was identified as the optimal depth [18]. The downside was, once again, that the thick PDMS layer limits the image quality and maximum magnification.

Petreus et al. explored how tumour spheroids respond to pharmaceutical treatments. The spheroids were cultured separately and then placed inside the commercially available Ibidi chips in a Matrigel droplet. After the hydrogel has polymerised, the chip could be perfused with a cell culture medium mixed with pharmaceuticals in the desired concentrations. To perfuse the chip, an Elveflow OB1-4 flow controller was supplied with air + 5% CO^2 to push the medium through the system. Ibidi chip is manufactured from a polymer impermeable to gas (in contrast to PDMS which is also known to bind some of the drug molecules). The permeability of PDMS allows the CO^2 from the incubator to diffuse into the system which is widely used. The air bubbles were trapped with a bubble trap [19]. This approach does not allow for culturing of as many spheroids as in previously described papers, but the use of Ibidi chips simplifies the whole process. Also, the low thickness of the coverslip allows for higher magnifications. Thus, those chips could later be considered as a potential alternative to the Twente PDMS chips. The gas permeability of the widely used PDMS chips is a property which needs to be kept in mind when designing our system.

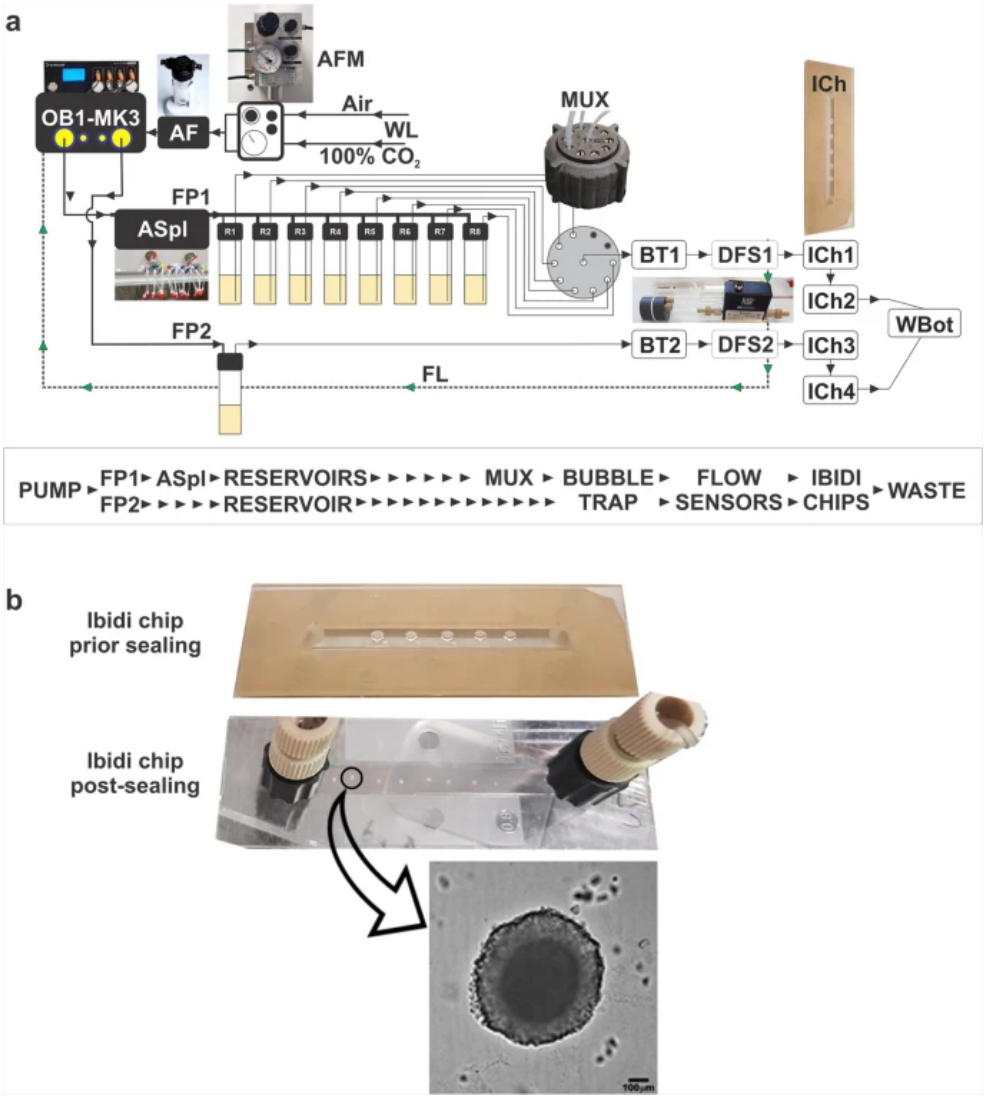

Figure 2.7: The system schematic based on Ibidi chips and Elveflow controller [19]

2.2.3. Microfluidic chips for spheroids

Ibidi has two chips which can be used for spheroid perfusion: µ-Slide Spheroid Perfusion with 3 channels of 7 microwells each (figure 2.8), the other is µ-Slide III 3D Perfusion and it's specifically made for culturing and imaging spheroids in the hydrogel (figure 2.9). The important features to be noted:

1. Chips are based on a 0.17mm coverslip which allows for up to 60x objectives.
2. Chips are made from a polymer which is not permeable to gas. That makes them more bubble-safe than PDMS chips especially when the negative pressure is used as the driving force of the flow and the chip is heated.
3. 21 wells and three channels on the first chips and six wells and three channels on the second chip allow for higher throughput than the now-used Twente chips. The disadvantage is that two different mediums cannot be introduced into one chamber.
4. Both chips allow the culturing of spheroids as well as the life support of pregrown ones.

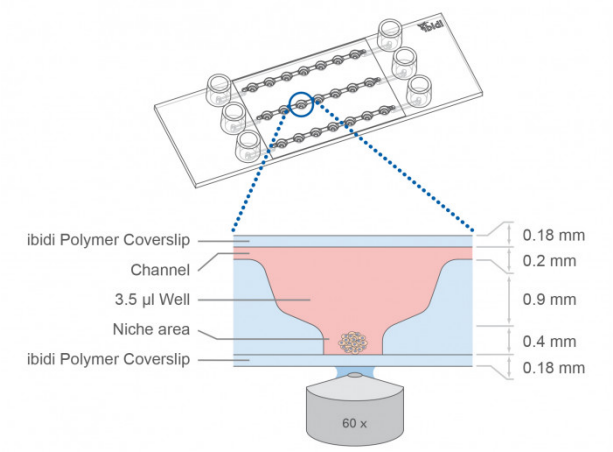

Figure 2.8: Ibidi spheroid microwell slide. Image courtesy ibidi.com

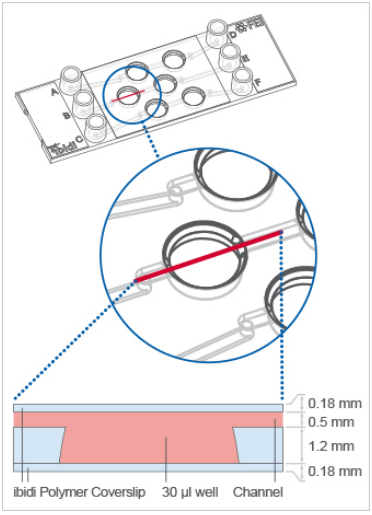

Figure 2.9: Ibidi spheroid hydrogel slide. The chambers are filled with hydrogel up to the channel surface, the chip is sealed with the top coverslip. After the gel is polymerised, the chip can be perfused. Image courtesy ibidi.com

Another commercially available chip which can provide life support for spheroids is Memetas OrganoPlate Graft. It's a platform containing 64 independent chips with three channels and one chamber. Spheroid can be encapsulated in the hydrogel in the central chamber. The side channels can be used for perfusion or for growing vascular tissue (angiogenesis). The newly formed capillaries can reach the spheroid so that later on the drug and treatments could be delivered to the spheroid via the capillaries.

Biond, an OoC startup from Delft, has also developed a chip suitable for spheroid culturing. It consists of 3 channels sharing the same single inlet and outlet passing at the bottom of the 3x3mm microwell where a spheroid can be implanted. The chip can be perfused with a 1-300 µl/min flow rate. An obvious downside is that only one type of medium can be supplied at a time.

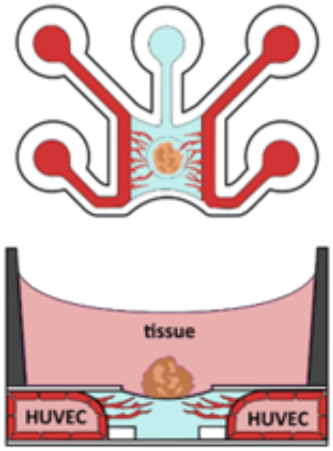

Figure 2.10: Mimetas OrganoPlate Graft chip. HUVEC stands for human umbilical vein endothelial cells. Image courtesy mimetas.com

Figure 2.11: Biond tri-channel microwell chip. Image courtesy biond.com

2.2.4. Hanging drop approach in microfluidics

The hanging drop method can also be replicated in a microfluidic device. Aijian et al. developed a nanofabricated microfluidic chip which allows the precise transportation of ul volumes of the cell-containing medium via an application of electric potential. The medium is transported to a 2.5mm-wide opening where a 7-10 µl hanging drop contains cultured cells. The critical part is that the cells require the medium exchange to survive and thus once a day under 25% of the hanging drop volume was extracted and replaced with the fresh medium using the same transportation channel. The authors archived a 300 µm+ spheroid diameter after 72 hours of culturing [20].

To conclude, most of the researchers are focusing on developing high-throughput systems to do pharmaceutical trials on spheroids. Microwell approach is trending. Growing hundreds of spheroids on a single chip proves advantageous for therapeutical trials. Spheroid and CTL interactions in the microfluidic environment are still understudied.

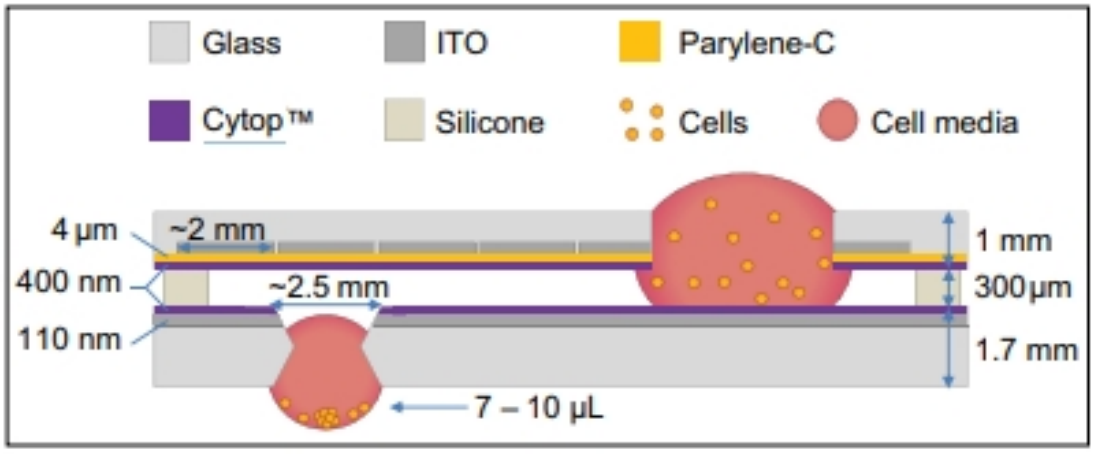

Figure 2.12: The schematic of the microfluidic hanging drop spheroid culturing device. Cytop is a transparent hydrophobic fluoropolymer. Parylene-C is a transparent biocompatible dielectric. [20]

2.3. Microfluidic platforms

In the second part, I'll look into the microfluidic platforms available on the market and compare them with the available functionality of the TU Delft portable microfluidic platform to see if there are any systems which already match the requirements. The downsides and upsides of each platform will be discussed as well as the applicability to spheroid research.

The chapter focuses on commercially available platforms because if a solution which fully covers the needs for EMC's spheroid experiments already exists then it could be considered an alternative to further developing the TUD platform.

2.3.1. Emulate human emulation system

Emulate has created a modular system which starts with organ-chips (the company produces slightly different chips for different types of tissues). For example, lung-on-a-chip also supports stretch and provides a liquid-air interface for gas exchange. Generally, each chip contains two channels and one chamber.

The next element is called the "POD portable module" and it serves as an interface between the chip and the medium containers. The PODs are put on racks and are installed in the Zoe culture module which provides the chips with the necessary environment. The flow can be adjusted to prevent excessive strain on the cells.

Up to 4 Zoe modules can be connected to an Orb: another module which is in turn connected to lab gas outputs and provides Zoe with gas and stretch.
Upsides of the system:

1. Supports complex models like lung and gut on a chip which require stretch.
2. All the components are available from Emulate and thus there will be no compatibility issues.
3. Each chip can be perfused with different mediums.

Figure 2.13: Orb on the left and Zoe on the right. POD modules mounted on racks within Zoe. Image courtesy: emulatebio.com

Downsides of the system:

1. Compatible only with Emulate chips which are unsuitable for every application (f.e. spheroids).
2. Chips can only be imaged when disconnected and removed from the system.
3. There's no temperature control.
4. The system is bulky and not portable.
5. Throughput of just sixteen chips per module is not that high given the dimensions of the system.

Overall it's a curious system which looks great but is not at all appropriate for our intended application.

2.3.2. Mimetas OrganoFlow

OrganoFlow is a platform which supplies up to 16 384-well plate-size OrganoPlate chip platforms with perfusion. In the case of spheroids and Graft chips (Figure 2.10) each plate contains 64 individually perfused chips. The temperature and environment control is done by placing the OrganoFow in the incubator.

Upsides of the system:

1. Very high throughput
2. Very simple and thus probably reliable mechanism
3. No compatibility issues
4. Individual perfusion for each chip

Figure 2.14: Organoflow system in S and L sizes. Image courtesy: mimetas.com

5. No bubble issues

Downsides of the system:

1. Temperature control for microscopy must be implemented separately
2. Imaging under perfusion is not possible
3. The system is not portable.
4. Total dependency on the Mimetas chips

This system looks very promising for high-throughput trials on spheroids and can be implemented in immunotherapy trials if the temperature control solution for microscopy is found.

2.3.3. Omi, automated organ-on-chip platform from Fluigent

Fluigent, a company which is known for its microfluidic flow controllers and other components has recently announced an ”automated OoC platform” Omi. It can be connected to any kind of microfluidic chip (up to standard slide size) and provided with nutrients (up to 4ml of cell culture medium, re-circulation is possible). The system is fully incubator-compatible.
Upsides of the system:

1. Possible to image under flow
2. System is portable and can function for up to 2 hours from the battery
3. Can function with any kind of chips

Downsides of the system:

1. Temperature control during imaging and while transferring the chip to the microscope is not implemented
2. Just 1 chip can be connected to only 1 inlet and 1 outlet
3. Complex setups like Lung-on-a-chip are not supported

The system exhibits potential as a solution for basic experiments and models. Nonetheless, in order to perfuse a two-channel chip, the user needs to employ two separate devices, which results in a cumbersome apparatus. The absence of temperature

Figure 2.15: Omi microfluidic chip perfusion platform. Image courtesy: fluigent.com

regulation is an unfavourable attribute, especially given the system works with just one chip. Ultimately, the system is unsuitable for conducting spheroid and CTL experiments.

2.3.4. Biond comPLATE

Biond comPlate is an interface to connect Bionds InCHIPit chips to a perfusion system (syringe or pressure pump). Up to six chips can be connected via the platform including

Figure 2.16: Biond comPLATE for up to six spheroid-compatible chips. Image courtesy: gobiond.com

Biond's tri-channel chips are applicable for spheroids (figure 2.11).

This system is the least advanced one from what's been covered so far. It basically gives the user an easy way to connect to the chip. However, it allows for some flexibility because it can be integrated with any perfusion system. There's no heating solution yet (apart from an incubator) designed for this platform.

2.3.5. Stage top incubators

Several companies like Ibidi, Okolab, LCI, Tokai and others produce incubators tailored to be used right under the microscope. They're mainly made to be used with Petri dishes or well plates. However, some solutions allow imaging of microfluidic chips under flow. The most common features specified by the manufacturers include:

- Heated glass bottom (via a transparent conductive layer of ITO - Indium Tin Oxide)
- Heated glass top to prevent condensation
- Heated sides and heated inserts for tubing if used with a chip
- Humidity control to prevent excessive evaporation from the dish or well plates
- CO^2 and O^2 control in the chamber. 0^2 can be used at concentrations below atmospheric to mimic cell hypoxia. CO^2 levels control the pH of the medium.
- Ability to put an additional thermocouple right in the sample for the temperature control to be more precise
- Microscope objective heater to be used with oil objectives to prevent heat loss through the oil.

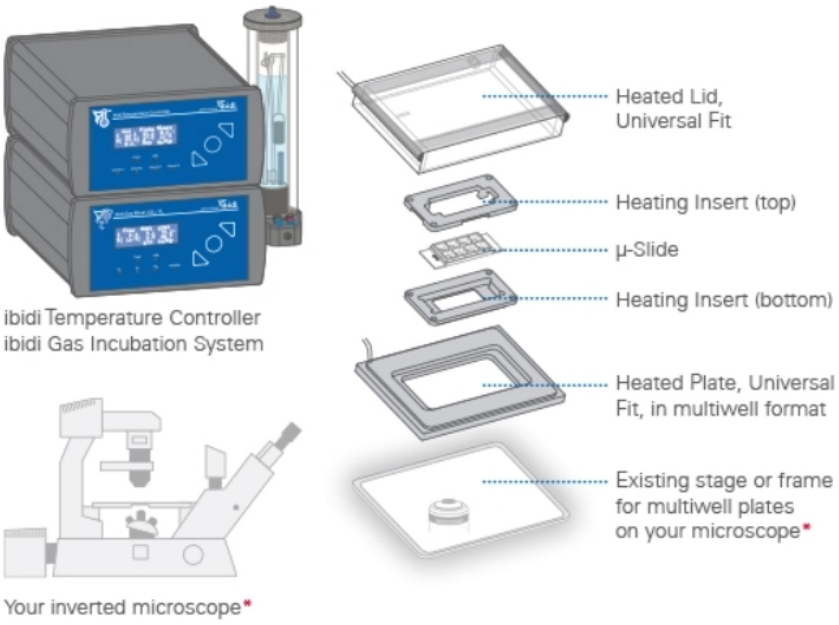

Figure 2.17: Schematic of the Ibidi stage top heater. Image courtesy: ibidi.com

Ibidi produces a heater which can be used with µ-slides 2.8. It allows for the highest imaging quality because it's heated from the sides and top and the bottom coverslip of the chips remains fully exposed for a reversed microscope. However, the power consumption of this system is quite high (up to 160 W) and it has a bulky temperature controller which limits the portability. Also, no publications yet use the heater for spheroid applications.

2.3.6. Elveflow stage top incubator beta

Elveflow recently announced a beta product which is a stage-top incubator specifically designed for microfluidic chips. According to Elveflow it has the following features:

- Fits up to two chips.
- Temperature control with 0.5 °C accuracy.
- Thickness of the bottom glass with ITO coating is 1.1 mm.
- Compatible with most microscopes.
- The chamber is not gas-tight and only provides temperature control.
- The outer chamber is made of aluminium.

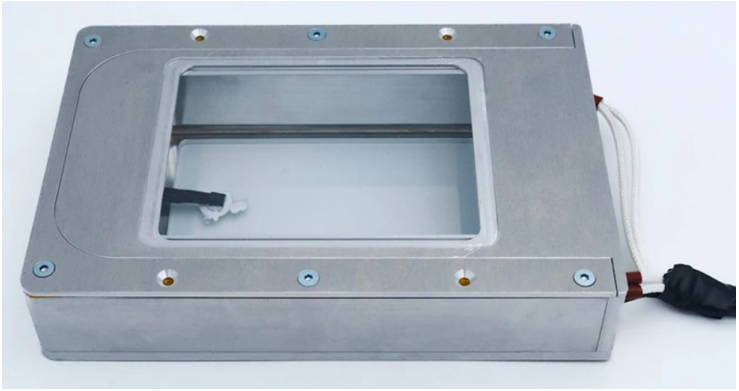

Figure 2.18: Elveflow stage top incubator beta. A thermal sensor is attached to the surface of the heated glass using thermal paste. Image courtesy: elveflow.com

The main shortcomings which can be observed in this device are a lack of portability and quite thick bottom glass which may be a limitation for high-magnification objectives. Also, it's still a beta product so the exact specifications are not yet clear.

2.3.7. TUD platform

The TUD platform was designed in 2020 by a MSc student Haoyu Zhu [21]. The platform has the following key components assembled on one base:

- Two Bronkhorst flow controllers with the flow range from 1.5 to 68 µL/min.
- A vacuum pump which provides up to -0.6 bar negative pressure to drive fluids through the chips.
- A waste reservoir to which the negative pressure is applied.
- Six medium reservoirs.
- A switch valve with six inlets and one outlet to pick the desired medium.
- Arduino Mega to integrate the components.
- 2000mAh 24V battery to provide portability.
- Controlled vacuum valve for Lung-on-a-chip applications.
- Chip slot for securing the chip up to microscope slide size and accessing it with the microscope objective.

The platform is compatible with any chip and can support two independent flow circuits. When the platform was examined to find out whether it was compatible with my project requirements several issues hindering its immediate use were identified:

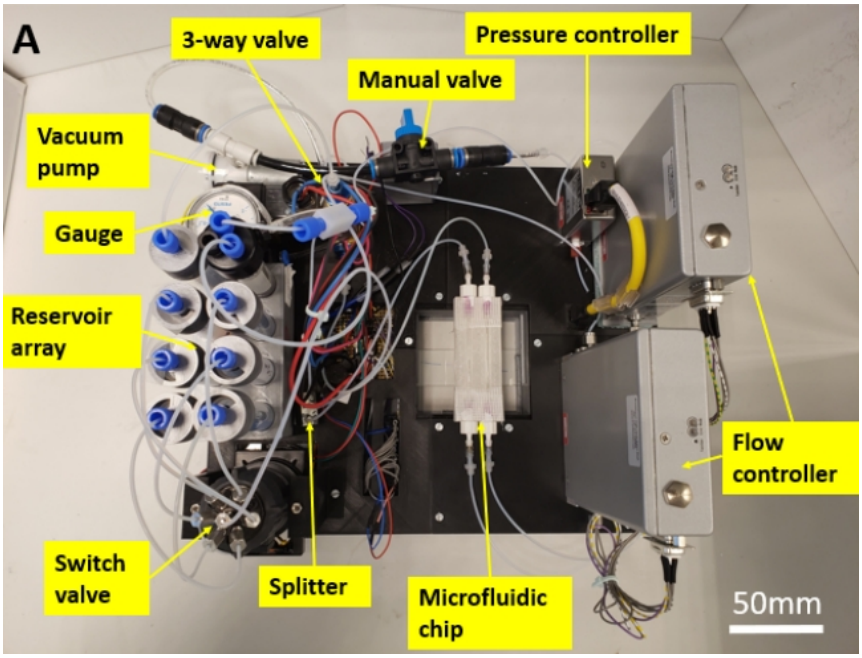

Figure 2.19: Fluidic components of the microfluidic platform. [21]

1. The platform can only be powered from a stationary 24V DC power supply which limits the portability. There's no way to power the platform up from the wall socket.
2. The battery cannot be easily accessed, replaced or recharged.
3. Arduino is powered separately either from a USB connection to a PC or from a single-use 9V battery. The 9V battery can only last a few hours and cannot be easily replaced.
4. If the chip is positioned in the window in the middle part of the platform then it can be used with the microscopes for fluorescent and luminescent imaging. Because the chip will be too far away from the objective and also the window position is not a fit for every type of microscope.
5. Platform does not have an integrated heating system. The external heating solution designed in the PME department will be described and discussed in the following chapter.
6. Platform wasn't ever used in an actual experiment and may have malfunctioning parts (valves, vacuum pump) because it wasn't in use since 2020.
7. There's no user interface so the software can only be configured or adjusted by re-uploading the code from a PC with Arduino IDE to the Arduino Mega of the platform. For example, if the experimenter wishes to change the flow rate from 10 to 15 µl/min.
8. The platform does not support re-circulation.
9. Perfusion of the medium is driven by a pull mechanism (negative pressure created by the vacuum pump) which can cause bubble issues and limits the usage of commercially available bubble traps.

To conclude, the platform can be used for the spheroid experiments, given that the issues above are taken care of. It already has the main features I need like precise flow

control and portability but is still limited on the user-friendliness and temperature control side.

2.3.8. Platform comparison and conclusions

Multiple companies recognise the need for more precise mimicking of physiological conditions and introduce relevant devices to the market. However, there is no ”ultimate solution” and most of the platforms are in the early development stage and don’t cover all or most of the requirements presented for this project. Even expensive commercial solutions need significant adaptations to the design. The comparison table of the examined solutions is presented below.

Brand		CO2/O2 control	Temperature control	Incubtor compatibility	Temperature control during imaging	Portability	Flow control	Imaging under perfusion	Chips compatibility
Emulate	Human emulation system	yes	no	no	no	no	yes	no	Only Emulate
Elveflow	Stage top incubator beta	Only CO2	yes	no	yes	no	yes	yes	any
Fluigent	Omi	no	no	yes	no	2 hours	yes	yes	any
Mimetas	OrganoFlow	no	no	yes	no	no	yes	no	Only Mimetas
Biond	comPLATE	no	no	yes	no	depends*	external**	yes	Only Biond
Ibidi, Okolab, etc.	Stage top incubators, heaters	yes	yes	no	yes	no	external**	yes	Adaptable***
TU Delft	TUD platform	possible	possible	no	possible	yes	yes	yes	any

Figure 2.20: The list of examined solutions. *The Biond comPLATE can be connected to any perfusion system. If the perfusion system is portable then the whole system can be considered portable as well. **These solutions don’t have a built-in flow control system but are compatible with various external controllers. *** The required holders can be 3D printed from heat-conductive materials and later tested if the heating is suitable for the user’s needs. Requires significant additional design investments. Sources: company websites.

The TUD microfluidic platform has the potential to become the most versatile research solution. Only research because archiving high throughput would be challenging and needs a different overall architecture. The platform needs a versatile heater, a CO2 and O2 control system (in the medium) and improved user-friendliness. This project won’t focus on dissolved gases since there are no such requirements posed by the Erasmus MC research group. The possible heating solutions and ways to improve the user experience will be discussed in further chapters.

2.4. Microfluidic heating solutions

The previous part already touched on the heating solutions developed in the industry. This chapter will focus more on how researchers approach this problem, especially in application to 3D cell culturing and PDMS chips.

2.4.1. TU Delft microfluidic heater for Micronit chips

MCs student Shieema Elhassan designed a heating platform to be used with glass chips produced by Micronit. The system is composed of several Peltier heaters which were chosen because having an option to cool the chip was also important. The sensing is done by up to twelve RTD (resistance temperature detector) sensors for up to four Micronit chips.

Based on the information presented in the MSc thesis of Shieema Elhassan this design has the following advantages:

- High precision of temperature sensing because of the use of multiple highly accurate Pt100 sensors.
- Low power consumption: about 1.5W per chip.
- 4.5 hour battery life.
- Up to 4 chips.
- Fast response time (2 minutes).

However, it also has shortcomings:

- Temperature distribution along the channel varies up to 1.6 °C.
- The system comes with a bulky controller box which limits its portability.
- Only compatible with the Micronit chip of specific size (45x15x2.1mm).

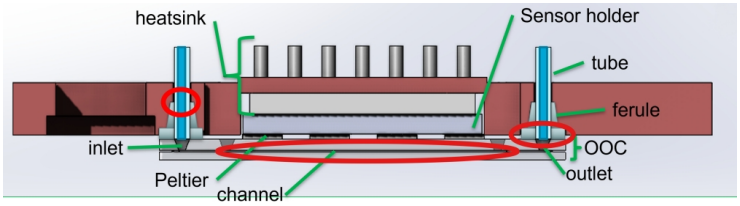

Figure 2.21: Micronit chip heater. Source: MSc thesis of Shieema Elhassan

It can be concluded, that this system cannot be readily applied to this project but some of the findings can be like heater PID (proportional–integral–derivative) control algorithms and sensor choice. In her literature survey, Shieema established that PLA (Polylactic acid), a popular material used in 3D printing, makes a good material for heater shells due to its low (comparable to wood) thermal conductivity.

2.4.2. Heatchips system

Aspert et al. designed a low-cost (under 100 euros) heater for PDMS chips from off-the-shelf components. It's comprised of ITO-coated heated glass, PI (proportional integral) controller and IR (infrared) probe [22].

Most important advantages of this approach:

- Only 0.4W of power is consumed at thermal equilibrium.
- Very low-temperature deviations from the 30C target (measured only at one point, though).
- Very simple design and assembly.
- High compactness and low cost of the system.

The downsides should also be noted:

- Only heats a single PDMS chip with side fluidic connections. Many PDMS chips have fluidic connections at the top of the chip, f.e. the ones used by the EMC group.
- Low accuracy of the sensor. IR probes do not go below 0.5°C accuracy, and repeatability of the measurements is also generally low [23].
- No battery. Although the low power consumption allows adding a battery to this design.
- The probe is mounted directly to the objective which is not always possible or fast and convenient for the user.
- The system wasn't extensively tested by the authors. The target temperature was only 30 °C.

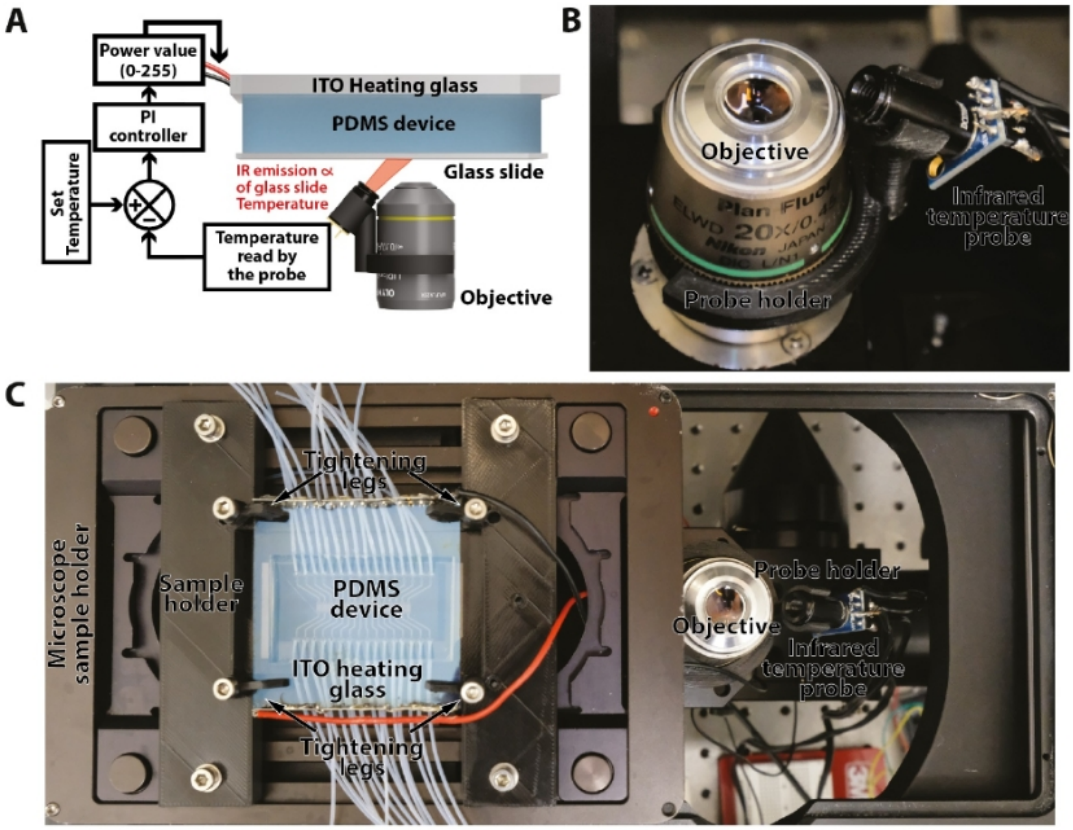

Figure 2.22: General scheme and implementation of the heater [22]

This paper shows a concept which can be applied to our setting because of the simplicity and the low cost of the system. However, the sensing part needs to be reconsidered because IR sensing is not precise enough to match the requirements. Also,

the fact that our chip has fluidic connections on top will not allow me to implement exactly the same design approach.

2.4.3. Compact microfluidic platform with a custom-built heater

Contoni et al. highlight that the devices which allow the transfer of a microfluidic device from the incubator to the microscope while maintaining perfusion and temperature are still not widely available [24]. They designed a system which fits into a 127x85 mm box comprised of two 1.5ml Eppendorf tubes for medium storage, two micropumps for chip perfusion, one chip pressed to the heater by a magnetic holder, and one K-type thermocouple for temperature control.

The heater was etched into PCB substrate and glued to a polyamide backing with holes for microscope use. The heater was controlled with a PI (same as PID but with no derivative component) controller using the on-off principle. The system allowed for under 0.5 °C gradients in the desired region when the flow was 10 µl/min. When the flow increased to 50 µl/min the temperature dropped to 35 °C. Thus, the authors propose to use an intermittent flow profile (switching the flow on for 10 seconds with a pause of a few minutes) for high flow rates.

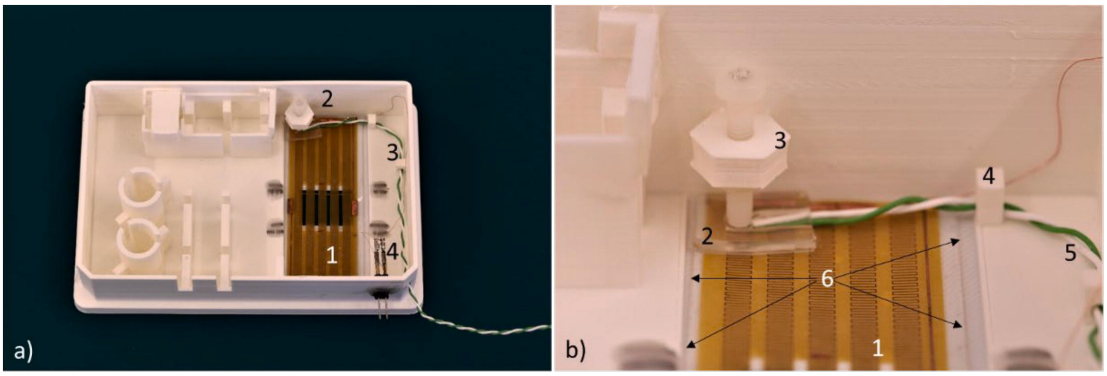

Figure 2.23: 1 is the heater. 2 is the thermocouple pressed to the heater. [24]

Advantages of the project:

- Very compact, portable and microscope-compatible setup.
- Low power consumption and thus easy to use with a battery. No battery is present in the original design.
- Mitigating the temperature shifts with the intermittent flow is an approach which can be applied to my project.
- PI control was managing to keep the temperature within the desired range at a low (10 µl/min) flow rate, the same flow rate as in my project. Thus, it can be an option.
- The objective can be in direct contact with the chip glass layer which keeps the working distance minimal.

Shortcomings:

- Micropumps deliver a very pulsatile flow which can be harmful to cells due to the shear stress on the membrane [25]. However, the measurements of the flow pulsation of the used piezo pumps conducted by the authors showed that the flow rate was quite constant.

- The device had some bubble issues.
- Very limited reagent storage. Need to drill holes in Eppendorf tubes.
- Only compatible with a specific chip. The positioning of holes in the heater does not allow for use with other chips.
- The precision of a K-type thermocouple is lower than that of the RTD sensors. Thermocouple needs to be calibrated from time to time.
- Heater was manufactured using cleanroom facilities which is expensive and complicated.

The authors present a simple and compact concept for heating and perfusion of microfluidic chips. Some of the ideas can be utilised like small reservoirs for expensive mediums, intermittent flow to reduce temperature gradient and save medium, and PI control.

2.4.4. Spheroid heater concept

Khan et al. introduced an organoid/spheroid 3D-printed bioreactor and imaging chamber. It's comprised of a heater, an organoid bioreactor with four wells for four organoids encapsulated in hydrogel and temperature and perfusion control system [26]. The bioreactor is 3D printed from a biocompatible resin and can be autoclaved and reused. The bioreactor is encased in an aluminium "oven" to improve thermal distribution and is heated with a resistive heater controlled by a PID algorithm using a single thermistor as a temperature sensor.

Key takeaways from this design:

- The medium delivered to the organoid chambers is preheated in the bioreactor which improves the temperature distribution even with high flow rates. The resulting temperature deviation was under 0.4 °C (from the setpoint of 37.4 °C).
- The bioreactor is just 6x4cm in size which will allow it to fit in most upright microscopes if secured on a stage plate.
- The bioreactor is 3D printed from a biocompatible resin which is easier than the long and multi-step production of PDMS chips.

Key downsides:

- The assembly is very complex and may leak.
- The working distance from the spheroid to the objective is 3mm which won't allow for high magnifications. Inverted microscopes are not supported.
- It may be complicated to sterilise the heated channels properly after use.
- Utilised resistive heater is very power consuming so it's hard to make this setup portable.

This prototype is mainly interesting because it's a rare project focusing on heating for a spheroid-specific application. However high power consumption and a large distance between the objective and the chamber don't allow me to apply the approach to my project.

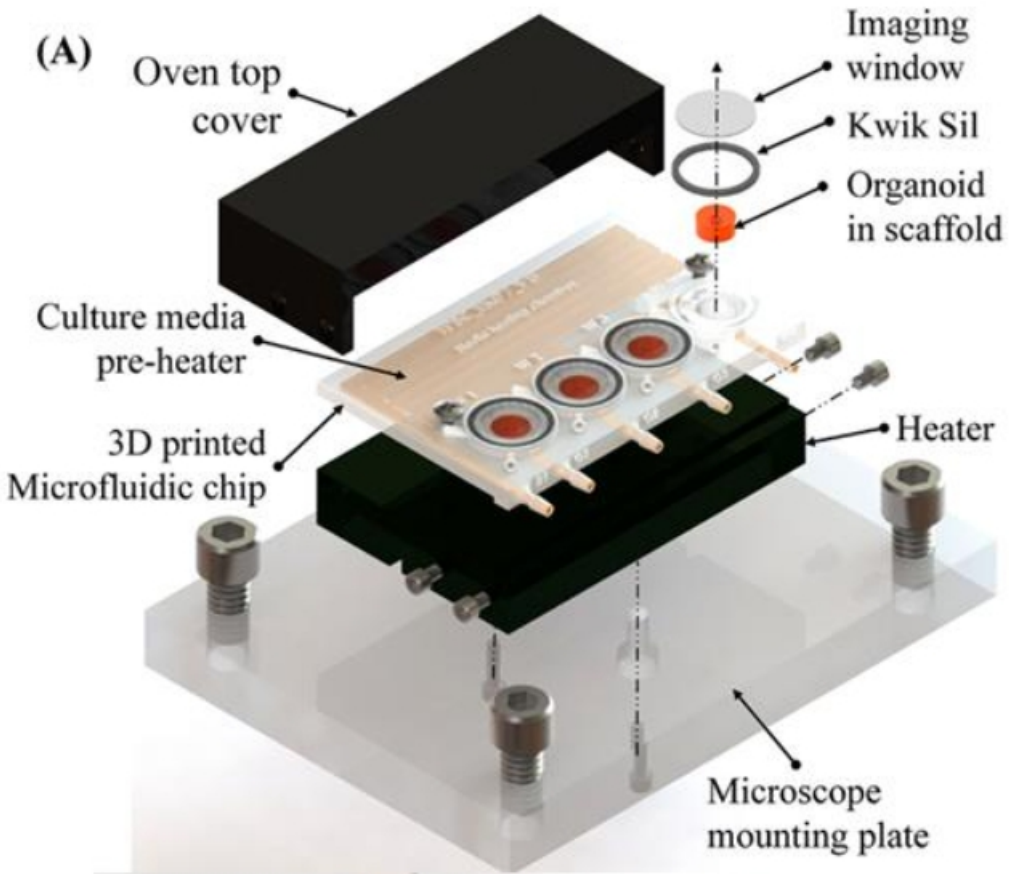

Figure 2.24: 3D-printed organoid bioreactor with a built-in heater [26]

Erasmus MC spheroid experiment protocol To come up with the exact specifications it's essential to know the protocol for the experiment. The desired sequence of steps was collected from the EMC research group. This protocol wasn't ever implemented because of the absence of suitable equipment. Currently, it's impossible to perfuse multiple chips, maintain temperature, place them under the microscope and image for a prolonged time without severely disturbing the environment in the chamber.

Important notes on the protocol:

- The T-cell suspension is prepared in a tiny quantity (matching the volume of side channels of the chips); thus, it cannot be perfused (and go to waste).
- Interleukin-2 (IL-2) solution is expensive and thus the wastage should be minimised.
- The chip may not ever dry out. A trial needs to be conducted to see if the chip can be properly sealed when placed on a heater to make sure the T-cells survive for 24 hours.
- The temperature in the central chamber should be kept as uniform as possible to minimise stress on the cells.

#	Stage	Step description	Duration	Channel	Temperature
1	Preparation	Grow spheroids of MC38 cells	10-14 days	-	36.5
2		Prepare hydrogel (Fibrin) solution	30 mins	-	Room
3		Mix spheroids with hydrogel	90 mins	-	Room
4		Pipette the mixture into the central chamber	1 min	central channel	Room
5		Fill the side channels with medium, for the chip to not dry out	5 min	both side channels	Room
6		Place into the incubator, gel (fibrin) crosslinks	1 hour	-	36.5
7	Spheroid life-support	Connect the chip to the perfusion system	30 mins	both side channels	Room
8		Perfuse with medium	12 hours	both side channels	36.5
9	T-cells introduction	Prepare T-cell suspension	90 mins	-	Room
10		Disconnect first side channel from perfusion	10 mins	first side channel	36.5
11		Pipette T-cell suspension inside the chip	5 min	first side channel	36.5
12		Seal the T-Cell channel	5 min	first side channel	36.5
13		Perfuse IL-2 mixed with medium	5 min	second side channel	36.5
14		Wait for T-cells to diffuse to the central chamber	24 hours	-	36.5
15	Imaging	Place the chip under the microscope	30 minutes	-	36.5
16		Pipette Luminescence substrate dissolved in medium (optional)	5 minutes	first side channel	36.5
17		Image	up to 24 hours	-	36.5

Figure 2.25: The intended spheroid and T-cells experiment steps

2.5. Research question

The examined literature, collected preliminary requirements and imaging protocol allow me to formulate the research question for this project.

Research Question

How to implement a stable body-temperature environment inside a microfluidic chip to perform high-resolution fluorescent and luminescent imaging of the 24-hour-long interaction of CTLs and spheroids?

A number of tasks can be identified:

1. Design a heater which is compatible with the microscope at EMC, the Twente chip and other chips suitable for spheroids (Ibidi µ-slide);
2. Integrate the heater with the perfusion system which will match the requirements of the EMC team;
3. Perform 24-hour imaging of the CTL and spheroid interaction;
4. Investigate the influence of temperature control on CTL activity.

2.6. Required specifications

Based on the obtained protocol the required specifications were collected and presented in figure 2.26.

Specification	Requirement from EMC
Chip dimensions	50x22x0.17mm
Number of chips	2
Chip fluidic connection location	Top
Temerature in the central chamber	36.5±0.5C
Response time from room temperature	5 minutes
Battery life	30 minutes
Portability	yes
Incubator compatibility	no
Oxygen and carbon dioxide control	no
Miscrosope type and model	Inverted, Zeiss Elyra PS1
Flow rate	10 ul/min
Perfusion duration	24 hours
IL-2 reservoir volume	<2ml
Objective working distance	<1mm
Optical transparency	yes, 450 to 600nm
Top lid (not transparent)	yes

Figure 2.26: The required specifications for perfusion and heating systems

2.7. Design and materials considerations

To ensure that the spheroids are always at the optimal temperature, we need to find a way to heat the chip and control the temperature. Thus, at least the following basic design blocks are required:

- A heating element. Produces heat.
- A sensor. Measures the temperature as close to the chamber as possible.
- A controller. Reads the sensor and adjusts the heating power.
- A holder. Ensures the chip is in contact with the heater.

This chapter will go into possible parts and materials to be used for those four elements based on the requirements and papers studied in parts 2 and 3.

2.8. Heater design considerations

The first consideration for the implementation of this project was to integrate the heater right on top of the TUD PMP. However, after the initial visit to Erasmus MC and inspection of the two microscopes, compatible with luminescence applications, it became evident that the platform won't fit and needed to be redesigned. Moreover, the top one priority microscope (Zeiss Elyra PS1) has an incubator installed which greatly limits the size of the object which can be placed under the objective.

An observation was made that most microscopes support stage top incubators (described in section 2.3.5. Thus, the heater could be an external device on which the chips are mounted and it could be connected with wires and tubings with the PMP where all the electronics, reservoirs and fluidic components are based. The block scheme of the design idea is presented in figure 2.27.

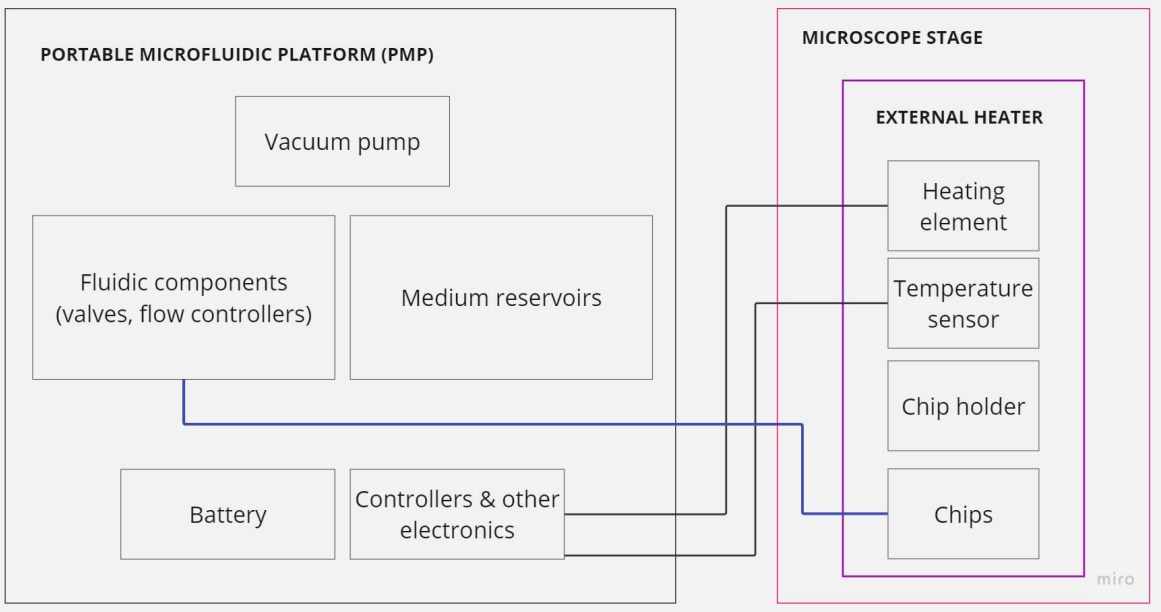

Figure 2.27: Block-scheme of the overall design. Only simplified connections between the external portable heater and PMP are shown.

S. Elhassan in her literature study examined the suitable materials for microfluidic chip heaters. Her finding was that the widespread 3D printing material PLA has a thermal conductivity of 0.15 W/m*K (similar to wood) and thus can be considered as the material for chip holder and casing. TU Delft also has an abundance of 3D printers with up to 0.15mm resolution for PLA. PLA will be used as the material for all 3D-printed parts of this project.

2.9. Heating elements

To come up with a more detailed design for the heater, the actual heating element first has to be selected. The design examined in parts 2 and 3 used the following heating element types:

- Conventional resistive heaters.
- Peltier elements.
- Transparent resistive heaters (ITO-coated glass).

Conventional resistive heaters are not transparent and thus they should either be placed on the opposite side from the objective or have windows in them. Our chip design has tubings connecting to the chip on the opposite side from the objective, so this side cannot be conveniently used for placing a heater. Also in this case the heater would have to transfer the heat through the thick layer of PDMS which is a thermal insulator (0.15 W/m*K thermal conductivity). The bottom side of the chip is in direct contact with the glass coverslip thus if heated from the bottom there's just 0.17mm of glass (1.3 W/m*K thermal conductivity) in the way to the chamber.
The chamber area has to be kept clear for the imaging, so if non-transparent heaters are used they cannot be positioned directly under the chamber. This will impact the evenness of temperature distribution and will make the heater design not universal because the

chambers are of different sizes for each chip.
The use of Peltier elements was thoroughly evaluated by S. Elhassan in section 2.4.1. It was decided not to use them in this project because they have the same disadvantages as resistive heaters (not transparent, heating is not uniform). Multiple Peltier elements are required to mitigate the non-uniformity of heating which complicates the design.
It's also possible to preheat the fluid delivered into the chip or use specialised channels in the chip for heating only. The second option requires a special chip design so it won't be considered. The first option requires enough flow to transfer a sufficient amount of heat. The flow rates used in this project are low (10 µl/min) so this option won't be considered either.

ITO-coated heaters have five major disadvantages:

1. Additional thickness of at least 0.7mm between the objective and the chip.
2. Possibility to scratch or break.
3. ITO layer is not 100% transparent, see Figure 2.28.
4. ITO-coated glass is generally more expensive than other off-the-shelf resistive heaters.
5. Establishing a reliable electrical connection with the glass can be challenging.

The advantages are also evident:

1. Very high uniformity of heating (given the coating is uniform).
2. Compatibility with any chip design.
3. Possible to heat right under the chamber.

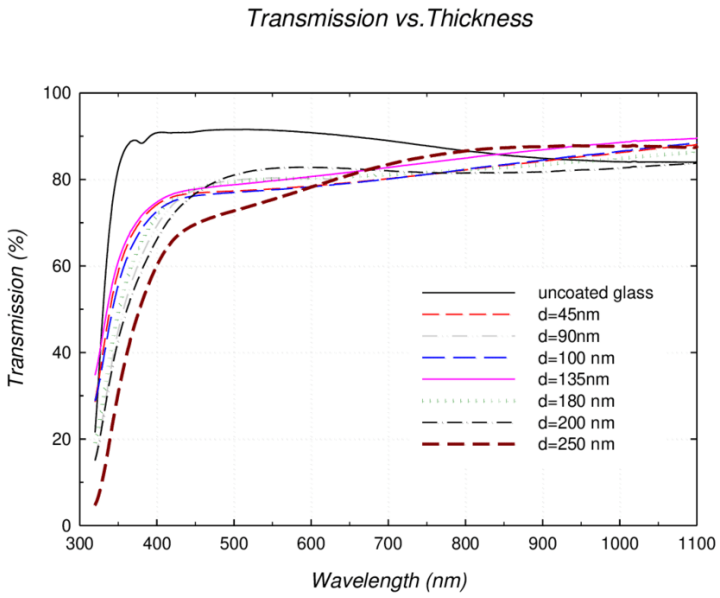

Figure 2.28: The transmission rate of ITO-coated glass with various ITO thicknesses compared to uncoated glass. [27]

Disadvantage (1) will still allow matching the requirements. The coverslip thickness is just 0.17mm, so the total minimal distance between the objective and the chamber

bottom will not exceed 1mm. Disadvantage (2) can be mitigated by a reliable glass holder design. Also, the ITO glass can be oriented downwards to reduce the scratching risk. Disadvantage (3) has to be experimented with on a microscope. It's certainly a risk. A possible mitigation is removing the ITO right under the chamber with a laser. However, the advantage (3) is also removed. To mitigate disadvantage (5) the ITO glass can be ordered with busbars (metallic, usually silver, bars on the sides of the ITO layer) to which the wires can be soldered.

ITO glass slides were found which have the desired thickness (0.7mm), size (50x75mm, enough for the chip sizes up to a microscope slide size and for two coverslip chips) busbars and an affordable price (13.5$ per unit 330$ for 25 pieces)[28]. Thus, it was decided to design the heater using the ITO glass, the suggested scheme is presented in figure 2.29.

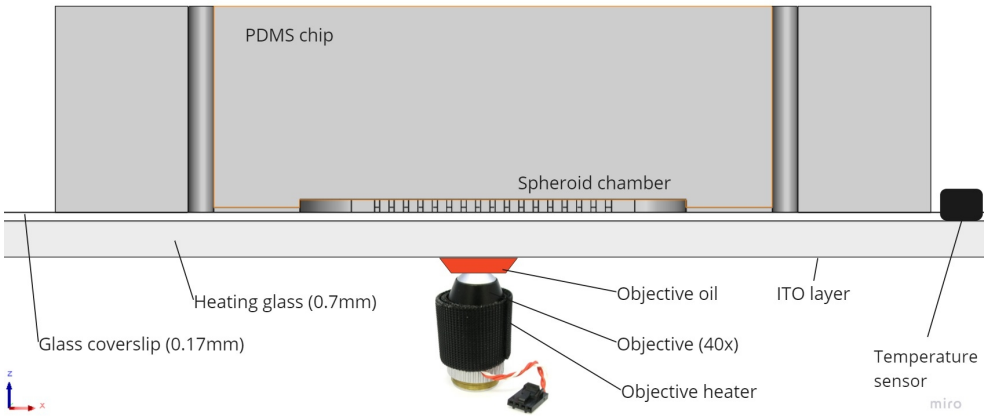

Figure 2.29: The suggested heating scheme with ITO-coated glass. The high-magnification objectives require the use of oil and an objective heater for the heat to not escape. The objective and the temperature sensor are shown out of scale with the rest of the elements.

2.10. Temperature sensors

To control the temperature, it needs to be measured and compared with the desired value to adjust the heating power. The design approaches examined in Chapters 2 and 3 use the following sensors:

- Thermocouples.
- Thermistors.
- RTDs.
- Infrared sensors.

It has to be noted that the chip surface is flat so it's desirable that the sensor is compatible with that geometry.

The datasheets of all the types of sensors priced under 50€were studied on the website of one of the TUD suppliers nl.farnell.com. The results are presented in Figure 2.30.

Type		Price	Maximum accuracy	Response time	Suitability for surface	Stability	Connection to Arduino
	**Thin-film RTDs**	**2€+**	**±0.1** ºC	<30s	**+**	**0.05°C/year**	Via Amplifier
	Surface thermistors	0.2€+	± 0.05 °C	<10s	±	0.2°C/year	Simple
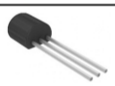	IC (LM335)	2€+	±0.1 ºC	<60s	-	1°C/year	Direct
	Infrared	5€+	±1 ºC	<1s	+	Unknown	Direct
	Surface thermocouple	3€+	±0.5ºC (type T)	<10s	±	Variable	Via Amplifier

Figure 2.30: The comparison table of various types of temperature sensors. Arduino is a commonly used single-board microcontroller. Source:nl.farnell.com

Thin-film RTD sensors like Pt100 and Pt1000 look especially beneficial to this application because of unmatched accuracy and superior surface compatibility. The downside is that an additional component (amplifier) is required to connect the sensor to the controller.

2.11. Design risks and mitigations

The design concept proposed in section 2.8 has a number of risks:

1. Placement of the heater outside of the platform lengthens the fluidic path from the reservoir to the inlet of the chip leading to more dead volume, resistance in the system, and medium wastage.
2. Some ITO glass restrictions and mitigations were discussed in section 2.9.
3. The flow in the chip's channels can cause a thermal gradient in the central chamber.
4. The capacity of the PMP's medium and waste reservoirs may not be sufficient for 24-hour operation.
5. Overall reliability of the platform is unknown.
6. Other complications related to PMP use are described in the section 2.3.7.
7. Bubble and leakage risks.
8. The sensor will be pushed to the glass on the same side as the chip. This means that the temperature measured by the sensor will not perfectly reflect the temperature of the central chamber. Even provided a quality calibration is done, the change of conditions like air temperature or surrounding air speed may lead to a discrepancy between the sensor and chamber temperature.

Let's estimate the dead volume and the time for the medium to reach the chip given the length of the tubing from the platform to the heater is 500 mm (l), the inner diameter of the tubing is 0.8 mm (D), and the volumetric flow rate is 10 µl/min (Q).

$$V_{dead} = \pi * R^2 * l = 251\mu l \tag{2.1}$$

$$t_{dead} = V_{dead}/Q = 25min \tag{2.2}$$

Risk (1) can be dealt with by placing the reservoirs right on the heater. It, of course, greatly limits the reservoir volume but also radically decreases the dead volume.

Risk (3) can be addressed by reversing the flow in one of the channels so that the flow directions in the channels oppose each other. COMSOL models showed the efficacy of this approach (results for conventional and reversed flow presented in figures 2.31 and 2.32 consequently). The temperature gradient in the central chamber is reduced from 0.5°C to 0.2°C.

For the COMSOL simulation, the following interfaces were used:

- Electric Currents in Shells (current in the 300 nm-thick ITO layer due to the applied voltage of 19 volts to the short sides of the layer).

  $$J = d * \sigma * E \tag{2.3}$$

  Where J is the current density, E is the electric field strength, σ is the electrical conductivity and d is ITO layer thickness.
- Joule Heating (ITO heating due to the electrical current).

  $$Q_e = J * E \tag{2.4}$$

  Where Q_e is the heat produced due to electric current.
- Heat transfer in solids and liquids (conduction of heat from the ITO to the glass substrate and further into the glass coverslip, PDMS chip and medium inside the channels and chamber of the chip). Convective heat loss to the surrounding layer was accounted for with a convective heat transfer coefficient h=5 W/m. ^{2}*K. The initial chip and surrounding air temperature were set to 293 K.

  $$Q_c = h * (T - T_{ext}) * S \tag{2.5}$$

  Where Q_c is the heat lost due to convection, T_{ext} is the temperature of the environment and S is the surface area.
- Non-isothermal laminar flow (for the 10 µl/min flow in the inlets of the side channels and zero pressure at the outlets). For the microfluidics applications Stokes (creeping) flow equations are used.

  $$\nabla \cdot \sigma + f = 0 \tag{2.6}$$

  Where σ is the sum of viscous and pressure stresses and f is the applied body force.

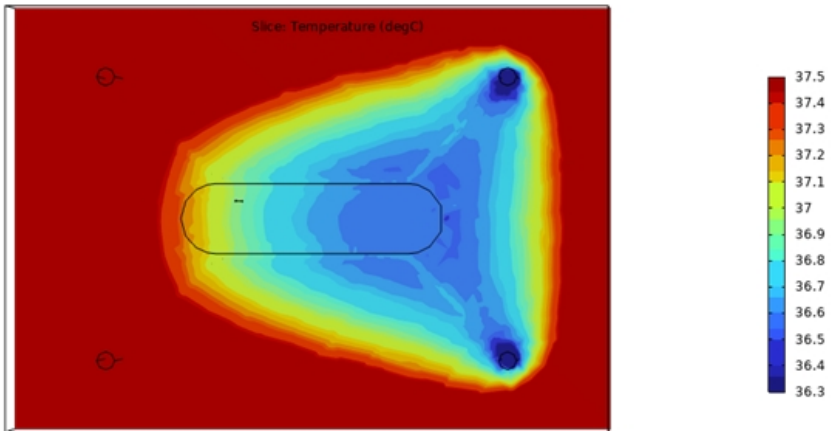

Figure 2.31: COMSOL model of the temperature distribution at equilibrium in the middle of the central chamber of the chip with the flow in the side channels directed flow left to right

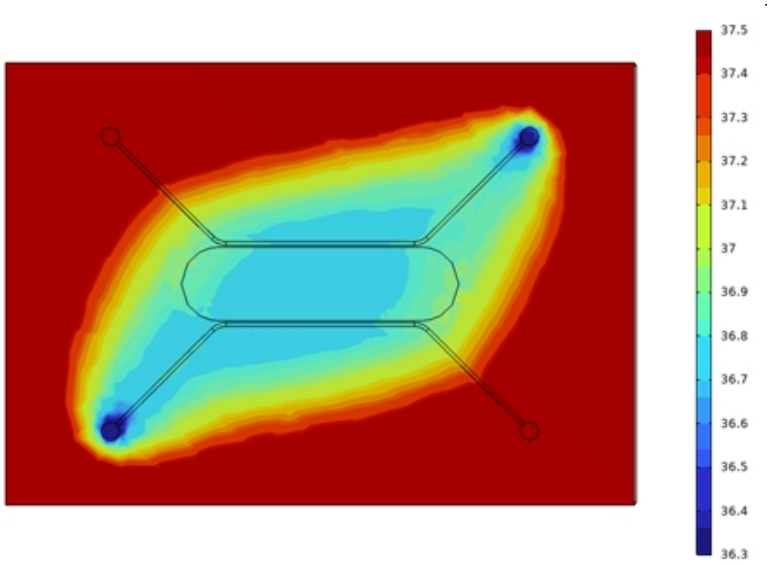

Figure 2.32: Same as 2.31 but with the reversed flow direction in the lower side channel

Risk (4) can be reduced by either redesigning the reservoir rack and increasing the volume of the tubes or by changing the flow mode from constant to intermittent (with pauses).

To investigate risk (5) preliminary overnight trials of the PMP should be conducted before proceeding to spheroid experiments.

Risk (7) is present in all microfluidic devices. In our case the flow rate is low thus the leakage in the fluidic connections with the chip is unlikely. It can be further minimised by ensuring tight connections between the L-shaped stainless steel PDMS couplers, tubing and PDMS chip itself. Immobilising the tubes in proximity to the chip can be advantageous as it will prevent the couplers from moving inside the holes. Bubbles may emerge, especially because the protocol entails switching the fluidic connections manually. However, in our case, the tumour is encapsulated in hydrogel and thus small

bubbles in the side channels should not be harmful to the spheroids. They can indeed harm the T-cells. This can be dealt with by carefully pipetting (instead of perfusing) the CTLs.

2.12. Chip perfusion scheme

Based on the risks discussed in the previous section and the required specifications (stated in section 2.6) a scheme with the intended design was created (figure 2.33). This design involves applying intermittent flow (one-minute flow, ten-minute pause) through the chip to spare the expensive medium (especially IL-2). The small (1-2ml) Eppendorf tube reservoirs are placed on the heater itself. The medium from the reservoirs is pulled through the chip via the negative pressure in the waste reservoir. The flow controller, waste reservoir, pump and all the controllers are based on the PMP.

The Eppendorf tube reservoirs and the short tubings leading from them to the chip inlets can be easily replaced to avoid any conditioning and cleaning protocols.

This configuration can be used for steps 9 to 17 of the imaging protocol (figure 2.25). For step 8 both channels can be connected by using a microfluidic splitter (splits 20 µl/min flow into two 10 µl/min flow paths).

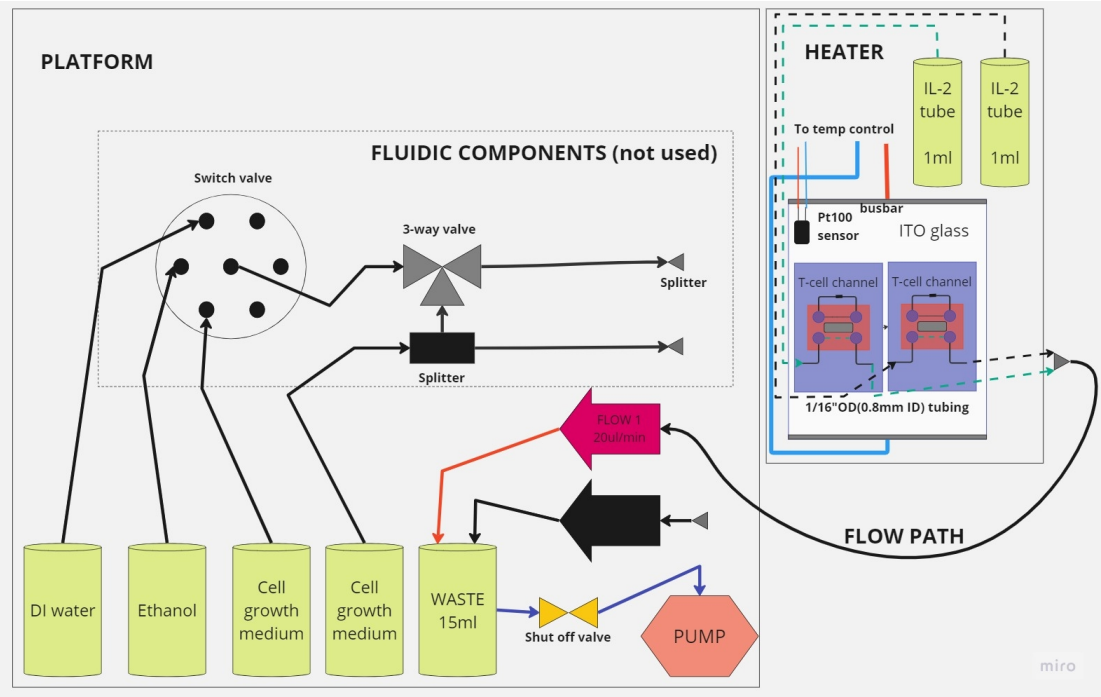

Figure 2.33: Proposed design of the system based on the existing PMP architecture

2.13. Power supply and control system

The block scheme of existing electrical and vacuum connections between the platform components is presented in figure 2.34. The system doesn't allow to power the PMP from the wall socket (to avoid the use of a bulky external 24V power supply unit), the Arduino can only be powered from the USB port or a very low-capacity 9V battery. I'm going to redesign the system to accommodate the new components and also improve the comfort of the user. The new design is presented in figure 2.35. The user will be able to turn the perfusion and the heater on and off separately. All the components will be based on the platform without the need for a USB connection, battery replacement and external power supply unit.

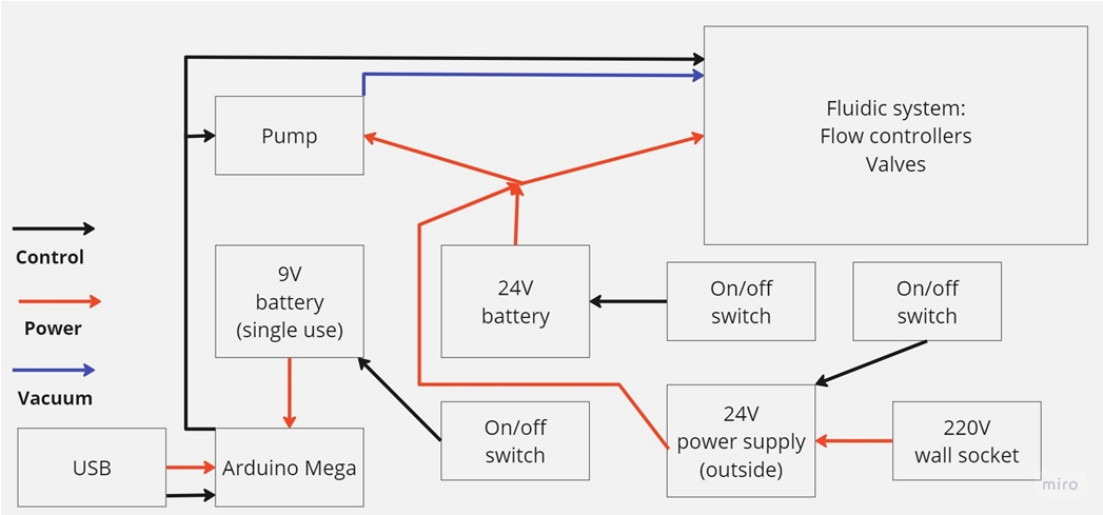

Figure 2.34: Current power supply and control block scheme of the platform

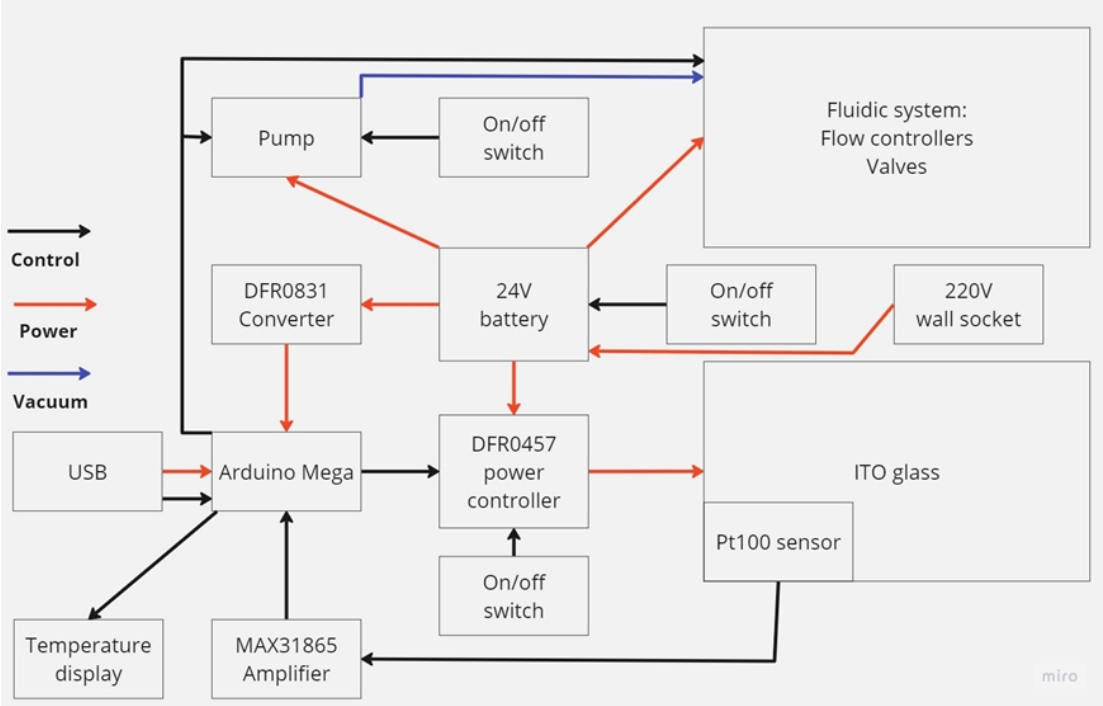

Figure 2.35: Proposed power supply and control block scheme of the platform

Main shortcomings of the proposed design of the electrical part:

- The absence of the possibility of data logging when not connected to a PC. There will be no way to tell if the temperature was maintained (e.g. throughout the night) unless by direct observation. To allow data logging an Arduino shield with an SD card reader needs to be introduced.
- The reliability of the system will remain unclear even after trials given that some components may be prone to failure (e.g. pump, various electronic components).

2.14. Project plan

The Gantt chart of the project was designed based on the requirement to graduate before September 2023.

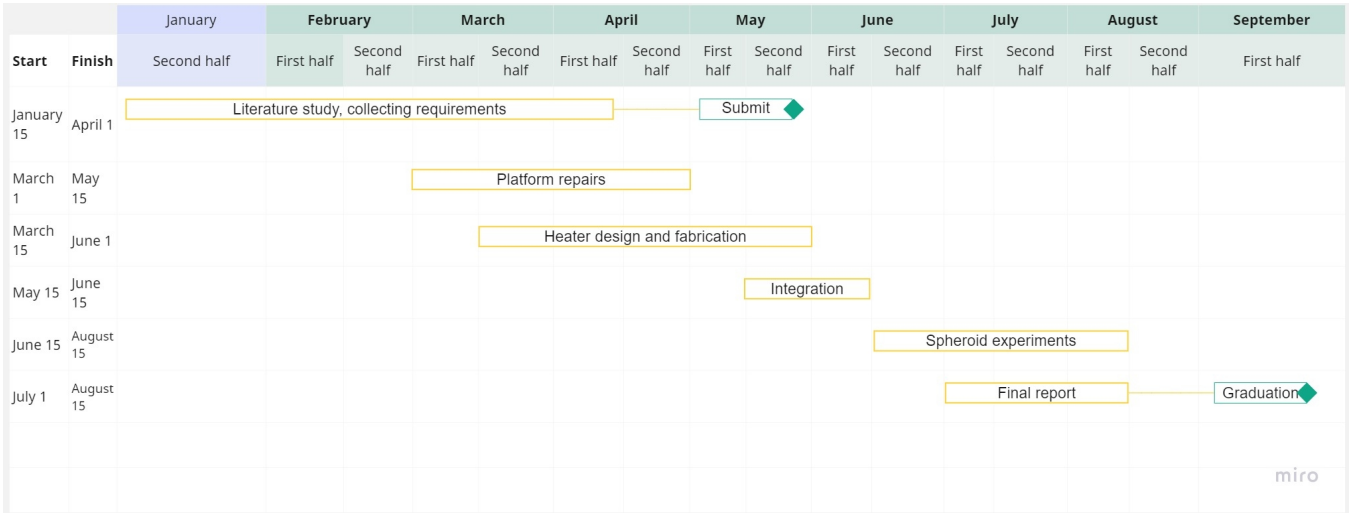

Figure 2.36: Gantt chart of the project

The key checks and experiments to be conducted after the heater is integrated with the PMP and before the start of trials with cells:

1. Check if the chips are drying out with the sealed channel (step 12 of the experiment protocol 2.25).
2. Check if the splitter (figure 2.33) is splitting the flow rate evenly between the two channels by pipetting the same amount in two Eppendorf tubes and checking how much is left in each tube after several hours of perfusion.
3. Evaluate the precision of the temperature control without flow using the thermal camera. Calibrate the sensor setpoint to ensure that 36.5 °C is maintained in the central chamber.
4. Make sure the ITO layer and two layers of glass (ITO substrate and coverslip) do not hinder the obtainment of images.
5. Ensure leakage-free flow with the chip placed on the heater and connected to the new Eppendorf tube reservoirs.
6. Measure if the flow in the system corresponds to the programmed values by measuring the volume which was pumped through the system over a period of time.
7. Perform an 8-hour experiment of the platform and heater running under perfusion to see if any malfunctions are observed. E.g. due to overheating of electronic components.
8. Perform a one-hour experiment on battery power. Check if the temperature and flow rates are maintained.

Portable microfluidic chip perfusion and heating solution for high-magnification optical microscopy

***Abstract*—A stage heater for inverted optical microscopy was developed as an add-on to TU Delft portable integrated microfluidic platform. The platform was modified to gain additional functionality and portability. The stage heater was designed to work with custom PDMS microfluidic chips and commercial polymer chips which highlights the adaptability of the setup. The on-off temperature control was evaluated via an external thermocouple sensor, and the standard deviation of temperature in the cell chamber did not exceed 0.3 °C. An intermittent flow mode (flow for 1 minute at 10 μl/min, pause for 10 minutes) was introduced to match the requirements of an experiment involving T-cell and tumour spheroid interaction. The stage heater was deemed compatible with fluorescent and transmission imaging modes for up to 20x magnification when equipped with a PET ITO-coated bottom heater with a window underneath the cell chamber. An increase in T-cell activity was observed with enabled heating. The process of T-cells attacking a spheroid via a time series of images was captured.**

I. Introduction

Organ-on-a-chip models have emerged as prominent tools for drug discovery and disease research. Their capacity to mimic organ functions and behaviours enhances the value derived from experiments. This principle extends to 3D tumour models, referred to as spheroids or organoids, wherein the tumour microenvironment (TME) profoundly influences the responses of cancer cells to drugs or therapies [4]. An important parameter governing the natural environment of human cells is physiological temperature. Its significance is frequently overlooked, even within high-impact studies involving microfluidic chip models [6]. This partly arises due to the customized design and fabrication of chips by researchers. The challenge lies in identifying a commercial solution that aligns with both experimental requirements (e.g., prolonged imaging sessions) and chip specifications. Thus, temperature control is often ignored, at least in some stages of the experiment.

Cell incubation during experiments is often limited to specific phases, with temperature regulation during microscopy disregarded. Navigating temperature fluctuations when transferring chips between incubators and microscopes, or even between different laboratories or facilities, further complicates matters. An optimal scenario envisages consistent chip conditions, granting researchers the freedom to manipulate and subject chips to microscopy without the cells experiencing environmental perturbations. Furthermore, a versatile solution able to accommodate a diverse array of chip types is preferred, so that a researcher could identify the most suitable chip for the experiment.

This paper introduces an updated iteration of the TU Delft integrated microfluidics (iMicrofluidics) platform [7]. The central focus resides in assessing perfusion, heating, and temperature control attributes while striking a balance between the portability, functionality, and adaptability of the platform. The platform's functionality was tailored to meet the prerequisites of a live cell experiment involving high-magnification fluorescent imaging. This specific case entailed examining interactions between spheroids of colon adenocarcinoma (MC38) cells expressing Green Fluorescent Protein (GFP) and Cytotoxic T-cells (CTLs) expressing Red Fluorescent Protein (RFP) within a microfluidic chip. The MC38 cell line spheroids are encapsulated inside hydrogel (Matrigel) inside the chamber or a well of the chip. The CTLs are deposited along with IL-2 medium in the side channels (or top channel for Ibidi Polymer chips) and should cooperatively destroy the spheroids. The metabolic activity and thus the effectiveness of CTLs in spheroid destruction is expected to depend on the temperature. This process has not yet been researched and imaged in a microfluidic chip with temperature control during all the stages of the experiment.

The requirements are as follows:

- Temperature in the cell chamber of 36.5 $\pm$ 0.5 °C.
- Battery life of at least 30 minutes.
- Uniform flow rate of 10 μl/min.
- Minimum wastage of Interleukin-2 medium used to activate the T-cells (medium reservoir volume under 2ml).
- Compatible with 10x and 20x dry objectives as well as with 40x and 63x oil objectives.

II. Materials and methods

A. Microfluidic chips

The system was designed to be compatible with three types of chips:

- Custom PDMS chips (17x12x4mm^3) plasma bonded to glass slides (75x25x1 mm^3).
- Same PDMS chips but plasma bonded to coverslips (50x22x0.17mm^3). Chips were manufactured at the University of Twente.
- Commercially available microscope slide size polymer chips used for 3D cell modelling (μ-Slide III 3D Perfusion and μ-Slide Spheroid Perfusion, Ibidi Gmbh, Germany) [2], [3].

PDMS chips consist of a central chamber with 7.5 x 2 x 0.25 mm^3 and a volume of approximately 4.5 μl. The inlets and outlets are 500 μm in diameter. The side channels have a 100x100 μm^2 cross-section and are separated from the optical detection chamber by an array of sixteen trapezium-shaped pillars. Up to two PDMS chips can be bonded to a coverslip or slide. Both polymer chips have three independent flow paths with multiple wells (7 or 2 wells in each path). Small wells have a 4.5 μl volume and large wells have 40 μl volume. According to the company specifications, only the chip with

large wells is applicable for usage with hydrogel. Petreus et al. however did successfully use the 4.5 μl well-chip in combination with hydrogel [5].

Fig. 1: Polymer chips specifically designed for 3D culturing. Each chip has three independent channels with multiple wells. The bottom (also polymer) coverslip of the chips is 0.17mm thick. Image courtesy: Ibidi Gmbh

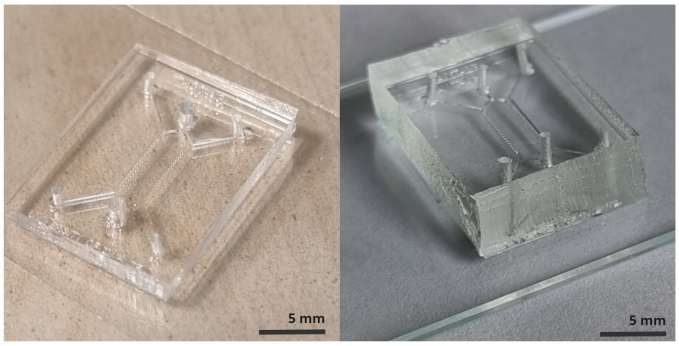

Fig. 2: PDMS chips on a 0.17 mm coverslip (left) and 1 mm microscope slide (right)

B. Microscopy

The system was designed to fit the Zeiss Elyra PS1 microscope with a 128x85 mm^2 Tokai Hit stage top heater. It can also fit other inverted microscopes with a similar stage size. The microscope has installed 10x and 20x dry objectives and a 63x oil objective. The images were processed with Fiji software.

C. iMicrofluidics platform and flow control

The used platform is extensively described by Haoyu Zhu [7]. To match the scope of this project some modifications were made, mainly due to the addition of the microscope stage top module (Figure 4). The top layer of the platform consists of a vacuum pump, a pressure gauge, a waste reservoir and two flow controllers (Bronkhorst, The Netherlands). The vacuum pump delivers a negative pressure to the waste reservoir, the pressure can be observed with the pressure gauge. A deliberate vacuum leak in the waste reservoir was created to lower the vacuum depth from -0.6 bar to -0.2 bar and thus reduce flow surges. The waste reservoir is connected with outlets of the flow controllers (FC) with tubes with 0.8 mm inner diameter. Inlets of the flow controllers are connected to the outlets of a chip. The inlets of a chip are connected with the medium reservoir made out of an Eppendorf tube and positioned right on the stage top heater module. The CAD drawing of the stage heater is presented in figure 6.

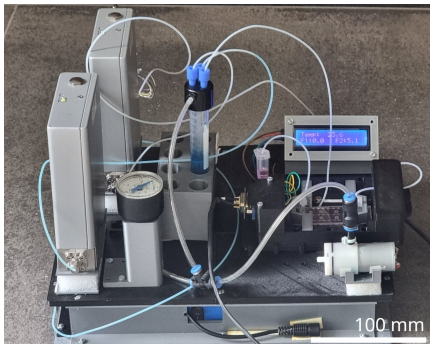

Fig. 3: Integrated microfluidics platform. Flow controllers are on the left; the pressure gauge and water reservoir are in the middle; the display, microscope module on a holder and pump are on the right.

D. 3D Printing

The stage heater and iMicrofluidics platform parts were designed in SOLIDWORKS, and 3D printed on a Prusa i3 MK3S out of PLA (Polylactic acid). The chip holders connect to the stage top heater with high-force neodymium magnets.

E. Finite element method

The heat distributions in the PDMS chip on a coverslip were modelled using COMSOL Multiphysics 6.1. The following packages were used for the model: heat transfer in solids and liquids; electrical currents in layered shells; creeping flow; electromagnetic heating in layered shells; and nonisothermal flow. Convective heat loss to the environment was accounted for.

F. Spectroscopy

The transmission rates of the transparent heaters were measured using AvaLight-DH-S-BAL light source (Deuterium and Halogen lamps) and AvaSpec-ULS2048CL-EVO-RS spectrometer, data was collected with AvaSoft-Basic software (all from Avantes, the Netherlands). The transmission was measured for regular microscope slide (1mm thick), ITO-coated glass and ITO-coated PET film (three samples each).

G. Bottom heating

Commercial microscope stage incubators (Tokai Hit, Ibidi) heat the environment around the sample, i.e. using a glass ITO lid heater and heating the sides of the incubator chamber with resistive heaters. This leads to high power consumption and the inability of a similar setup to function from a battery. Stage incubators also control the environment in the chamber, ensuring desired humidity, oxygen and carbon dioxide concentration. Those incubators are usually tailored to be used with well plates or microscope dishes and don't support microfluidic chips. To ensure maximum adaptability of the platform, namely the ability to work with multiple chip types, and to minimise power consumption, the design approach involves an unconventional transparent bottom heater. The heating scheme is presented in figure 7.

The heating element is based on ITO-coated PET film (0.2mm thick), size 75x50mm^2 (Thor labs). The film has

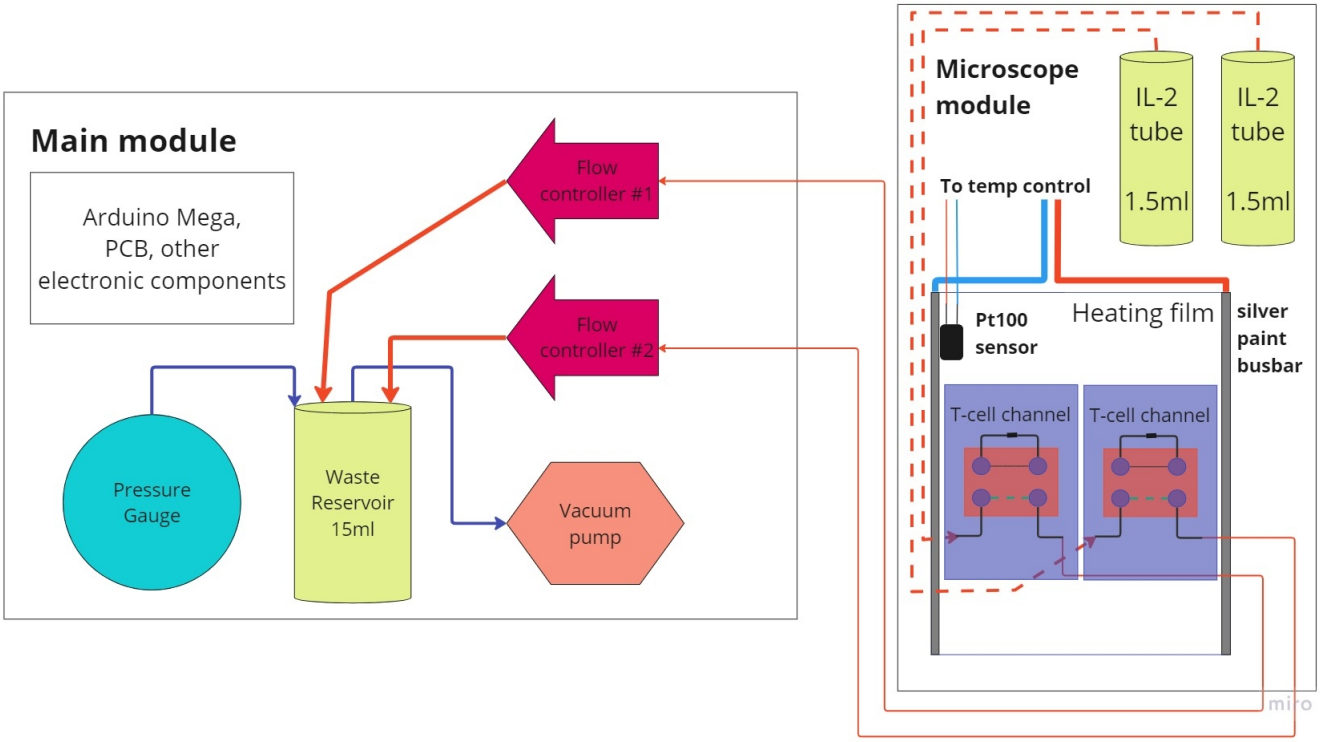

Fig. 4: Schematic of the integrated microfluidic platform. The modules are connected with an 80 cm wire bundle and one or two 0.8mm ID PTFE tubings. Placement of the 1.5 ml medium reservoirs reduced the dead volume by 250 μl but limits the reservoir volume. If more volume is desired then the larger 15 ml medium reservoirs can also be positioned on the tube rack of the main module. The inlet path and reservoir can easily be replaced to avoid contamination.

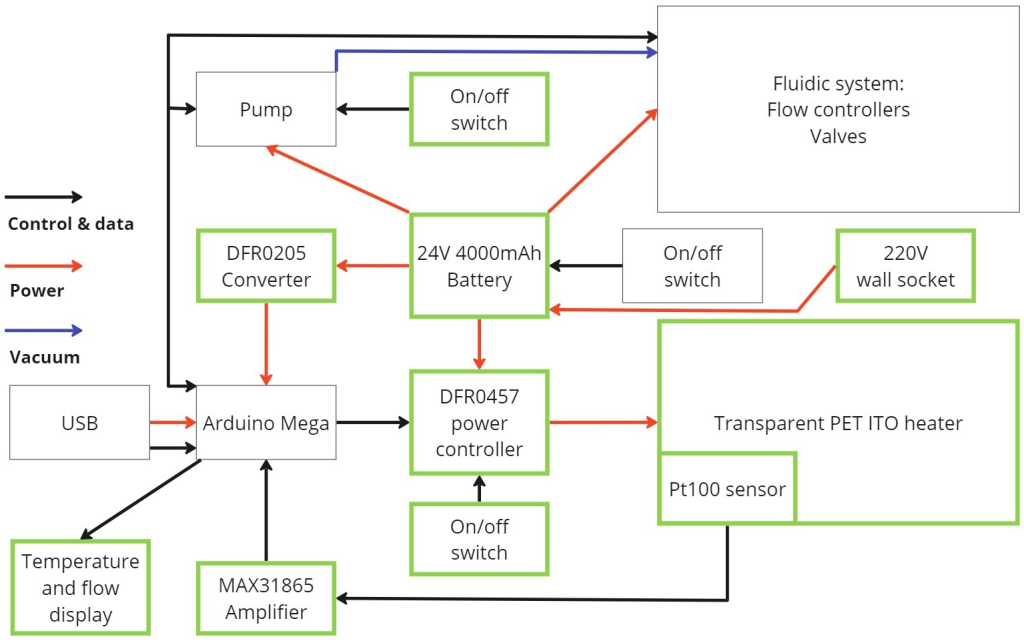

Fig. 5: Block-scheme of the electronic components of the integrated microfluidic platform. The new components compared to the original design are in green frames. Only key connections are shown. Most components are connected through a PCB (not shown).

silver strips on the long side (painted with conductive silver paint) and is attached to a 3D-printed frame. The film is pressed to the frame with 3D-printed pads. The contact wires are inserted between the pads and the silver strips, and the assembly is held together with four bolts and nuts. As shown in the results, the imaging quality through the PET film was unsatisfactory. Thus, the heating elements with 'windows' were used. The 'windows' can be cut with a snap-off knife to allow direct access of the microscope objective to the cell containing parts of the chip. Windows are especially crucial

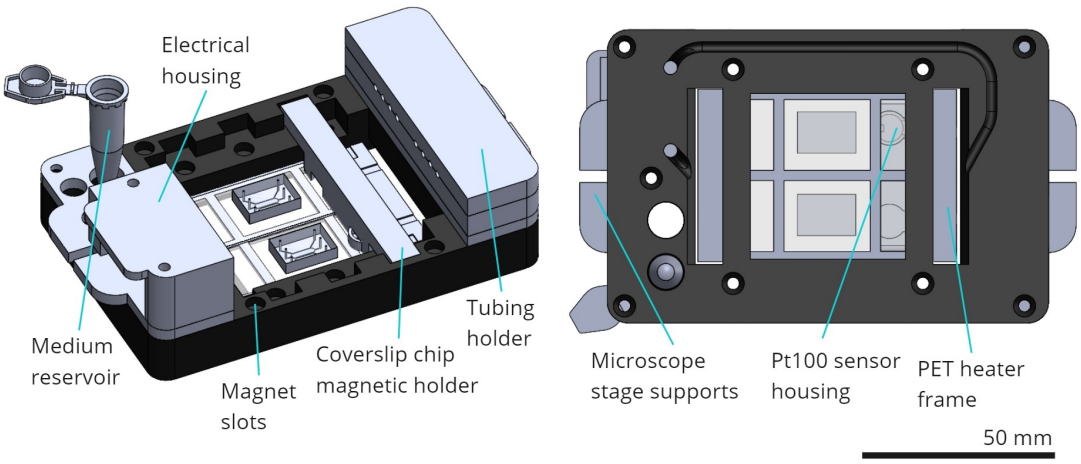

Fig. 6: Stage heater (microscope module) design and key components. The stage heater has three sets of magnetic slide holders (one pair for each chip type). The chips can be quickly swapped. The electrical housing contains a 9-pin D-SUB connector to which the sensor and the heater wires are connected with screws, to allow fast replacement. The sensor is inserted in a housing 10mm in diameter with a magnet on top and can either be mounted (by clicking in) in a slot on one of the chip holders or magnetically mounted (using a thin bottom magnet) right on the heater or chip surface, as the user desires. The configuration of the heater frame and thin bottom heater supports allow for a microscope objective to approach any cell-containing part of the chip.

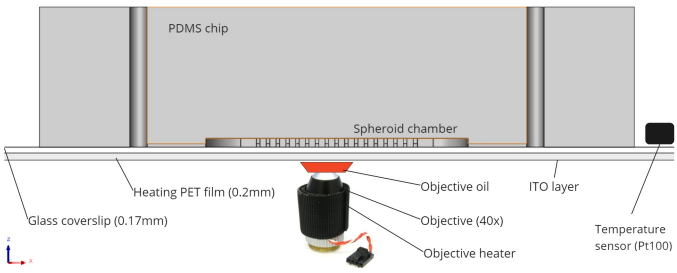

Fig. 7: Heating scheme. The imaging was intended to be done through the film or by cutting windows in the film and imaging only through the slide or coverslip of the chip. The trials showed that only the window approach is applicable to optical microscopy.

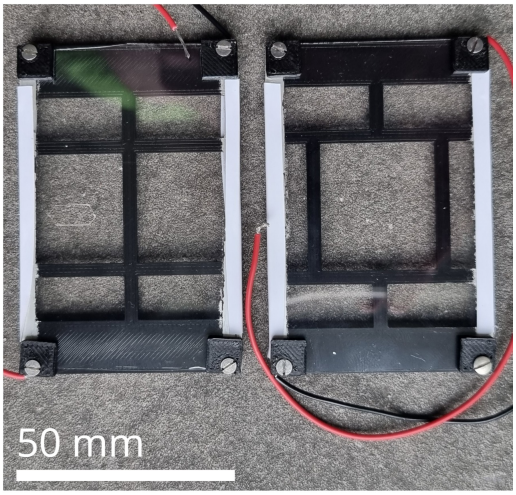

Fig. 8: The left heater is designed to be used with one or two PDMS chips on a coverslip. The heater on the right supports a single PDMS chip on a slide or a single slide-size Polymer chip. Switching heaters takes approximately five minutes. The size of each heater is 75x50 mm^2.

when wet objectives with very limited (usually under 0.5 mm) working distance are used. If a wet objective is used, it needs to be heated with an objective heater (widely commercially available) to ensure no heat loss from the cell chamber through the oil and the lens. Connecting to the film via the long sides ensures a 2.25 times lower overall resistance and thus higher power output (when heated by applying a constant direct voltage). The resistance of the film is calculated with the sheet resistance equation:

$$R = \rho * \frac{L}{W} \quad (1)$$

, where L is the length of the coated film and W is the width, ρ is the resistivity of the material. The measured heater resistance (including contact wires) was in the range between 250 and 280 Ω. That allows for a maximum output of around 2.2 - 2.5 W with a voltage of 24 V. The alternative type of heater considered was 75x50x0.7 mm^3 ITO-coated glass with silver busbars on the short sides (SPI-Supplies, USA). This heater was tested for optical transparency on par with the PET heater. Its thickness (0.7 mm) limits the range of compatible objectives and the highest attainable magnification. Also, soldering to the silver busbars does not provide a reliable vibration-resistant connection which complicates the use and transportation. Thus the PET heater was chosen as the main option.

H. Temperature sensing and control

Pt100 thin film RTD sensor is used to measure the temperature in the desired spot either on the surface of the heater or on the surface of the chip, slide, or coverslip (thin-film, NB-PTCO-058, Class T). The sensor can be either pressed to the surface with a magnetic chip holder or with its own magnet. The second scenario requires another magnet in a 3D-printed case to be present at the bottom surface of the heater. Pt100 was calibrated in an ice bath at 0 °C to account for the

wire resistance (0.4 Ω). The sensor is read with a MAX31865 amplifier and the corresponding Arduino library. The data from the sensor was recorded by connecting the platform to a laptop via USB and recording the log file with PuTTY software. The data points were recorded at approximately 400ms intervals. The temperature control is a simple on/off scheme using the DFR0457 power controller operated by Arduino code. The controller turns on when the temperature reported by the sensor is below the setpoint. The setpoint depends on the configuration of the heater (with or without windows), used chip and sensor location (on the slide, coverslip or on the heater itself). The chips were heated in a two to three-step process with a gradual increase of the setpoint, which allowed to avoid overheating as compared to heating with just one setpoint. Setups were tested using a K-type thermocouple inserted into the central chip chamber and read via NI 9211 input module, connected to the cDAQ-9171 USB chassis. the results were recorded with DAQ Express software (all National Instruments, USA). The data was aggregated in MS Excel and visualised with the Plotly Python library.

I. Spheroid and T-cell preparation. Chip filling.

The cells used are murine colon adenocarcinoma (MC38) cells expressing Green fluorescent protein (GFP). The cells are cultured into spheroids using the ultra-low attachment plates technology. This process takes about 7 days in the incubator, and the resulting spheroids average 100 μm in diameter. The spheroids then are mixed with the Matrigel hydrogel prepared according to the manufacturer's instructions. Afterwards, the spheroids mixed with the hydrogel are immediately pipetted into the central chamber of the chip (for PDMS chips) or deposited into the wells of the Ibidi Polymer Chips which are then sealed with a top coverslip. The filled chips are placed in the incubator at 37 °C, the hydrogel will polymerise in under an hour. To prevent drying out of the chip, the side channels (or the top channel for polymer chips) are filled with cell growth medium, also the droplets are placed on the inlets and outlets. Afterwards, the cytotoxic T-cells (specifically designed to target MC38 cells) expressing red fluorescent protein (RFP) are brought from the immunology lab and mixed with the cell growth medium and Interleukin-2 (IL-2) which is required to activate the CTLs. The mixture is pipetted into one of the side channels of the chip (or the top channel for polymer chips). The chip is placed in the incubator overnight to give time for the T-cells to migrate to the location of spheroids.

III. Results

A. Thermal control evaluation

The temperature of Pt100 (controlled with on-off protocol) was in a narrow range for all tested chip types. The average value after equilibrium had ±0.01 °C difference with the set value, the standard deviation did not exceed 0.05 °C and the maximum difference between the highest and lowest values was under 0.25 °C. Evaluation of thermal control with a K-type thermocouple inserted into the chip's chamber is presented in figures 9 and 10. Thermocouple values showed more variation than Pt100 data (standard deviations of 0.17 - 0.29 °C). However, the standard deviations after the equilibrium did fit the ±0.5 °C for all chip and heater (window or no window) types. The average chip temperature depends on the setpoint which can be adjusted in the software. The window heater (when the area directly under the chamber is not heated) performed even better than the heater without a window (standard deviation of 0.19 °C compared to 0.29 °C for uniform heater). The chips with higher thermal capacity (PDMS on a slide and Ibidi Polymer chip) performed better than the coverslip chip (standard deviation of 0.17 °C for polymer and PDMS slide chip and 0.29 °C for the PDMS coverslip chip) because the thermal capacity of the chip acts as a buffer to the temperature fluctuations. The same explanation stands for the better performance of the window heater because in this case the heat is not transferred directly to the cell chamber but through an additional volume. The thermal control trials were performed without flow in the chip (but with medium present and refreshed between each run). The reason is that when a thermocouple is inserted in the chip the flow path is no longer leak-free and flowing liquids becomes impossible. The perfusion system for the live cell experiment was intended to be used with intermittent flow (as pre-cultured spheroids can use the nutrients from the surrounding hydrogel without the need for constant replacement). Intermittent flow is mostly a state of no flow (and only 10% of the time the flow is present) so conducting the trials without flow was considered an acceptable simplification.

B. Constant and intermittent perfusion modes

The perfusion trials involved testing the chips under two programmable perfusion modes: constant and intermittent. The iMicrofluidics platform supports the flow range from 1.5 to 68 μl/min. For intermittent flow any duration of flow and pause period can be set, the pump switches off during the pauses when the intermittent flow is enabled. Due to many possible conditions (flow type, flow rate, duration of the experiment, chip type, battery or socket power, first or second flow controller, vacuum depth, etc.), only the flow rate of 10 μl/min was extensively tested. The measured flow rates are as reported by flow controllers and were not measured with an independent device. The correctness of the values reported by flow controllers was roughly checked by measuring the volume of liquid that went through the flow path over a time period. The average flow achieved for intermittent flow (during the flow interval) is 9.56 ± 1.67 μl/min for the PDMS chip. The plot is in figure 11. The average flow rate achieved for constant flow (PDMS chip) is 9.99 ± 0.68 μl/min. For the Ibidi Polymer chip, the numbers were similar: 9.97 ± 0.28 μl/min. Very short (under 1 second) spikes to approximately 50 μl/min are a common occurrence after the first hour of operation. Their frequency varies depending on the unknown conditions but usually averages around one spike an hour. Influences like a bubble or congestion in the flow path, variations in the pressure, vibration of the platform, transportation and others may induce spikes. The plot of the flow rate is presented in figure 12.

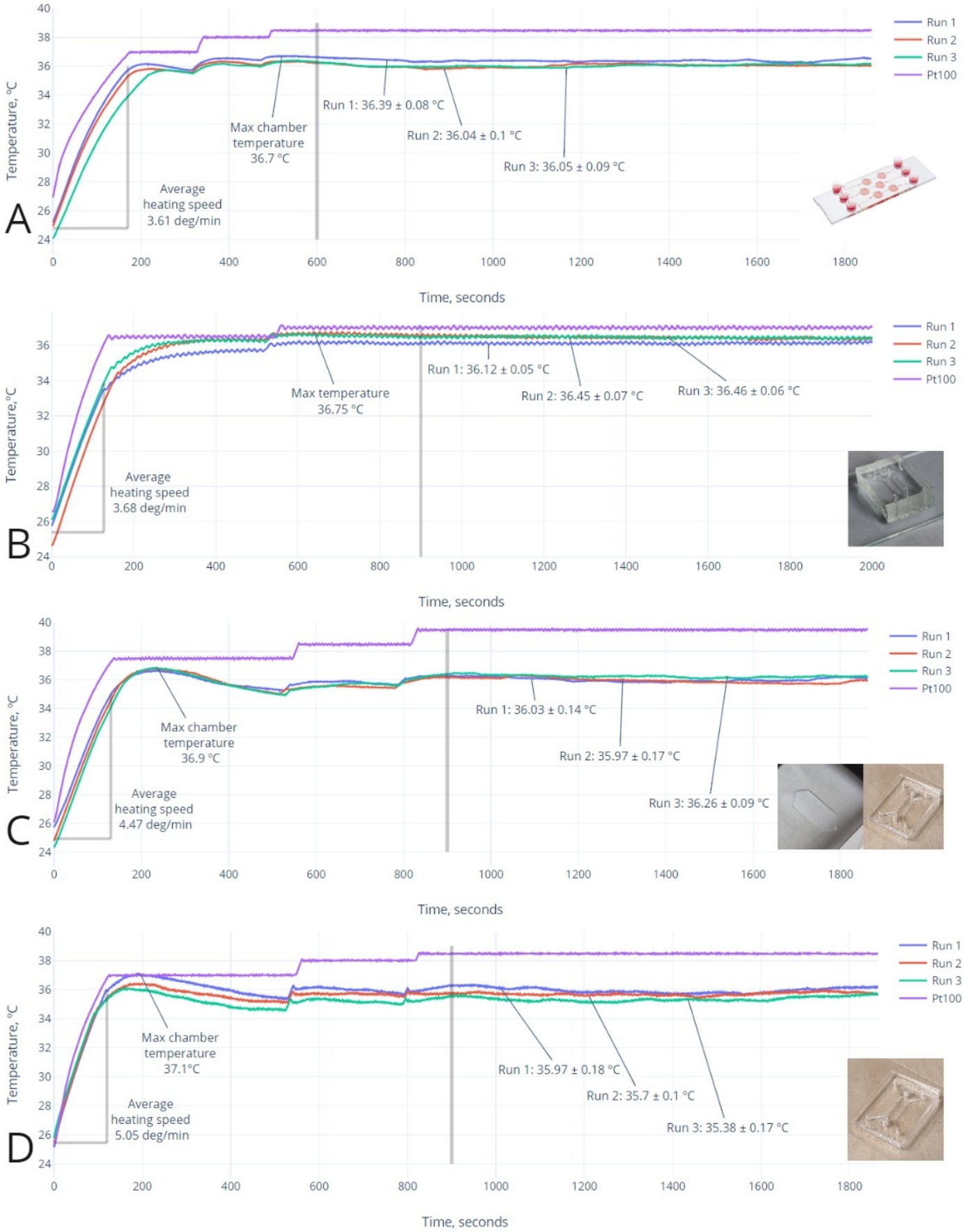

Fig. 9: A-D show 3 heating runs, heating speed calculation and set temperature (measured by Pt100 sensor, purple line) for four experiments. A - Ibidi Polymer chip (40 μl well). B - PDMS chip on a slide. C - PDMS chip on a coverslip, heated with a window heater. D - PDMS chip on a coverslip, heated with a heater without a window. The vertical line at 600 seconds for A and at 900 for B-D represents the approximate thermal equilibrium, it's shifted to 900 for B-D because slower heating protocols were used. Temperature values after the equilibrium line were used to calculate the average temperatures and standard deviations presented in the figure.

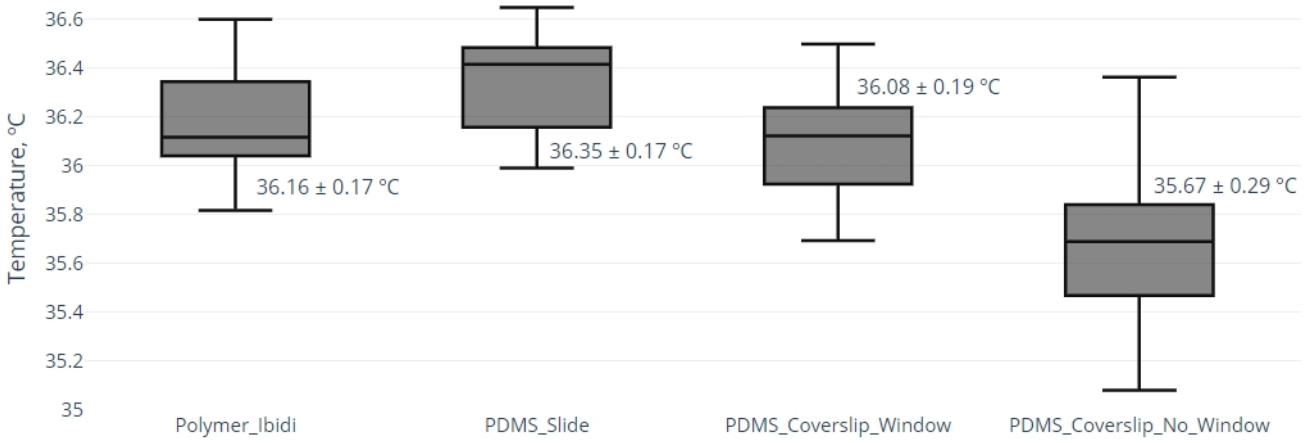

Fig. 10: The comparison of average (three runs for each box plot) temperature control performance after equilibrium for the same four experiments as in figure 9. The temperature settings for all four conditions can be increased and the overheating will still be avoided.

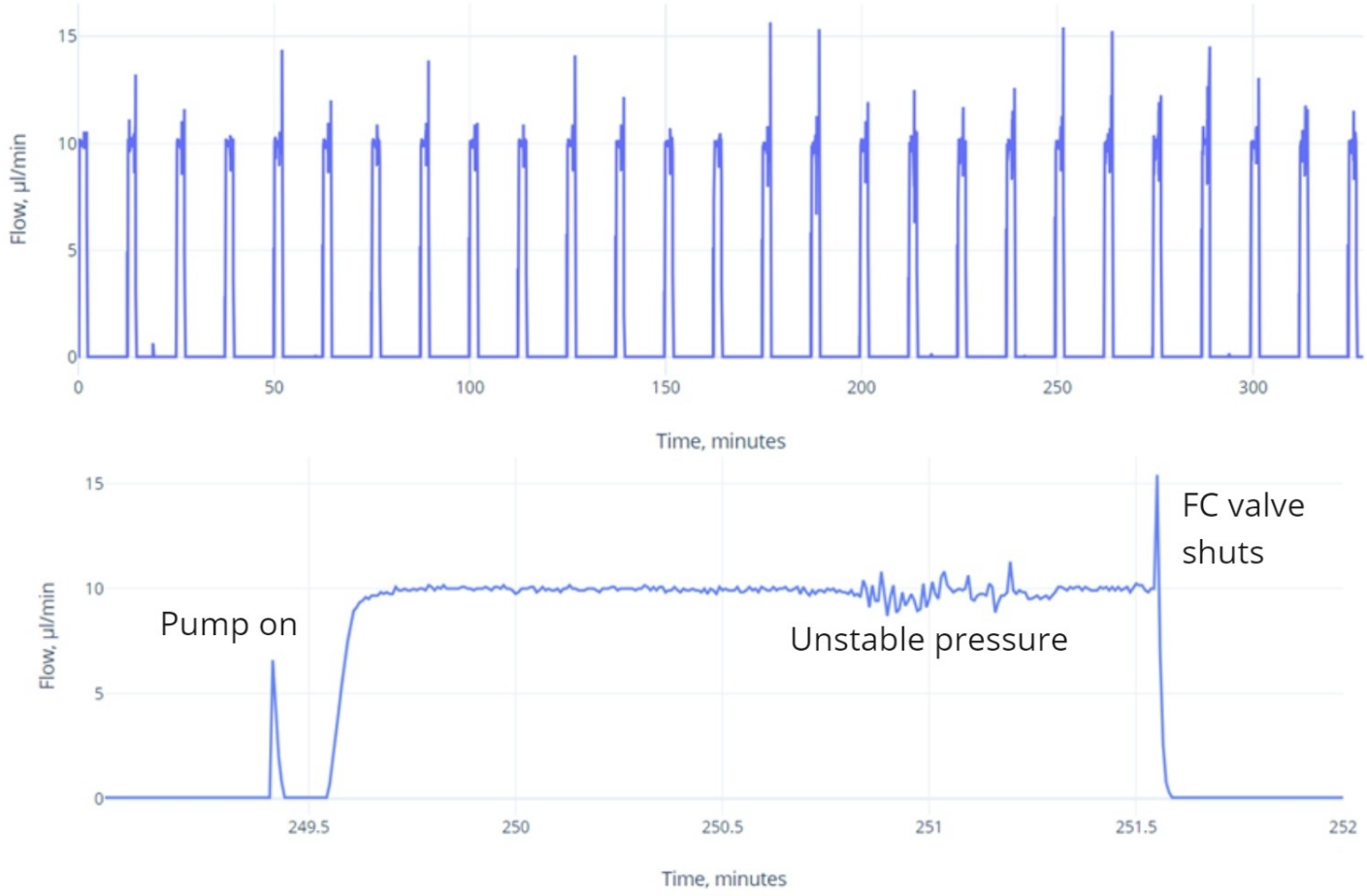

Fig. 11: Top: Flow rate in Intermittent mode on a 6-hour run. Bottom: an individual segment of the intermittent flow. In this case a spike up to 15 μl/min developed which is a common event during the rapid closing of the flow controller valve. The other disturbances on the graph are due to changes in the rotation frequency of the pump. These imperfections of the flow do not present any danger to the cells and were not deeply investigated.

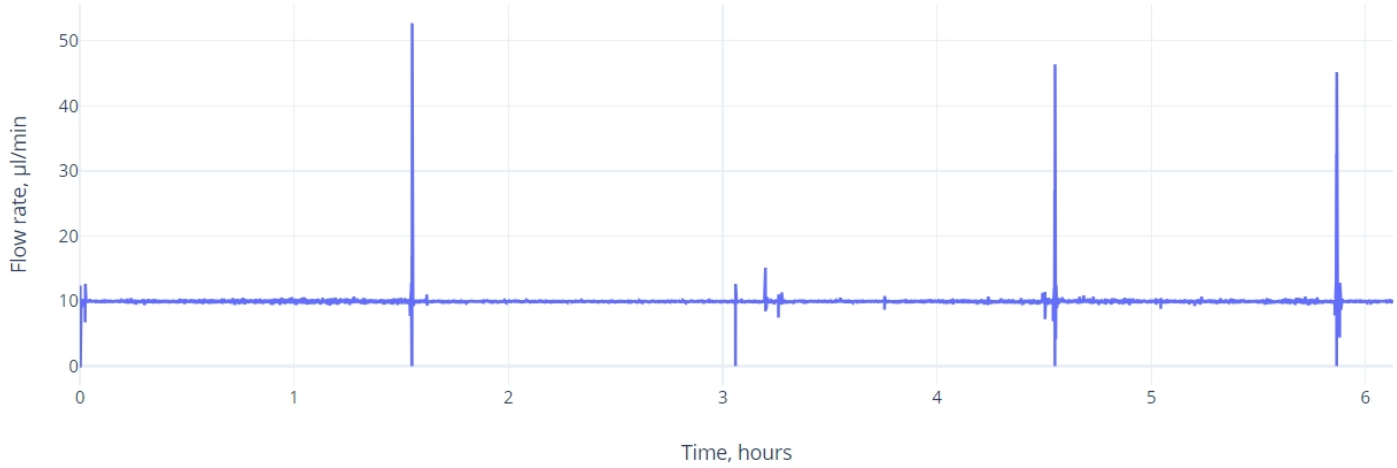

Fig. 12: Constant flow rate plot for a six-hour experiment. Significant spikes are more common for constant flow than for intermittent flow as the system runs continuously and thus more opportunities for flow controller errors occur and the chances of various disturbances like bubbles getting in the tubes are higher.

C. Heat distribution models

To evaluate the performance under constant flow as compared with no flow conditions for PDMS chips, simulations in COMSOL Multiphysics were conducted. The results are presented in Figures 13 and 14. The 5 μl/min flow was chosen because even when applied to a single channel, it's enough to refresh all the volume of the central chamber once every minute. If temperature distribution is a concern then the flow should be minimal, provided that the medium is delivered at room temperature. The temperature gradients described in figure 14 allow to draw the following conclusions:

1) In the absence of flow the temperature gradient with a perfectly uniformly heated bottom heater is almost zero.
2) Reversed (in opposite directions) flow allows great improvement (from 1.6 to 0.7 degrees) in the temperature distribution compared to flowing in one channel.
3) The gradient with the 10 μl/min flow in a single channel exceeded the requirement of 1 degree. However, if the intermittent flow is used (flow for one minute, pause for 10), then the distribution will be significantly closer to zero (as in no flow condition) than to 1.6 degrees and will satisfy the requirements. Where the chips, equipment and experiment conditions allow it, the reversed flow should be used. An alternative solution is preheating the medium. Even if the medium is at 30 °C in the inlet, the temperature gradient in this scenario is reduced from 1.6 to 0.75 °C. Delivering the medium at 36 °C almost eliminates the gradient.

As shown by the temperature control trials, polymer chips have a higher thermal capacity and are less prone to temperature fluctuations. Also, for Ibidi Polymer chips, the spheroids tended to reside on the bottom of the wells and the flow was almost a millimetre above. Consequently, the spheroids may not be as impacted by the gradient created by the flow.

D. Portability and battery life evaluation

The platform endured over fifty 10-minute to one-hour transportations by public transport, bicycle and by foot while being carried in a plastic box. Not a single significant malfunction or major durability issue was detected afterwards. Vibrations caused by transportation did however significantly alter the flow rate, usually increasing it up to 3-fold from the set value. The exact flow rate values during transportation are not available due to the lack of a logging module on the platform. The battery performance exceeded the 30-minute requirement. Flow controllers were delivering reliable performance for the first hour of battery operation, followed by an hour and 20 minutes performance with several flow spikes, after 2 hours and 20 minutes the performance of flow controllers became completely unstable. The temperature control maintained the setting for 7 hours.

E. Heater optical transmission tests

Both ITO glass and ITO PET film showed lower transmittance compared to 1mm glass. It may impact the quality of transmission imaging. Still, widefield and confocal fluorescence imaging will be especially affected as the light has to pass through both layers twice (once as excitation light from the bottom laser to the sample and once as emitted light from the sample to the detector).

F. Microscope compatibility

The 3D-printed microscope module did fit the stage of the Zeiss Elyra PS1 microscope, the stage was fully able to move in X, Y and Z directions to full extent with tubes and wires connected. With an exception being when Ibidi Polymer Perfusion Chips were installed on the heater, as their fluidic connectors were extending too high and interfering with the condenser. The use of different connector types would solve this complication. The not-perfect flatness of the supports of the microscope module allowed the module to slightly rock on the stage; the supports' design should be improved to restrict

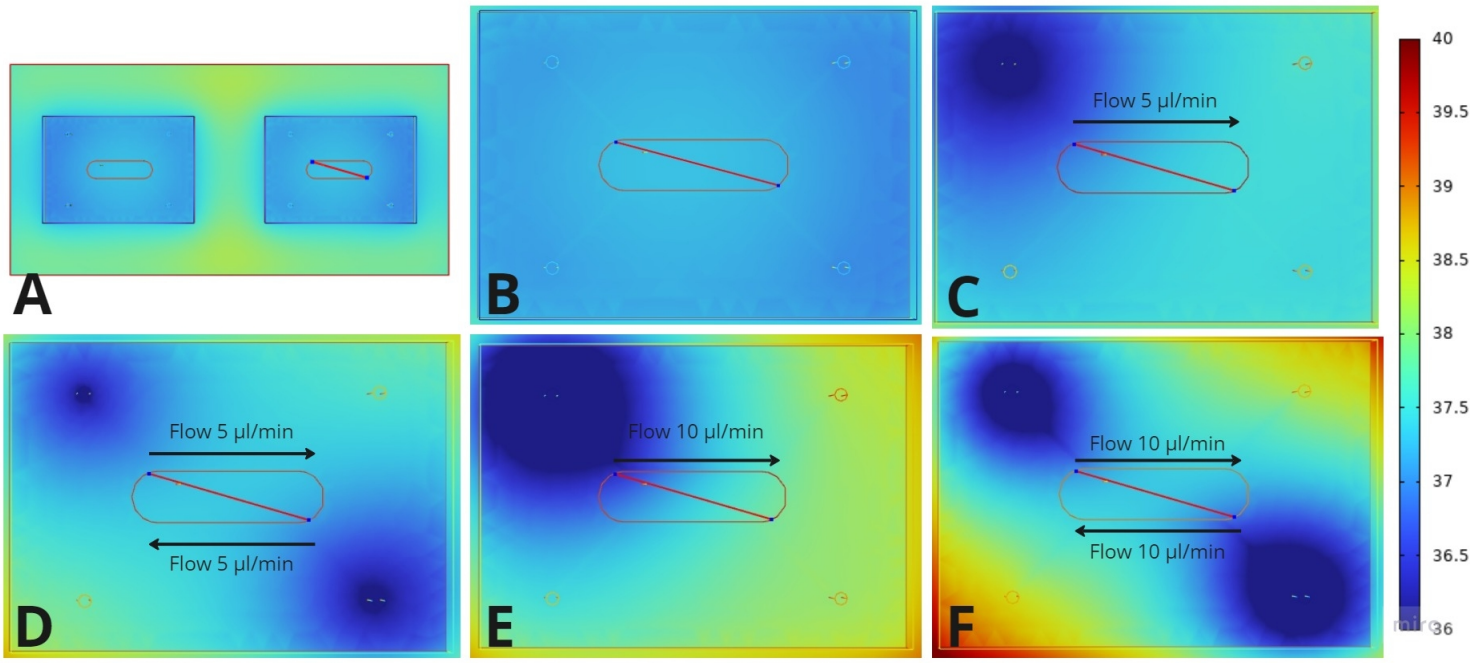

Fig. 13: The used model of the two PDMS chips on a coverslip is depicted in (A), the left chip was always without flow. The red line shows the line of measurements that were used for plotting graphs depicted in figure 14. For all scenarios, the temperature in the centre of the central chamber was maintained at 37.25 °C to simulate the worst possible scenario (heating to higher temperatures slightly increases the gradient). (B) shows temperature distribution without flow. (C) with 5 μl/min flow in a single channel. (D) same but in both channels in opposite directions. (E) 10 μl/min flow in a single channel. (F) both channels in opposite directions.

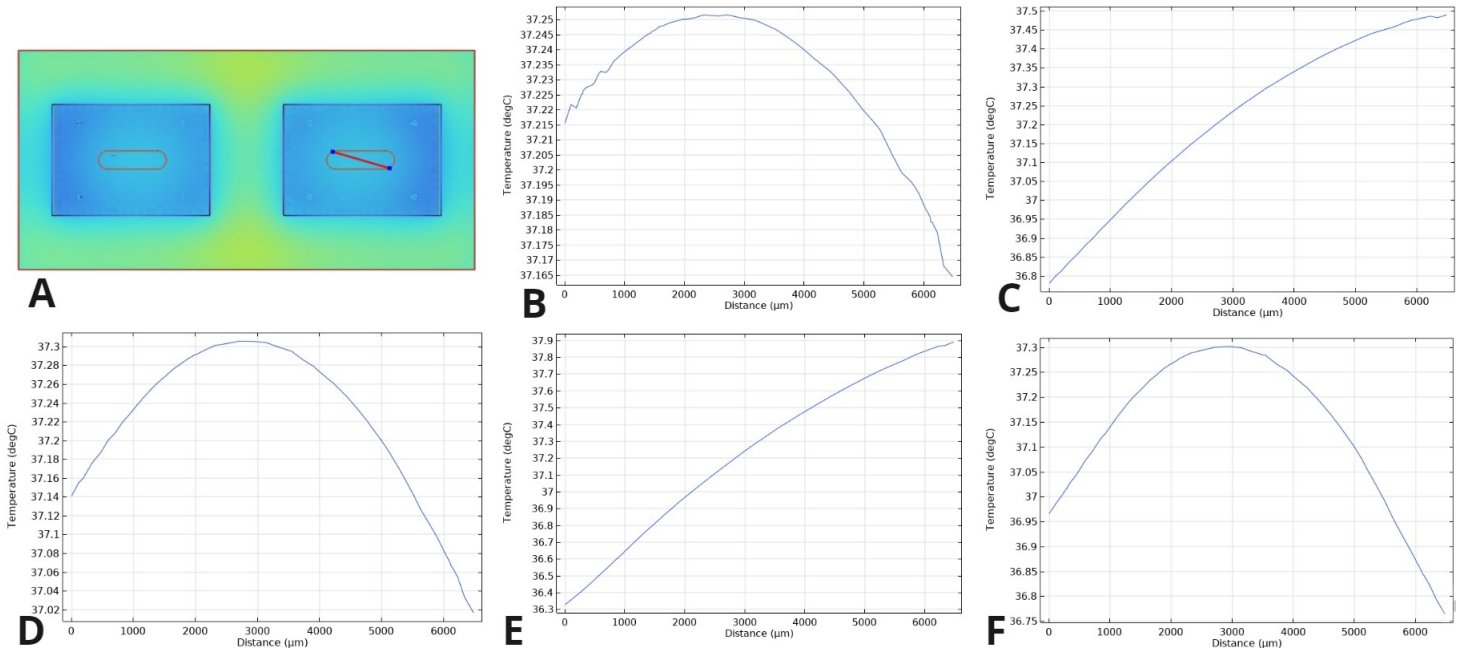

Fig. 14: (A) shows the used model, same as in figure 13. B-F are the same scenarios as in 13. The following maximal temperature gradients were obtained (with 37.25 °C maintained in the middle): 0.05 for no flow, 0.7 °C for 5 μl/min single channel, 0.3 °C for 5 μl/min reversed both channels, 1.6 °C for 10 μl/min single channel, 0.55 for 10 μl/min reversed both channels.

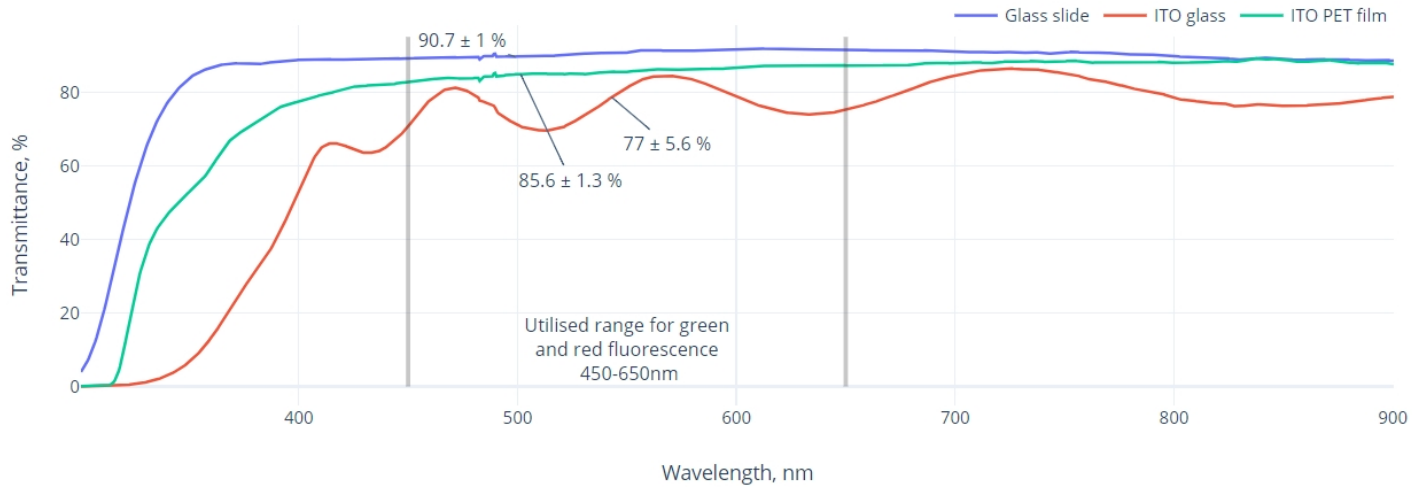

Fig. 15: Transmittance in the visible spectrum for three materials types. The thickness of ITO coatings was not specified by the manufacturers. ITO PET film has a sheet resistance of 350-500Ω and ITO glass 8-12Ω, so the layer of ITO on the glass is several times thicker.

that movement. It did not significantly influence the imaging quality. Attaching the heater to the microscope stage with bolts is a solution to that.

G. *Effect of heating on T-cell behaviour*

The increase in CTL activity of speed of spheroid destruction was not quantified in this study. However, it was observed that the RFP signal from CTLs is increased when the chip is heated 19. Also, the movement of CTLs was quicker. It may be however due to convection flow created in the chamber so further investigation and quantification of this aspect is required. A key moment captured during the imaging trials was an invasion of a T-cell into the spheroid captured via a 20-minute confocal time series with 30-second intervals 20.

IV. Discussion

A. *Flow controllers and pump performance issues*

The platform did comply with the experiment requirements by supplying the chips with the required flow rates with acceptable accuracy (up to 1.67 μl/min flow rate standard deviation in case of intermittent flow). However, those results don't allow for predicting whether the platform will be able to perform with the same accuracy with long durations (24 hours and above). The continuous running of flow controllers and pump in constant flow mode sometimes leads to one of the flow controllers displaying incorrect flow rates that do not correspond to the setting (i.e. 22-25 μl/min with a set value of 10). Turning the perfusion off, zeroing the malfunctioning controller according to the supplier's manual and restarting the program resolves the problem. If such an event occurs when the platform is not supervised, it can dry the chip out. Short (occurring during under 1 second) flow spikes (to 50-80μl/min) risk also cannot be entirely excluded. They may develop when a bubble gets into the flow path and increases the resistance. The attempt of the flow controller to mitigate the congestion leads to the resolution of the blockage, a rapid drop of resistance and a subsequent spike in the flow rate. A successful attempt to reduce this risk was made by adding a vacuum leak in the waste chamber and reducing the vacuum to -0.2 bar. Used "pull" (with negative pressure in the waste reservoir) type of perfusion may cause issues when combined with hydrogel-filled chips. Chunks of hydrogel (i.e. which ended up in the side channels of the PDMS chip when the central chamber was filled) may cause blockages in the flow and lead to spikes in the same way as described above.

B. *Chip perfusion limitations*

It was required to perfuse both channels of the PDMS chip at certain stages of the experiment. It also improves the thermal distribution if done in opposite directions. There are two approaches to that

1) Connecting one flow controller to each channel.
2) Splitting the flow path controlled by a single flow controller in two by using a Y-connector.

Both of those approaches don't work with the used setup. (1) leads to an interaction of the flow controllers and unexpected performance in terms of flow rates in the channels. (2) leads to the flow entirely picking the path of the lowest resistance (even when attempts are made to equalize the resistance as much as possible).

The volume of the PDMS chip chamber is approximately 5 μl, thus even flow rates of 5 μl/min and below may be considered applicable. However, the flow controller's lower limit of operation is also 5 μl/min which doesn't allow to guarantee a reliable performance for this flow rate.

C. *Chip considerations*

PDMS chips allow for more flexibility in the experiments which has a trade-off for ease of use. The flexibility stems from two channels, one of which can be filled with T-cells or a drug and sealed and the other one used for perfusing medium. The major downside of the coverslip chips is extreme fragility and in an experiment where many manipulations with the chip are required, they're likely to fracture. It happened on

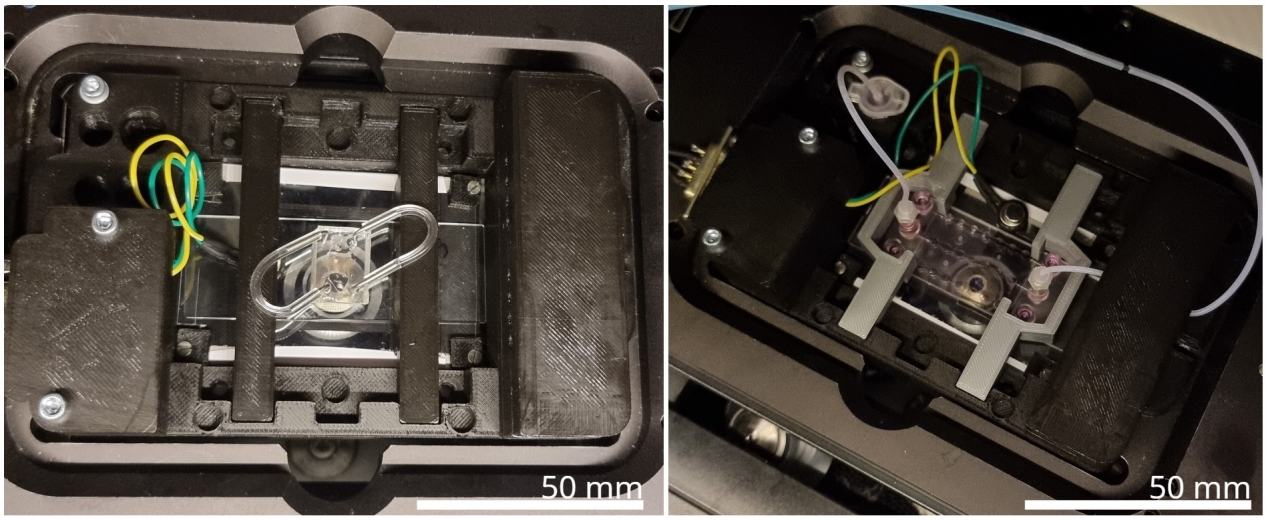

Fig. 16: PDMS chip on a slide (left) and Ibidi Polymer Chip (right) mounted on the microscope module on the Zeiss Elyra PS1 stage during an imaging session.

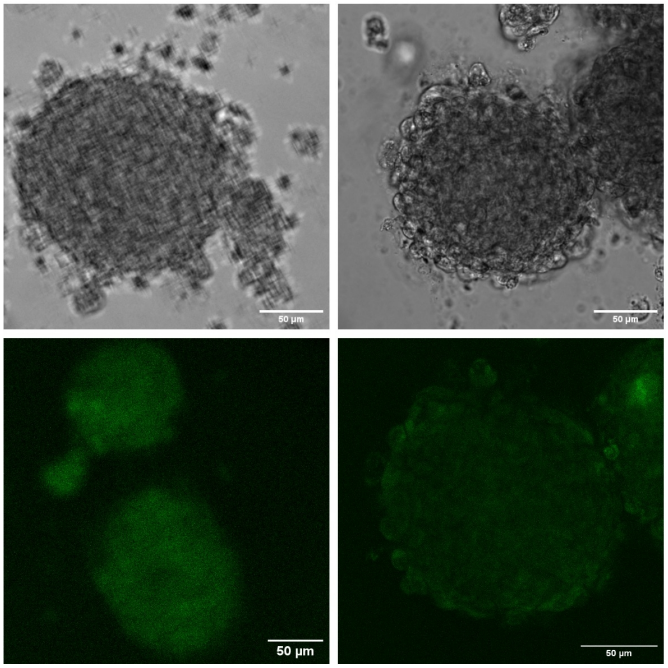

Fig. 17: Comparison of transmission (top) and fluorescent confocal (bottom) spheroid images with 20x objective. The left images are taken through a PET heater, right images are taken through a window in the heater. Ibidi Polymer chip. The scale bar is 50 μm for all images.

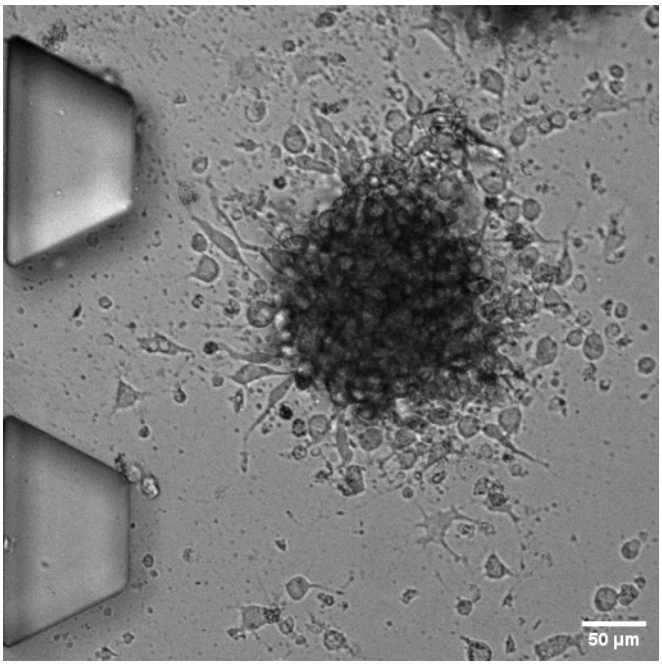

Fig. 18: Transmission image of a spheroid being attacked by T-cells inside the central chamber of PDMS chip on a slide. Pillars separating the channel from the chamber are on the left. Window heater. 20x objective.

several occasions during metal coupler insertion or spheroid deposition into the chip. The low volume of the chamber makes the chips prone to drying out. The bubbles easily infiltrate into the hydrogel chamber, affecting the outcome or making the chip unusable. The chamber has a flat profile (250 microns in the Z direction) and thus the bubble usually captures a large area of the chamber. Due to manual manufacturing chips sometimes had defective inlets, differing PDMS thickness and, at times, thicker central chamber diameters which complicated the sealing of the central chamber for reliable perfusion. Commercial polymer chips with multiple wells feature a more convenient and precise spheroid injection method. The hydrogel and spheroid solution are delivered into the wells before sealing the top coverslip. If the bubbles are formed in the process, they usually can be chased out of the chambers by delivering medium into the channel after the chip is sealed. For polymer chips establishing a leak-free connection was easier. The polymer does not allow gas diffusion (compared to PDMS) so these chips did not dry out as easily. The bubbles formed in the heating process tended to float to the top and not hinder the imaging or flow. The

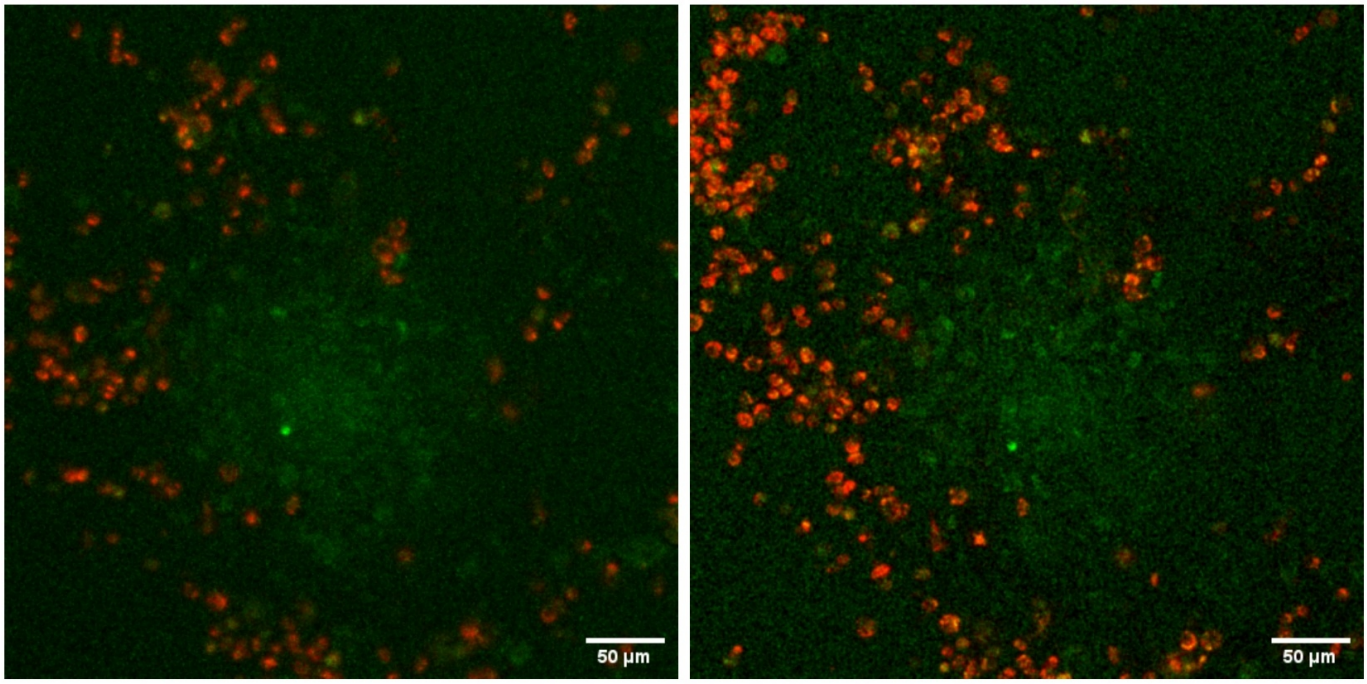

Fig. 19: A spheroid (green) surrounded by CTLs (red). Both images: PDMS chip on a glass slide. Left: under room temperature. Right: with temperature control enabled. Under temperature control, a brighter fluorescent signal from CTLs was observed as well as increased mobility.

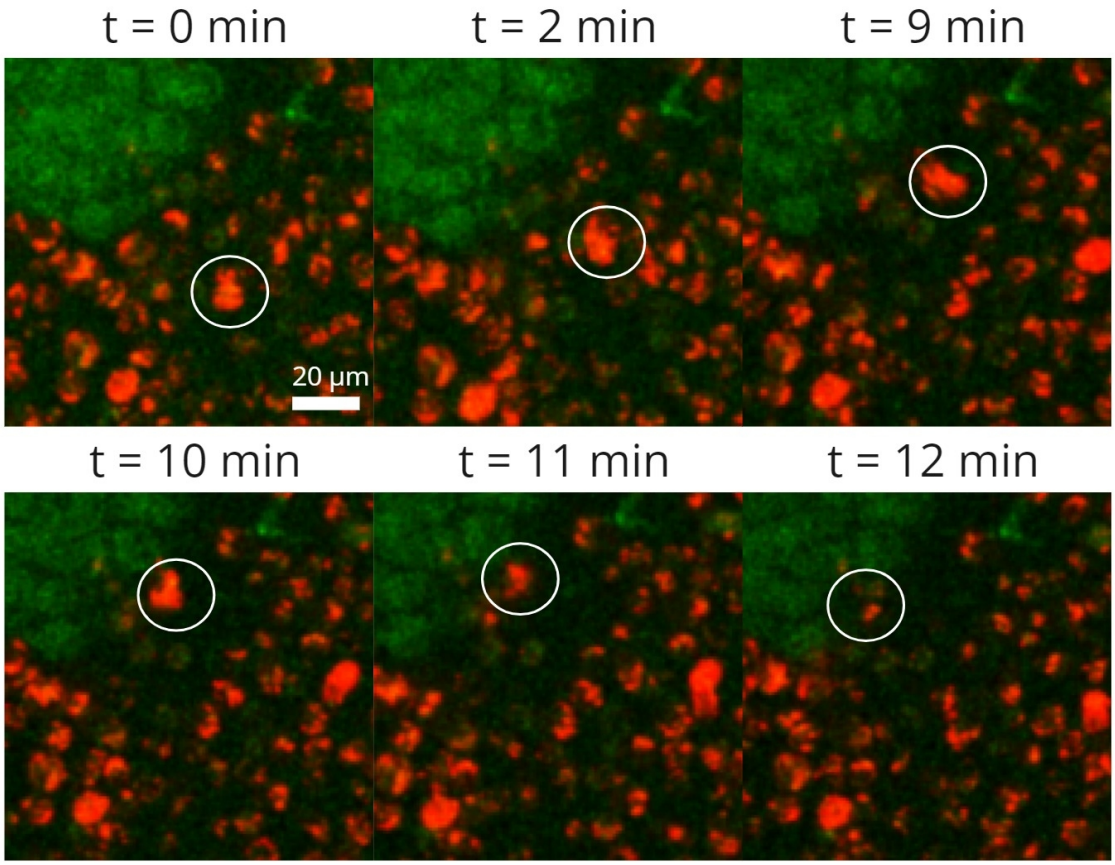

Fig. 20: Time series images of a CTL (red) invading a spheroid (green). Ibidi Polymer Chip (4.5 μl well). Temperature control.

polymer chips were not prone to breaking and the multiple well configurations paired with thin bottom coverslip allowed to acquire more quality images per chip compared to PDMS chips.

D. Limitations of temperature control

The main limitation of the utilised temperature control system is that the temperature is measured outside of the location of the cells. Although it's technically possible non-invasively to measure the temperature in the chamber (via an infrared probe), the accuracy will be very low ($\pm$ 1-2 degrees, depending on the sensor) [1]. IR temperature sensors are also significantly more expensive than Pt100 and their placement poses an additional design challenge. The ideal solution for this limitation would be a temperature sensor (or even a sensor along with a heater) embedded right into the chamber of the chip (by the chip manufacturer). The main parameter showing the adequacy of temperature control is the well-being of cells and the current temperature control solution showed it's capable of being configured to perform with the tested chips and seemingly (the effect was not quantified) improve the activity of CTLs. It's suggested to conduct a re-evaluation of the temperature control setpoints via an external thermocouple when a new chip type or sensor position is used.

E. Applicability of bottom heating to high magnification microscopy

Imaging through a double layer was deemed not compatible with inverted microscopy, both for transmission and fluorescence imaging. The extremely low cost of ITO PET film (under 1 euro for each heater) allows for cutting windows of the required size for each required scenario, especially if the chip has a single chamber. Windows greatly improve the imaging quality without compromising on heating quality as shown in heating trials. However, most of the wet objectives due to their geometrical properties (flatness and large area of the casing surrounding the front lens) require a larger window to be comfortably used. Imaging with wet objectives when temperature control is concerned is always done with an objective heater that will maintain the temperature in all the chip areas contacting with oil, thus a long-term wet objective imaging scenario is viable. The use of multi-chamber chips with a window heater is limited because the area of the chambers is a significant portion of the total chip area and requires further investigation.

F. Bubble issues

Bubbles did emerge in all the chip types when the heating was on. The most likely reason is the release of dissolved gases from the medium. Short-term imaging (under 30 minutes) was not impacted for any chip type. Longer protocols, especially with low-volume flat chambers (like PDMS chips) are likely to cause extensive bubble formation. Possible solutions include:

- Degassing the medium or making sure it contains as little dissolved gas as the experiment conditions allow.
- Using very slow heating protocols with gradual temperature increase.
- Heating the chip more evenly from multiple sides.
- Heating the medium reservoir. This approach will also improve the temperature distribution in the chamber.

The solutions and the process of bubble formation weren't thoroughly investigated and require further attention.

V. Conclusion

The portable microfluidic chip perfusion and heating system for high-magnification optical microscopy was designed, assembled and tested. This work improved all three foundations of the TU Delft iMicrofluidics platform (portability, adaptability and functionality) by employing a novel two-module approach and a unique transparent PET ITO-coated heater. The gains in portability stem from an updated independent power supply system running from a single high-capacity Li-ion battery. Functionality increased by adding a microscope module for inverted optical microscopy with a stage heater without compromising portability. The adaptability was proven by testing the platform with four microfluidic chip models and two perfusion modes. The required and obtained specifications of the platform with the microscope module are presented in the table I.

Images were successfully obtained with 10x and 20x dry objectives under flow and heating conditions for Ibidi Polymer chips (both for large well and small well models) and for PDMS chips on a slide.

The main constraints for using the platform for 24-hour and longer experiments are bubbles created in the process of heating and the long-term instability of the perfusion system (flow rate spikes are developed after several hours of operation). Addressing these issues is recommended in future work. The formation of bubbles can be potentially reduced by preheating the medium with an additional heater installed next to the reservoir slots. The improved heating unit design may allow for oil objective usage. Compatibility of the system with luminescence imaging also requires an additional trial.

Specification	Required	Obtained
Chip compatibility	PDMS on a coverslip	PDMS, coverslip +
		PDMS, slide +
		Polymer, slide-size, Ibidi +
Chip number	2	Coverslip-size 2
		Slide-size 1
Cell chamber temperature Polymer chip	36.5 $\pm$ 0.5 °C	36.16 $\pm$ 0.17 °C*
Cell chamber temperature PDMS chip	36.5 $\pm$ 0.5 °C	36.35 $\pm$ 0.17 °C* (slide)
		35.67 $\pm$ 0.29 °C* (coverslip)
		36.08 $\pm$ 0.19 °C* (coverslip, window heater)
Maximum temperature difference inside the chamber at 37 °C, PDMS chip	1 °C	Model, 0 flow: 0.05C
		Model, single channel 5 μl/min flow: 0.7 °C
		Model, reversed 5μl/min flow: 0.3 °C
		Model, single channel 10μl/min flow: 1.6 °C
		Model, reversed 10μl/min flow: 0.6 °C
Heating speed to 37 °C	-	3.6-5 deg/min
Flow rate	10 μl/min, spikes under 20 μl/min	Constant 9.99 $\pm$ 0.68 μl/min**
		Intermittent 9.56 $\pm$ 1.67 μl/min
IL-2 medium storage	2ml	1.5ml
	Minimum wastage	20 μl dead volume
Microscope	Zeiss Elyra PS1 fit	Size (128x85 mm) +
		Weight (200 grams) +
Optical transparency	-	100% (window heater)
		85.6% (PET heater)
		77% (Glass heater)
Magnification	10x, 20x, 40x (oil), 63x (oil)	10x + (window)
		20x + (window)
		40x not tested
		63x only without heater***
Imaging modes	Transmission	+
	Fluorescent	+
	Confocal	+
	Time series	+
	Luminescent	not tested
Battery life with heating	30 minutes	60+ minutes (12 W max power consumption)
Portability	Carry while ON****	+ (7kgs with box and spare parts)
	Bicycle while ON****	+
Bubbles in the chamber	No bubbles	Bubbles form when heated for 30 minutes
Leakage	Leak-free	+

TABLE I: Required and obtained specifications of the heating system. * - Heating setpoints can be adjusted to fit the specifications better. ** 50 μl/min spikes do occur with constant flow once every hour after the first hour of operation. *** - A special heater design has to be developed to work with oil objectives. **** - Flow controllers tend to increase the flow due to vibration. Transportation when ON is not recommended if precise flow without spikes is required.

REFERENCES

[1] Theo Aspert and Gilles Charvin. Heatchips: A versatile, low-cost and microscopy-compatible heating system for microfluidic devices. 11 2022.

[2] Ibidi. mu-Slide III 3D Perfusion, 2023.

[3] Ibidi. mu-Slide Spheroid Perfusion chip, 2023.

[4] Shang Menglin, Ren Soon, C.T. Lim, Bee Luan Khoo, and Jongyoon Han. Microfluidic modelling of the tumor microenvironment for anti-cancer drug development. 09 2018.

[5] Tudor Petreus, Elaine Cadogan, Gareth Hughes, Aaron Smith, Venkatesh Pilla Reddy, Alan Lau, Mark OâConnor, Susan Critchlow, Marianne Ashford, and Lenka OâConnor. Tumour-on-chip microfluidic platform for assessment of drug pharmacokinetics and treatment response. Communications Biology, 4:1001, 08 2021.

[6] Gustave Ronteix, Shreyansh Jain, Christelle Angely, Marine Cazaux, Roxana Khazen, Philippe Bousso, and Charles Baroud. High resolution microfluidic assay and probabilistic modeling reveal cooperation between t cells in tumor killing. Nature Communications, 13, 06 2022.

[7] Haoyu Zhu, Gurhan Ozkayar, Joost Lotters, M. Tichem, and Murali Ghatkesar. Portable and integrated microfluidic flow control system using off-the-shelf components towards organs-on-chip applications. 10 2022.

4

Conclusion

To conclude, the portable microfluidic chip perfusion and heating system for high-magnification optical microscopy was designed, assembled and tested. All the parts were 3D printed on an FDM printer from PLA. Compatibility (for simultaneous perfusion, heating and imaging) with all four tested chip types was achieved. The standard deviation of the temperature in the chamber was between 0.17 and 0.29 °C (without perfusion) depending on the chip type (when heated to 37 °C). The modelled central chamber temperature distribution for PDMS on a coverslip chip greatly depends on the flow rate and in the worst case (constant flow in a single channel at 10 μl/min flow rate) the gradient reaches 1.6 °C. The potential operating range of temperatures for the employed PET ITO-coated heater is between 20 and 45 °C covering the whole physiological range for human cells. The heater is only compatible with imaging when it has a window under the cell chamber. Otherwise, when imaged through the PET layer, the quality of microscope images deteriorates. This design lowered the heating speed by 11% (from 5.05 to 4.47 °C/min for a chip on a coverslip) but improved the standard deviation of measured temperature in the chamber from 0.29 to 0.19 °C when heated to 37 °C. The platform supports two flow types: constant and intermittent with 0.68 and 1.68 μl/min standard deviation of flow rate from the required set value (10 μl/min) consequently. The platform supports flow rates from 1.5 to 68 μl/min in two independent channels. The recommended range to ensure reliable performance and even temperature distribution is from 5 to 20 μl/min and should be picked for each individual case (chip type, flow type, single or double channel connection).

The microscope module hosts up to two chips on a coverslip, secured by magnetic holders, up to two 1.5 μl medium reservoirs and a single changeable heating unit. The module's weight (approximately 200 g) and size allow for compatibility with Zeiss Elyra PS1 microscope in transmission and fluorescent imaging modes with objectives up to 20x, as well as with other microscopes with the same or similar stage size. To achieve compatibility with oil objectives (40x and above), a redesign of the heating unit is required because the PLA frame of the heating unit restricts the approach of an oil objective to the surface of the film.

The battery life of the setup with enabled heating and constant double-channel perfusion is 60 minutes. The calculated maximum power consumption of the setup is 12 W, of which heating consumes 2.5 W, flow controllers 2.5 W each and the pump consumes 2 W. The platform can be carried during operation or transported over a long distance in a box (the weight including the box and spare parts is under 7 kg).

The major hindrance to long-term imaging using this setup is the appearance of bubbles in the cell chambers during heating.

4.1. Recommendations

The following can be done to improve temperature control performance:

1. Laser cutting the heaters and the windows a precise match to the chip's geometry.
2. Preheating the medium can mitigate both bubble formation and uneven temperature distribution. Installing a 2-watt resistive heater and a temperature sensor around the Eppendorf tube reservoir can be considered. The used D-Sub connector has enough pins to accommodate these two new devices.
3. Implementing a PID temperature control can help further reduce the temperature variations in the cell chambers.

Further improving the platform performance:

1. Adding an SD-card logging module to the platform to record temperature and flow rates without a USB connection to a computer.
2. The platform's inner electronics compartment lacks space for the integration of new components. The electronics layer either needs redesigning by removing the central window or all the components need to be integrated on a custom PCB.
3. Adding an input on the platform to be able to configure the flow settings would eliminate the need for software adjustments by the user.
4. A convenient way to control pressure in the waste chamber may prove a better solution than the current vacuum leak. The optimum pressure (in terms of flow spikes and overall evenness of flow) may lie between the current -0.2 bar and the maximum -0.6 bar.

5

Reflection

5.1. Slow start

I started out with the project without knowing almost anything about microscopy, FDM 3D printing, COMSOL models, temperature control, Arduinos and IDE, electronic components, microfluidic chips, etc. So in the initial months, the project wasn't moving forward too fast. Looking back, I'm impressed I was eventually able to deliver some results based just on common sense and willingness to learn. Of course, thanks to all the people who greatly helped me on the way (see 5.4). This initial lack of hard skills did however sometimes lead to imperfect design decisions.

5.2. Failure of the initial design approach

I was too much in love with the initial ITO glass idea and paying too much attention to the specifications of "some" objectives instead of closely looking at the installed ones. Also, I didn't invest in building an understanding of how modern microscopy works, although acquiring images was the end goal. It took a very long time for the ITO glass to arrive and in a few days, it became clear that it won't work. Luckily, the PET ITO heater was a way better option. Establishing contact with the optical imaging team would greatly help here and save me from that mistake. It's a pity they got involved only at a later stage.

5.3. Building up on Haoyu's platform

My initial experience with working with the platform designed by another student wasn't positive. Not much worked and I didn't understand why. It took around a month to figure out how this whole system operates on a level where I could start making some improvements. However, I did admire how much work Haoyu put into that and it motivated me to keep up. After I figured out the basics, it went much better. Removing several components from the platform allowed me to speed up the trials and eventually get some results. Although it still wasn't enough to understand some of the processes (f.e. the development of flow spikes) and parts of the code. The convenient structure of Haoyu's code (with separate tasks for each component) allowed me to easily integrate the new components.

5.4. Acknowledgements

I'd like to thank:

- Murali Ghakesar for gentle and firm supervision and for trusting in me to conclude this project on time.
- Laura Mezzanotte for optimism and enthusiasm and a lot of help and initiative in the final push for the great images.
- Massimo Mastrangeli for all the kind support and introduction to the OoC team.
- Zhilin Wang for support and lots of help with various matters.
- Giorgia Zambito for all the fruitless tries we had at the microscope, just to find out that nothing works. And not losing optimism in the process.
- Erasmus MC OIC team (Johan Slotman, Gert van Cappelen and Gert-Jan Kremers) for fruitful hours spent together at the microscope, lots of feedback and a crash course in optical microscopy.
- My wife Anastasia for supporting me throughout the way and then kindly going on a vacation without me so that I could occupy the kitchen table for a month for 24/7 microfluidics experiments.
- Haoyu Zhu for giving birth to the platform and helping with my questions about it.
- COMSOL support team for rapidly providing me with a 6.1 trial ”because I need to graduate” although they ”never do that”.

5.5. Conclusion

To conclude, I’m happy I took this project as I was able to learn a lot (significantly more than during my first MSc year), acquire valuable hard skills and move science a tiny bit further.

5.6. Timeline

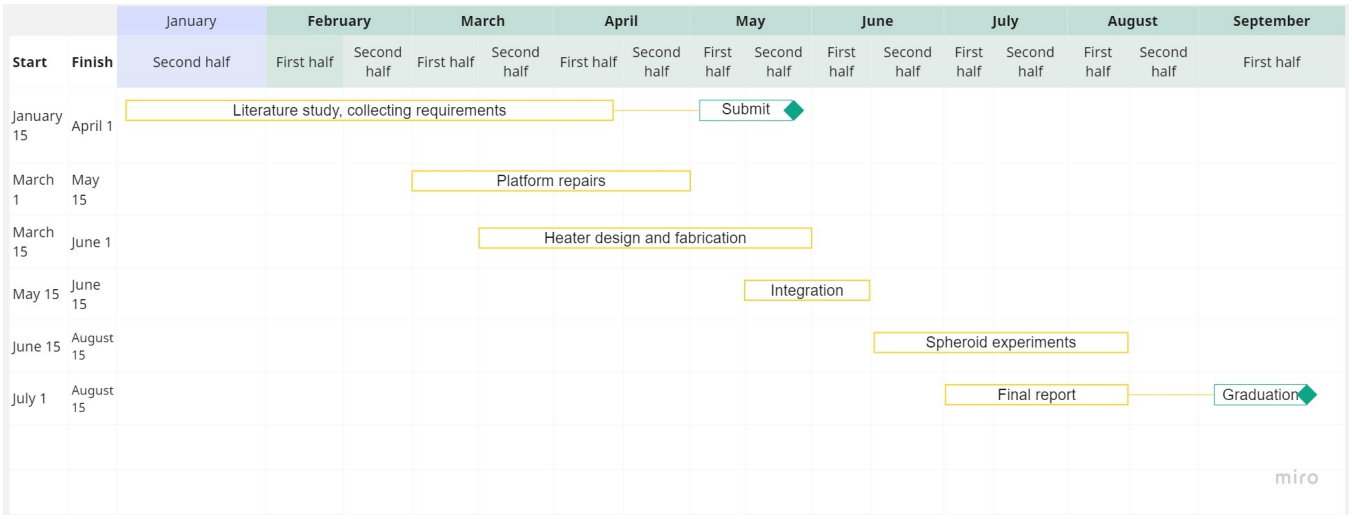

Figure 5.1: Gantt chart of the project

References

[1] Centraal Bureau voor de Statistiek. *Causes of death in the Netherlands*. 2021. URL: https://www.statista.com/statistics/520529/netherlands-causes-of-death.

[2] Pouya Safarzadeh Kozani et al. “Recent Advances in Solid Tumor CAR-T Cell Therapy: Driving Tumor Cells From Hero to Zero?” In: *Frontiers in Immunology* 13 (2022). DOI: 10.3389/fimmu.2022.795164. URL: https://www.frontiersin.org/articles/10.3389/fimmu.2022.795164.

[3] Shang Menglin et al. “Microfluidic modelling of the tumor microenvironment for anti-cancer drug development”. In: (Sept. 2018).

[4] Nanoluc. *NanoLuc Luciferase*. 2023. URL: https://nld.promega.com/resources/technologies/nanoluc-luciferase-enzyme/.

[5] Linfeng Xu et al. “Vacuum-driven power-free microfluidics utilizing the gas solubility or permeability of polydimethylsiloxane (PDMS)”. In: *Lab Chip* 15 (20 2015), pp. 3962–3979. DOI: 10.1039/C5LC00716J. URL: http://dx.doi.org/10.1039/C5LC00716J.

[6] Gustave Ronteix et al. “A Multiscale Immuno-Oncology on-Chip System (MIOCS) establishes that collective T cell behaviors govern tumor regression”. In: *bioRxiv* (2021). DOI: 10.1101/2021.03.23.435334. eprint: https://www.biorxiv.org/content/early/2021/03/23/2021.03.23.435334.full.pdf. URL: https://www.biorxiv.org/content/early/2021/03/23/2021.03.23.435334.

[7] Franziska Hirschhaeuser et al. “Multicellular tumor spheroids: An underestimated tool is catching up again”. In: *Journal of Biotechnology* 148.1 (2010). Organotypic Tissue Culture for Substance Testing, pp. 3–15. DOI: https://doi.org/10.1016/j.jbiotec.2010.01.012. URL: https://www.sciencedirect.com/science/article/pii/S0168165610000398.

[8] Dario Barbone et al. “Mammalian Target of Rapamycin Contributes to the Acquired Apoptotic Resistance of Human Mesothelioma Multicellular Spheroids*”. In: *Journal of Biological Chemistry* 283.19 (2008), pp. 13021–13030. DOI: https://doi.org/10.1074/jbc.M709698200. URL: https://www.sciencedirect.com/science/article/pii/S0021925820597548.

[9] Kleomenis Dardousis et al. “Identification of Differentially Expressed Genes Involved in the Formation of Multicellular Tumor Spheroids by HT-29 Colon Carcinoma Cells”. In: *Molecular Therapy* 15.1 (2007), pp. 94–102. DOI: https://doi.org/10.1038/sj.mt.6300003. URL: https://www.sciencedirect.com/science/article/pii/S1525001616312552.

[10] John W. Haycock. “3D Cell Culture: A Review of Current Approaches and Techniques”. In: *3D Cell Culture: Methods and Protocols*. Ed. by John W. Haycock.

Totowa, NJ: Humana Press, 2011, pp. 1–15. DOI: 10.1007/978-1-60761-984-0_1. URL: https://doi.org/10.1007/978-1-60761-984-0_1.

[11] Xinran Xiang et al. “The Development and Characterization of a Human Mesothelioma In Vitro 3D Model to Investigate Immunotoxin Therapy”. In: *PloS one* 6 (Jan. 2011), e14640. DOI: 10.1371/journal.pone.0014640.

[12] Yi-Chung Tung et al. “High-throughput 3D spheroid culture and drug testing using a 384 hanging drop array.” In: *The Analyst* 136 3 (2011), pp. 473–8.

[13] Guocheng Fang et al. “Gradient-sized control of tumor spheroids on a single chip”. In: *Lab on a Chip* 19 (Nov. 2019). DOI: 10.1039/C9LC00872A.

[14] Xian Xu et al. “Three-Dimensional In Vitro Tumor Models for Cancer Research and Drug Evaluation”. In: *Biotechnology Advances* 32 (Nov. 2014). DOI: 10.1016/j.biotechadv.2014.07.009.

[15] Khashayar Moshksayan et al. “Spheroids-on-a-chip: Recent advances and design considerations in microfluidic platforms for spheroid formation and culture”. In: *Sensors and Actuators B: Chemical* 263 (2018), pp. 151–176. DOI: https://doi.org/10.1016/j.snb.2018.01.223. URL: https://www.sciencedirect.com/science/article/pii/S092540051830248X.

[16] Sébastien Sart et al. “Multiscale cytometry and regulation of 3D cell cultures on a chip”. In: *Nature Communications* 8 (2017).

[17] Gustave Ronteix et al. “High resolution microfluidic assay and probabilistic modeling reveal cooperation between T cells in tumor killing”. In: *Nature Communications* 13 (June 2022). DOI: 10.1038/s41467-022-30575-2.

[18] Ebrahim Behroodi et al. “A combined 3D printing/CNC micro-milling method to fabricate a large-scale microfluidic device with the small size 3D architectures: an application for tumor spheroid production”. In: *Scientific Reports* 10 (Dec. 2020). DOI: 10.1038/s41598-020-79015-5.

[19] Tudor Petreus et al. “Tumour-on-chip microfluidic platform for assessment of drug pharmacokinetics and treatment response”. In: *Communications Biology* 4 (Aug. 2021), p. 1001. DOI: 10.1038/s42003-021-02526-y.

[20] Andrew Aijian et al. “Digital Microfluidics for Automated Hanging Drop Cell Spheroid Culture”. In: *Journal of laboratory automation* 20 (Dec. 2014). DOI: 10.1177/2211068214562002.

[21] Haoyu Zhu et al. “Portable and Integrated Microfluidic Flow Control System Using Off-the-shelf Components Towards Organs-on-chip Applications”. In: (Oct. 2022). DOI: 10.21203/rs.3.rs-2166950/v1.

[22] Théo Aspert et al. “HeatChips: A versatile, low-cost and microscopy-compatible heating system for microfluidic devices”. In: (Nov. 2022). DOI: 10.1101/2022.11.15.516605.

[23] Kimmo Keränen et al. “Infrared temperature sensor system for mobile devices”. In: *Sensors and Actuators A: Physical* 158.1 (2010), pp. 161–167. DOI: https:

//doi.org/10.1016/j.sna.2009.12.023. URL: https://www.sciencedirect.com/science/article/pii/S0924424709005494.

[24] Federico Cantoni et al. “A microfluidic chip carrier including temperature control and perfusion system for long-term cell imaging”. In: *HardwareX* 10 (2021), e00245. DOI: https://doi.org/10.1016/j.ohx.2021.e00245. URL: https://www.sciencedirect.com/science/article/pii/S2468067221000754.

[25] Gürhan Özkayar et al. “Toward a modular, integrated, miniaturized, and portable microfluidic flow control architecture for organs-on-chips applications”. In: *Biomicrofluidics* 16 (Mar. 2022), p. 021302. DOI: 10.1063/5.0074156.

[26] Ikram Khan et al. “A low-cost 3D printed microfluidic bioreactor and imaging chamber for live-organoid imaging”. In: *Biomicrofluidics* 15.2 (Mar. 2021), p. 024105. DOI: 10.1063/5.0041027.

[27] Salam Yousif et al. “Design and Preparation of Low Absorbing Antireflection Coatings Using Chemical Spray Pyrolysis”. In: *International Journal of Nanoelectronics and Materials* 11 (Oct. 2018).

[28] SPI Supplies. *ITO Coated Slides (Float Glass, Polished, 0.7 Ohms/sq, Busbar)*. 2023. URL: https://www.2spi.com/item/z06438/ito-coated-slides-float-glass-polished-07-busbar/.

[29] Bronkhorst. *mini CORI-FLOW™ ML120V21 manual*. 2023. URL: https://www.bronkhorst.com/int/products/liquid-flow/mini-cori-flow/ml120v21/.

A

Design

A.1. Changes in the original platform design

The platform was dissembled and several components were removed and added.

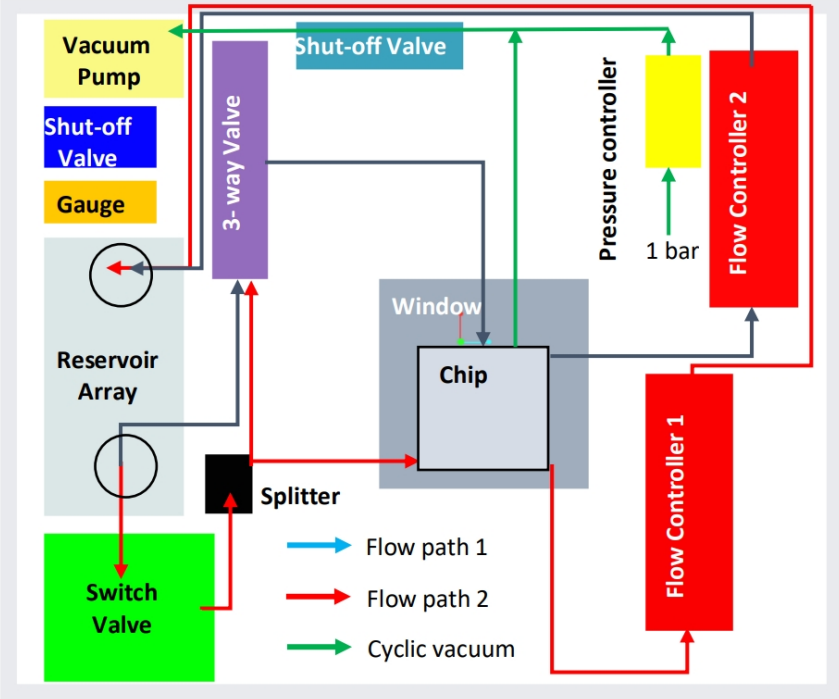

Figure A.1: Initial layout of the top layer of the platform. Source: thesis of Haoyu Zhu

A.1.1. Changes in the upper (fluidic) layer

The following components were removed from the platform (see Figure A.1):

1. Pressure controller and shut-off valve.
2. Switch valve, 3-way-valve and splitter.
3. Shut-off valve (between the vacuum pump and the waste reservoir).

(1) were removed because those components are only needed for lung-on-a-chip applications. There was also a suspected vacuum leak in the shut-off valve during the

initial inspection of the platform. (2) is not used in this experiment. It was decided to switch the delivery of mediums manually if needed to not overcomplicate the system. The project plan involves the delivery of small volumes of mediums from proximity to the chip positioned under the microscope, so it's undesirable to have long tubings from the reservoirs on the platform to the valve and then to the stage top heater. (3) The vacuum shut-off valve wasn't functioning correctly (jamming) when initially inspected so I decided to connect the pump to the waste reservoir directly to further simplify the system and improve reliability.

The following components were added to the top layer:

1. Stage top heater on a designated holder.
2. 16x2 LCD I2C display in a 3D-printed shell. Model courtesy: GrabCAD.
3. Foam pad for flow controller 1 and new foam pad for flow controller 2.

(2) is used to display the flow in µl/min in both flow controllers (as measured by the flow controllers themselves). Also, the temperature of the sensor positioned in the stage top heater is displayed here. (3) is used to reduce the cross-talk of the controllers as, according to Bronkhorst, the controllers cannot be placed near each other [29]. Haoyu mitigated that by placing the flow controller 2 (FC2) on a foam pad. My initial flow experiments showed that cross-talk is still significant (reported flow values had a variation of around 30 % from the set value). The problem was solved by replacing the old foam pad and putting flow controller 1 (FC1) on a foam pad as well. The pad consists of two 3D-printed PLA rectangles and electronics packaging foam of uniform thickness in between.

A.1.2. Changes in the bottom (electronics) layer

The core of the system (Arduino Mega 2560) allowed for significant expansion and thus several components were added to the electronics layer:

1. MAX31865 RTD to digital converter. It's an amplifier used to read the signal of a single Pt100 temperature sensor.
2. DFR0205 DC-DC Buck Converter. This module is used to power the Arduino from a rechargeable battery and not from a single-use 9V battery.
3. DFR0457 MOSFET Power Controller Module. It's used to power the heater from the 24V battery.
4. New 24V 4000mAh Lithium-ion battery. This battery allows connection to the 220V socket via the charger. It has an on/off switch which is used to power the platform on and off. Also, it has twice the capacity compared to the previously installed NiMH battery.
5. On/off switches for the vacuum pump and the heater. The switches are located in the right panel. They allow to run the platform without heating or to stop perfusion at any point without turning the platform off fully or changing the code.

It's important to note that on/off switches do not reset the program, they just put the power off from a single component. Due to that, turning the pump switch on when the program is running will result in significant spikes. To avoid that, the platform has to be turned off with a battery switch and then the pump switch can be turned on.

The only component removed was the 9V battery slot because it was no longer needed.

A.1.3. Redesigned or updated 3D-printed elements

The following components were changed or updated compared to the original design:

1. Four side panels.
2. Central microscopy window.
3. Pressure gauge holder.
4. Vacuum pump holder.
5. Most of the electronic modules were placed on 3D-printed bases.

(3) and (4) were easy to break during use so they were redesigned to be more durable.

(1) and (2) needed replacement because of the size of the new battery. Also, the original design couldn't fit some of the components (wire connectors didn't fully fit and the intended on/off switch didn't fit).

Also (2) wasn't wide enough to fit a microscope slide, so it was made 1mm wider. And it still seems not to be enough.

A.2. CAD drawings

A.2.1. Stage heater CAD drawings

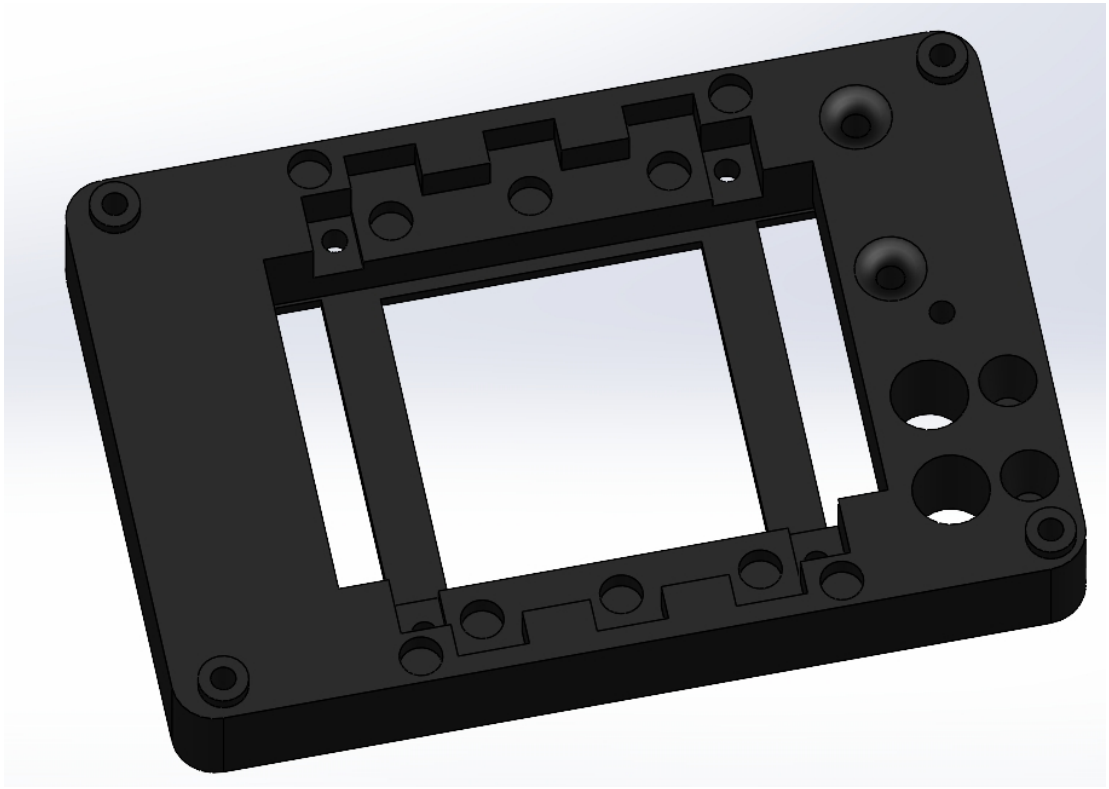

Figure A.2: Main part of microscope stage heater

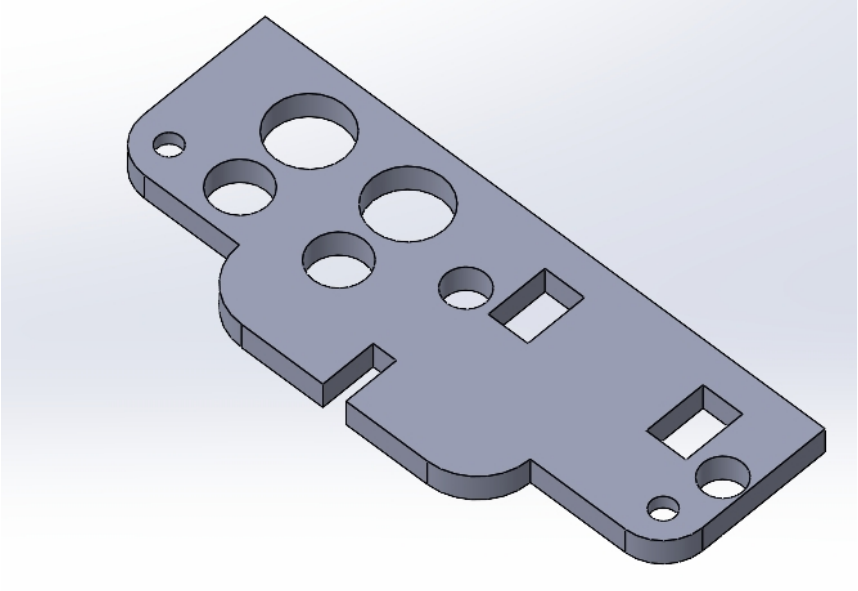

Figure A.3: Left microscope stage support part.

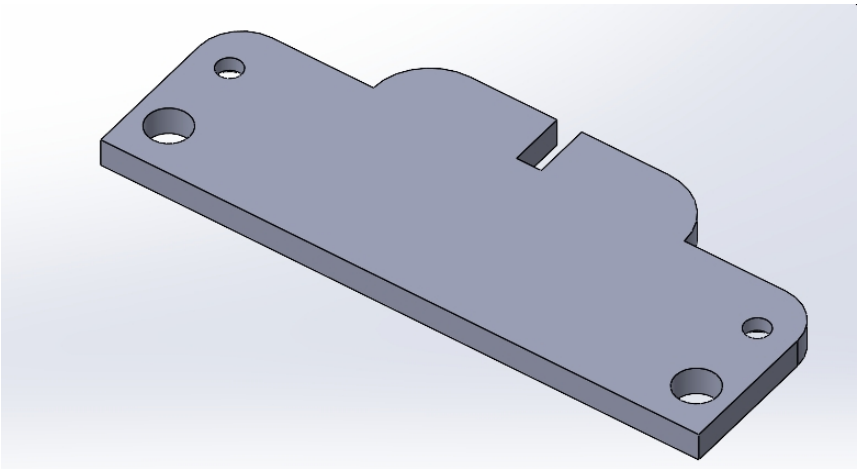

Figure A.4: Right microscope stage support part.

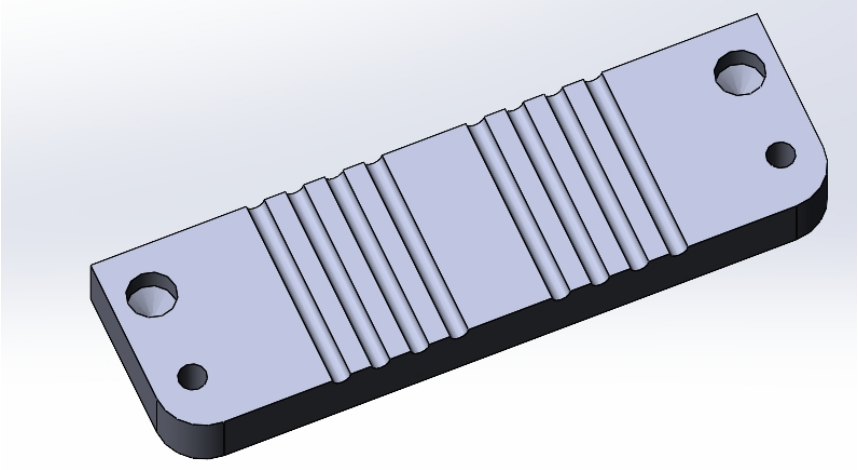

Figure A.5: Lower part of tubing holder.

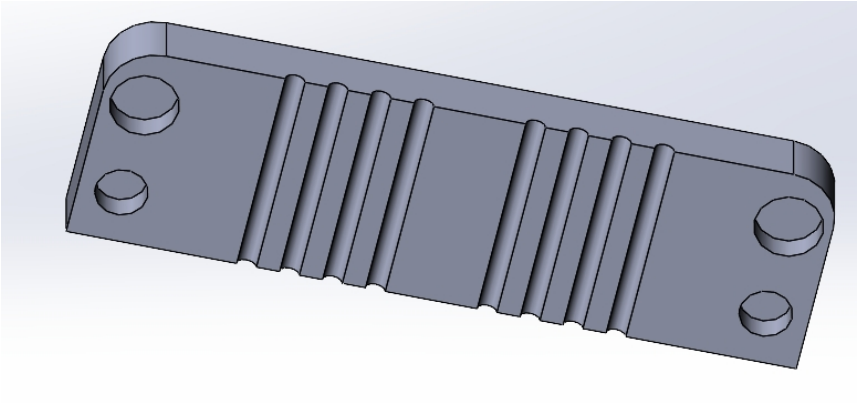

Figure A.6: Upper part of tubing holder.

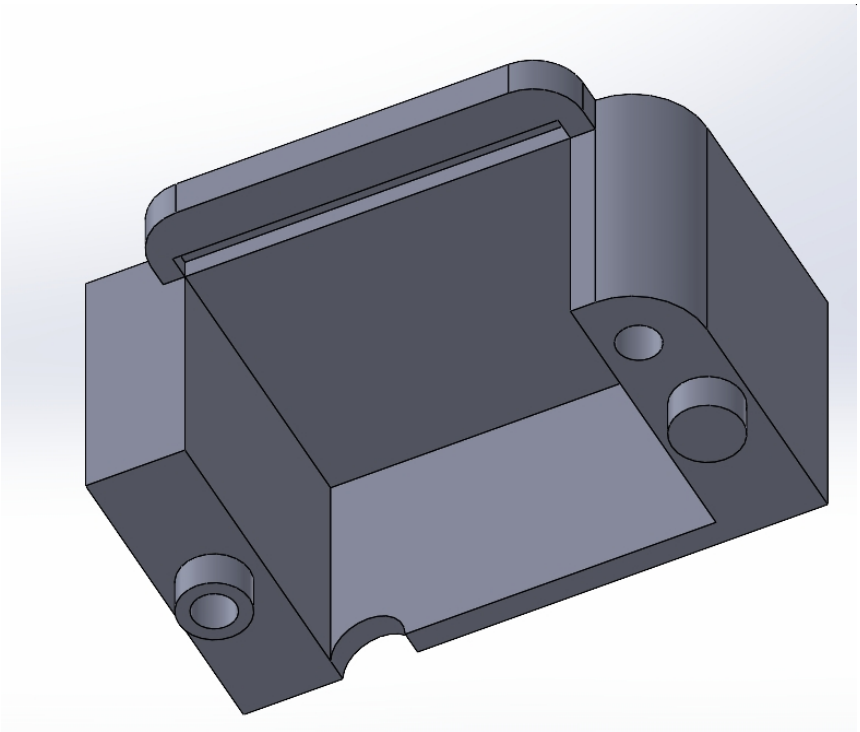

Figure A.7: Electrical housing part.

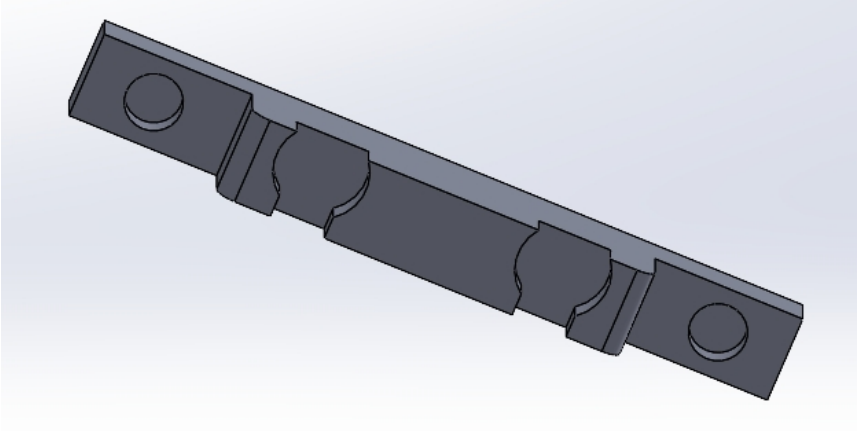

Figure A.8: PDMS chip on a coverslip holder with sensor holder slots.

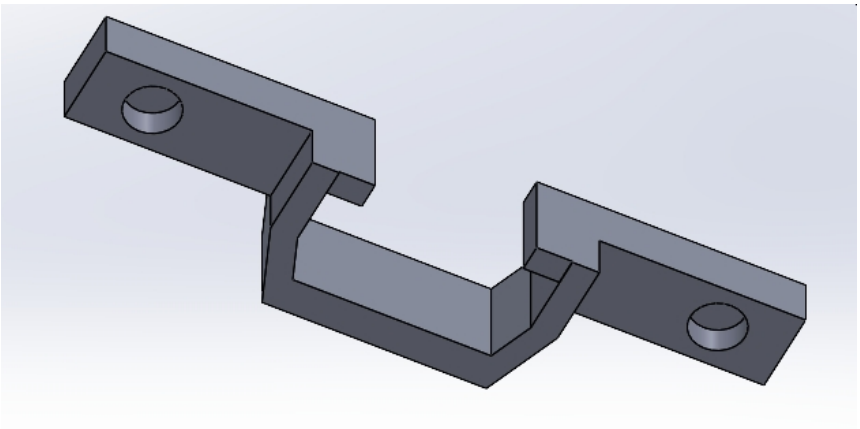

Figure A.9: Ibidi Polymer Chip holder.

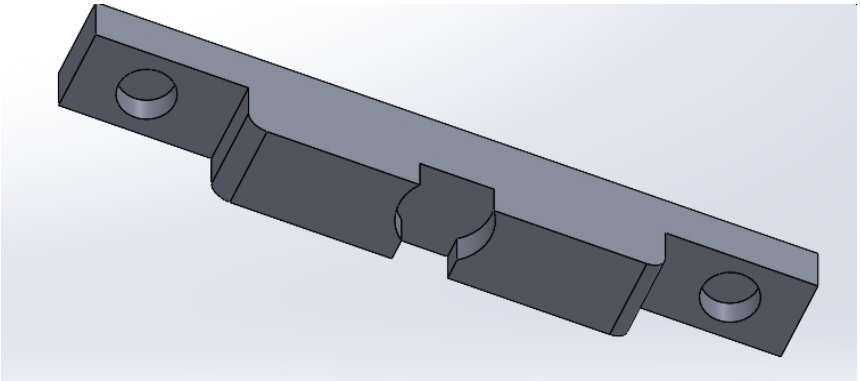

Figure A.10: PDMS chip on a slide holder with sensor holder slot.

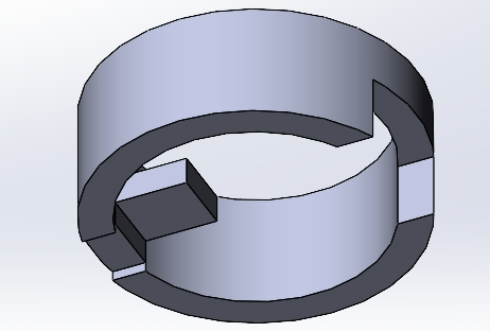

Figure A.11: Temperature sensor holder.

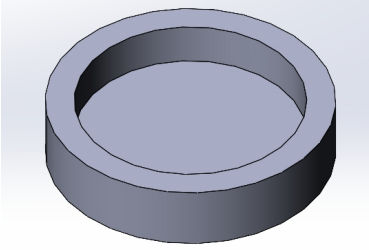

Figure A.12: Bottom magnet housing (to secure the sensor on the heater surface and not via insertion to one of the chip holders).

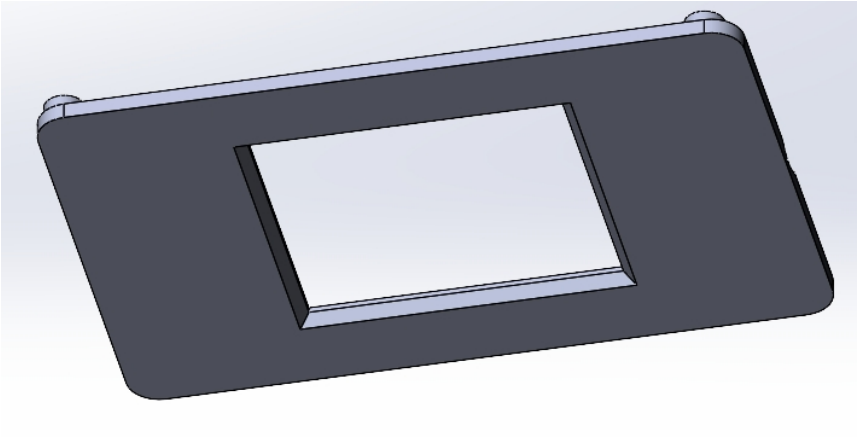

Figure A.13: Bottom lid of the stage heater (didn't fit the Elyra and thus wasn't used).

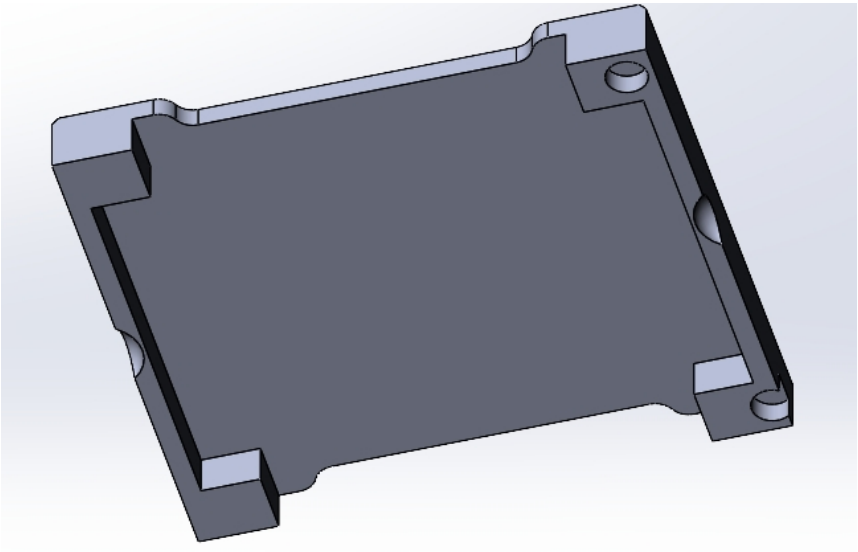

Figure A.14: Top lid of the stage heater. Used only for luminescence

A.2.2. Heater parts CAD drawings

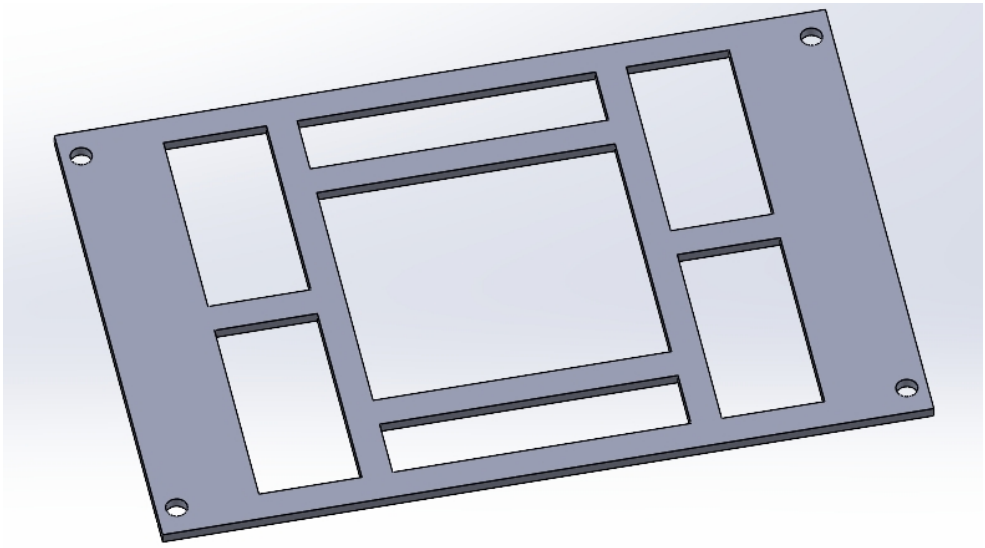

Figure A.15: PET heater frame for Ibidi Polymer chips and PDMS on slide chips.

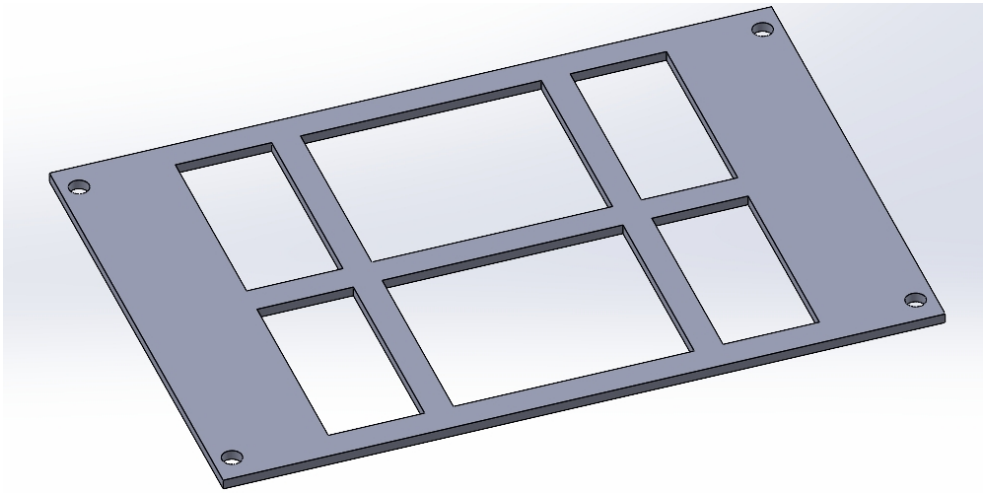

Figure A.16: PET heater frame for PDMS coverslip chips.

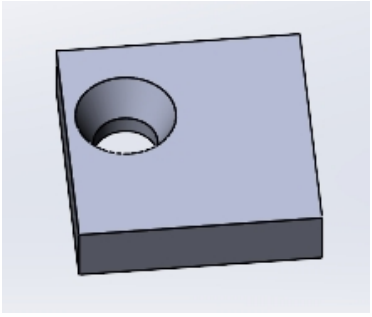

Figure A.17: Square which presses the PET film and wires to the frame

A.2.3. New platform parts CAD drawings

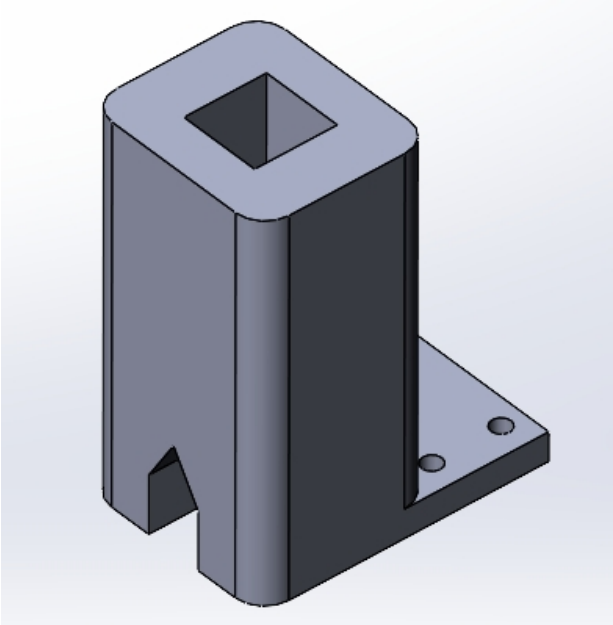

Figure A.18: A sturdier version of a pressure gauge holder.

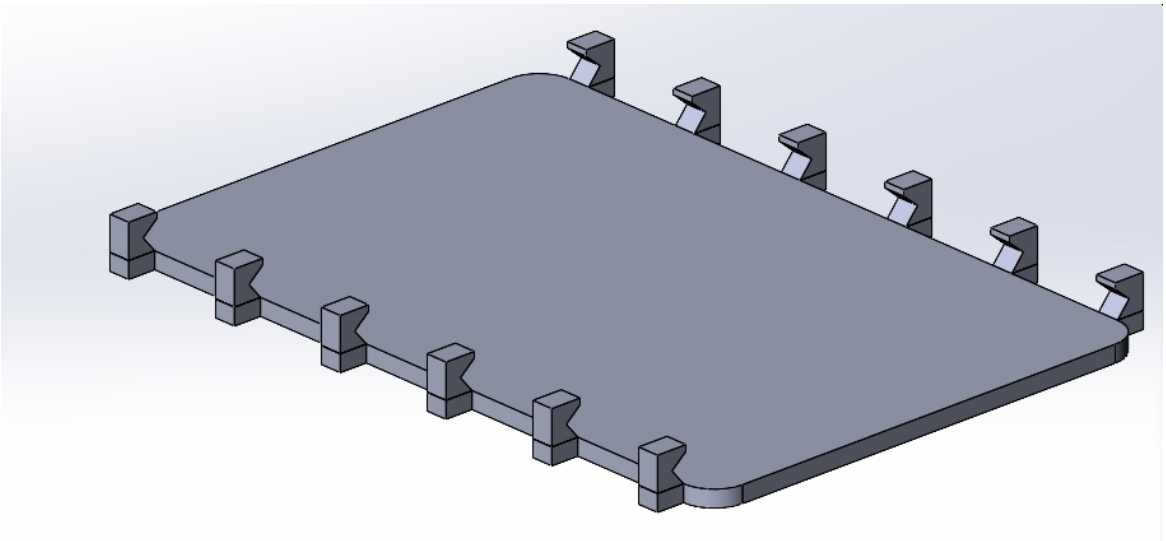

Figure A.19: A holder which allows to slide in the stage top heater.

A.2.4. Updated platform parts CAD drawings. Originals by Haoyu Zhu.

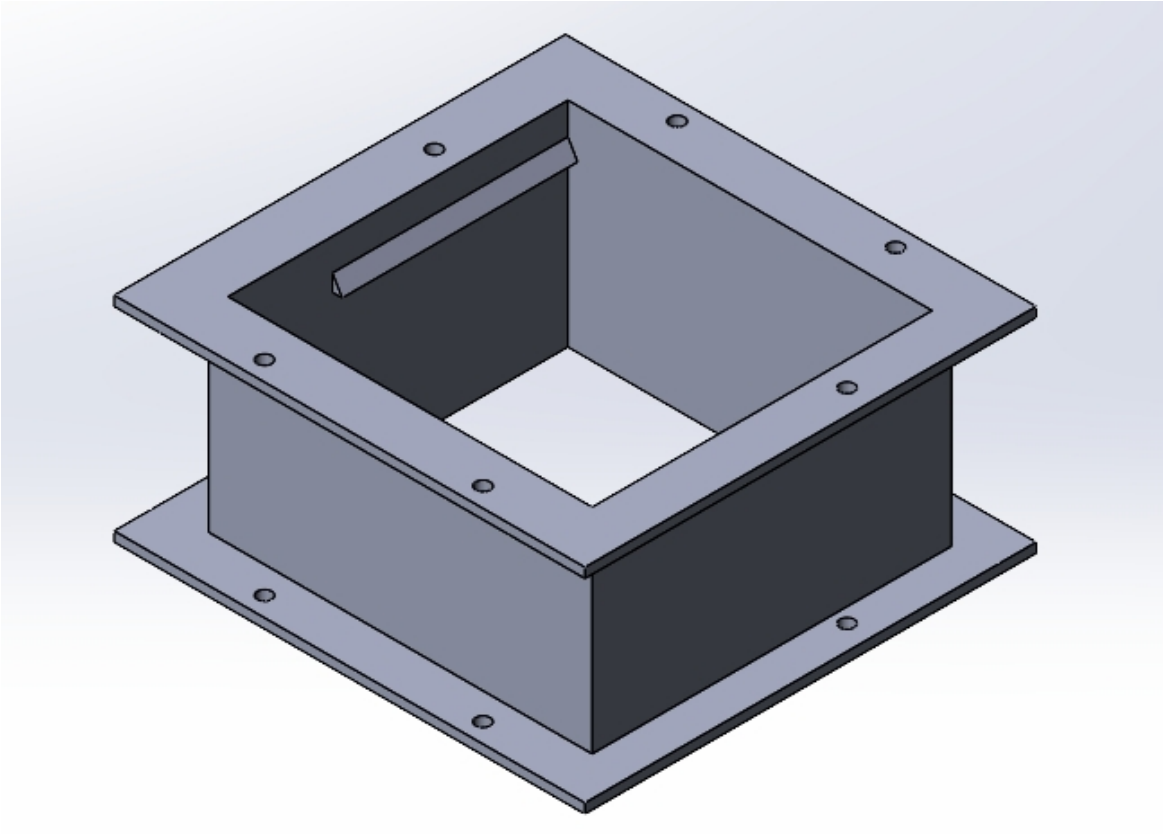

Figure A.20: Updated central square of the platform.

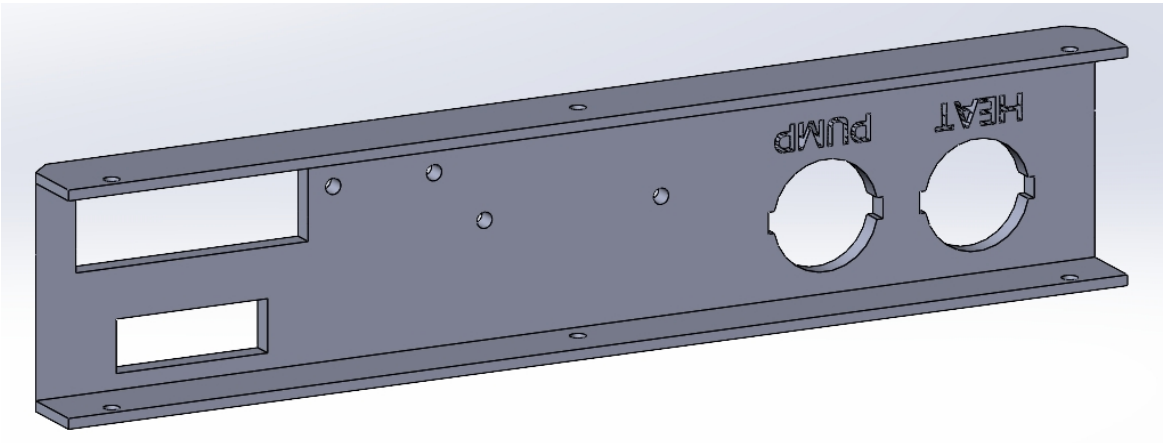

Figure A.21: Updated Arduino sidebar of the platform.

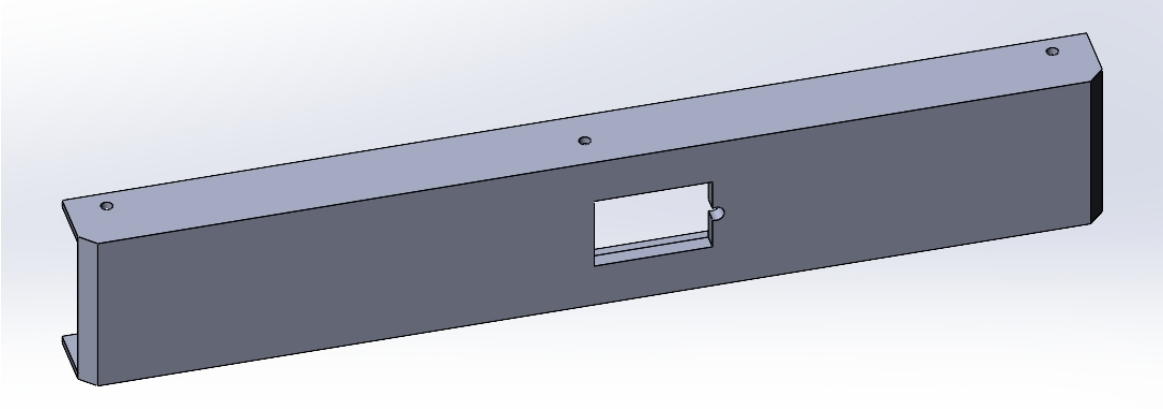

Figure A.22: Updated battery sidebar of the platform.

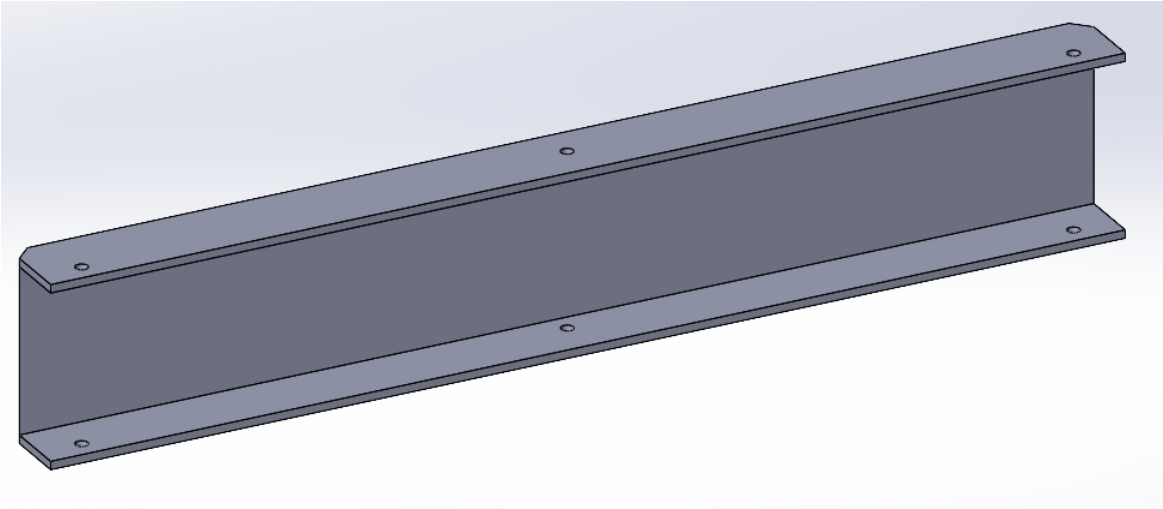

Figure A.23: Updated display sidebar of the platform.

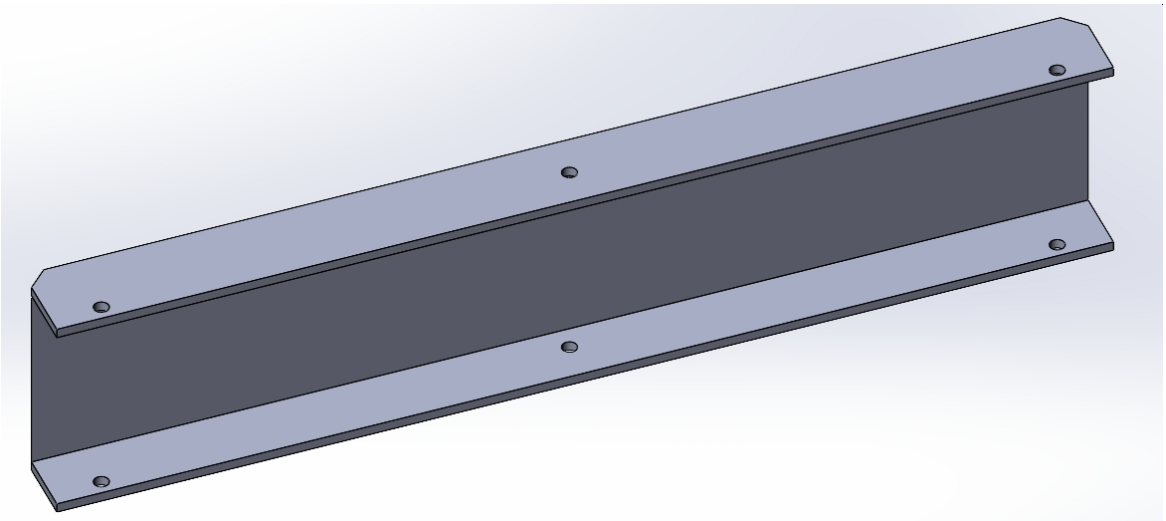

Figure A.24: Updated flow controllers' sidebar of the platform.

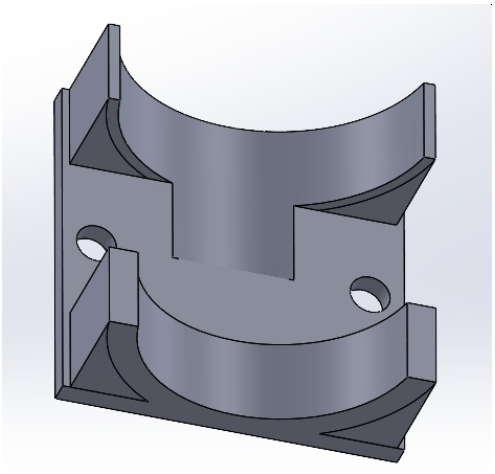

Figure A.25: A sturdier version of the pump holder.

B

Additional experimental results, videos and images

B.1. Temperature control

Imaging ITO PET heaters with a thermal camera showed a relatively even (12 °C gradient) and symmetrical heat distribution. The maximum temperature reached was well above 60 °C which allows heating the chips to the physiological range of temperatures (up to 40 °C). Further trials with the thermal camera were not conducted as it was deemed too inaccurate (after imaging an ice bath).

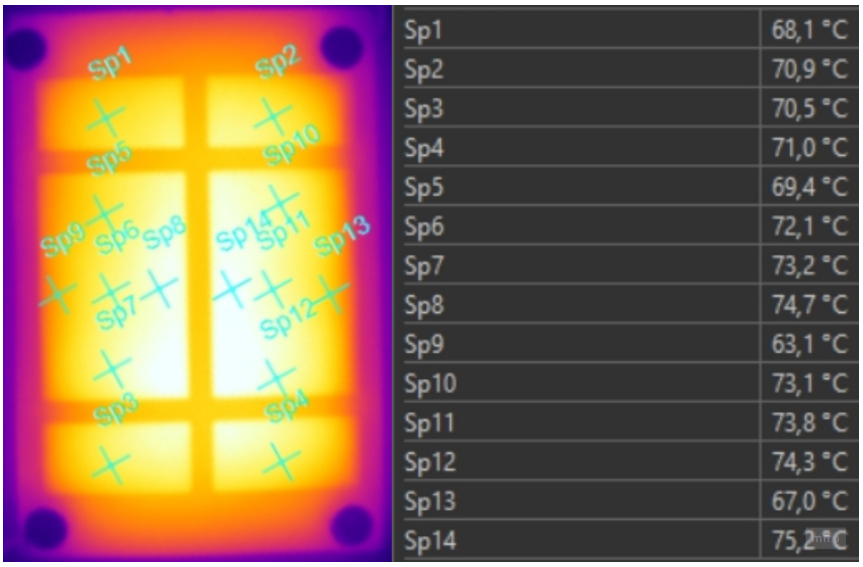

Figure B.1: ITO PET heater thermal camera image

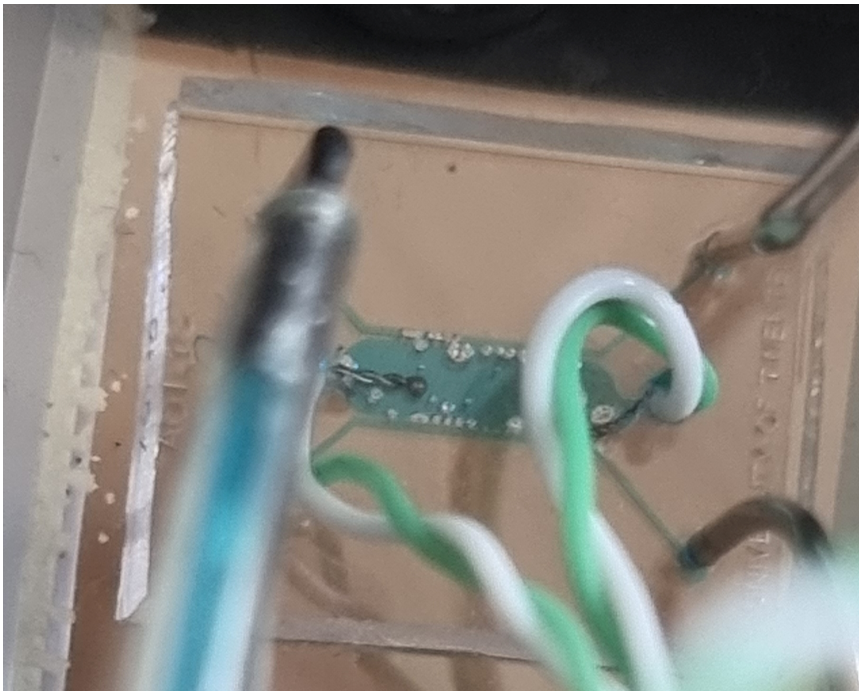

Figure B.2: Image depicting how the thermocouple was inserted in the central chamber of the PDMS chip. Bubble formation can be observed.

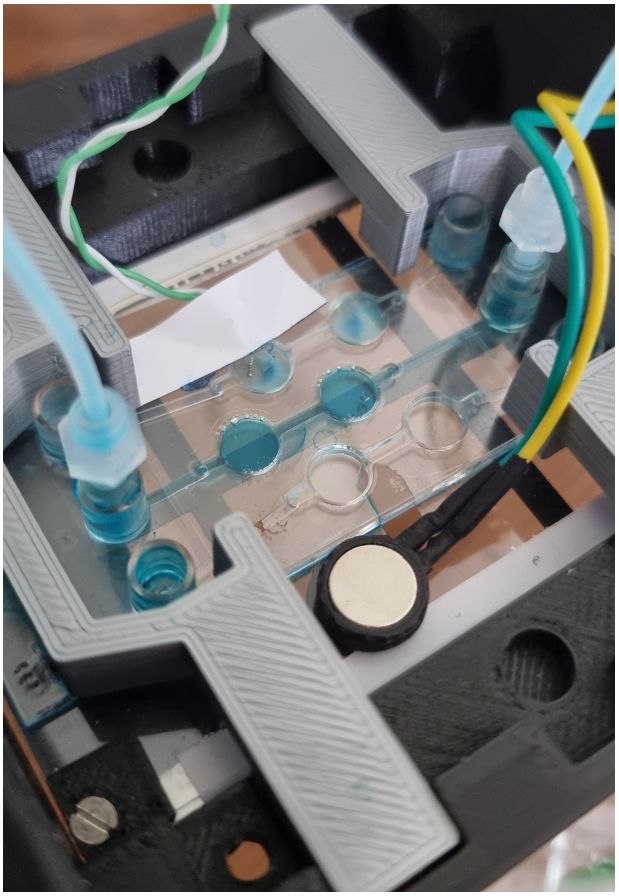

Figure B.3: Insertion into the polymer chip was more invasive. Some bubble formation in the central wells can be observed (due to heating).

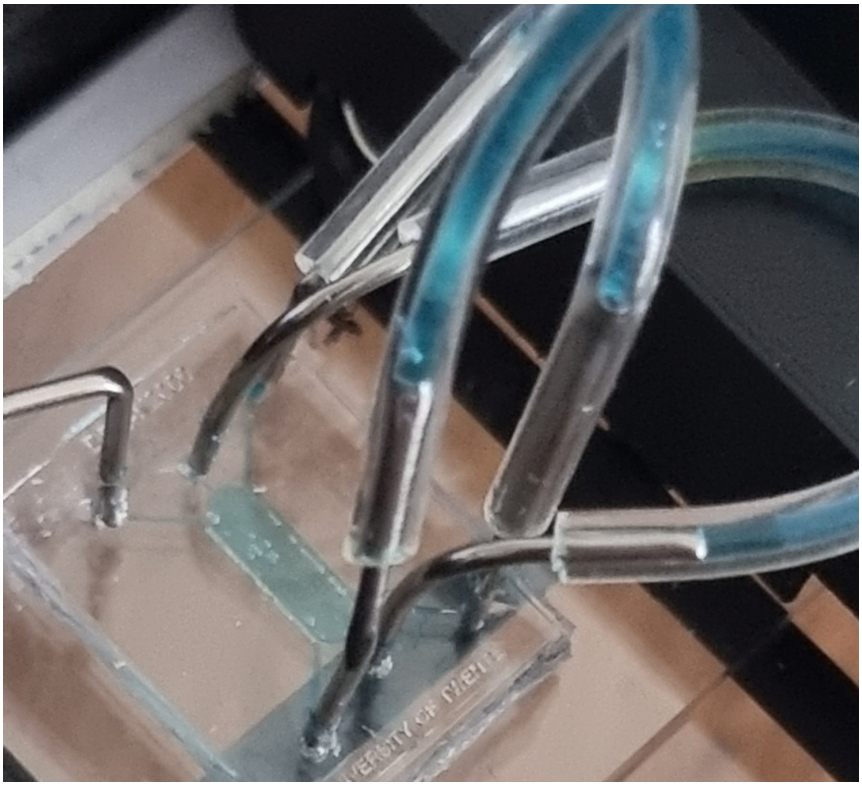

Figure B.4: Bubble formation in the PDMS chip central chamber under heating and perfusion

Figure B.5: Temperature control trial results for 3 runs for Ibidi Polymer chip. Top: thermocouple. Bottom: Pt100 sensor.

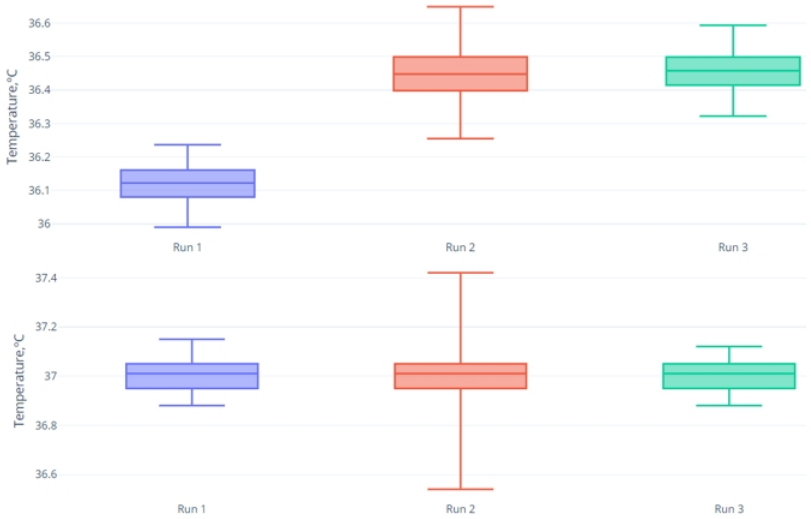

Difference within a run up to 0.4 ºC
Average 36.34 ± 0.17 ºC

One run showed abnormal 0.9 ºC min-max difference due to a single spike.
Average 37 ± 0.06 ºC

Figure B.6: Temperature control trial results for 3 runs for PDMS on a slide chip. Top: thermocouple. Bottom: Pt100 sensor.

Difference within a run up to 0.8ºC
Average 35.68 ± 0.29 ºC

Difference within a run up to 0.2ºC
Average 38.49 ± 0.03 ºC

Figure B.7: Temperature control trial results for 3 runs for PDMS on a coverslip chip. Top: thermocouple. Bottom: Pt100 sensor.

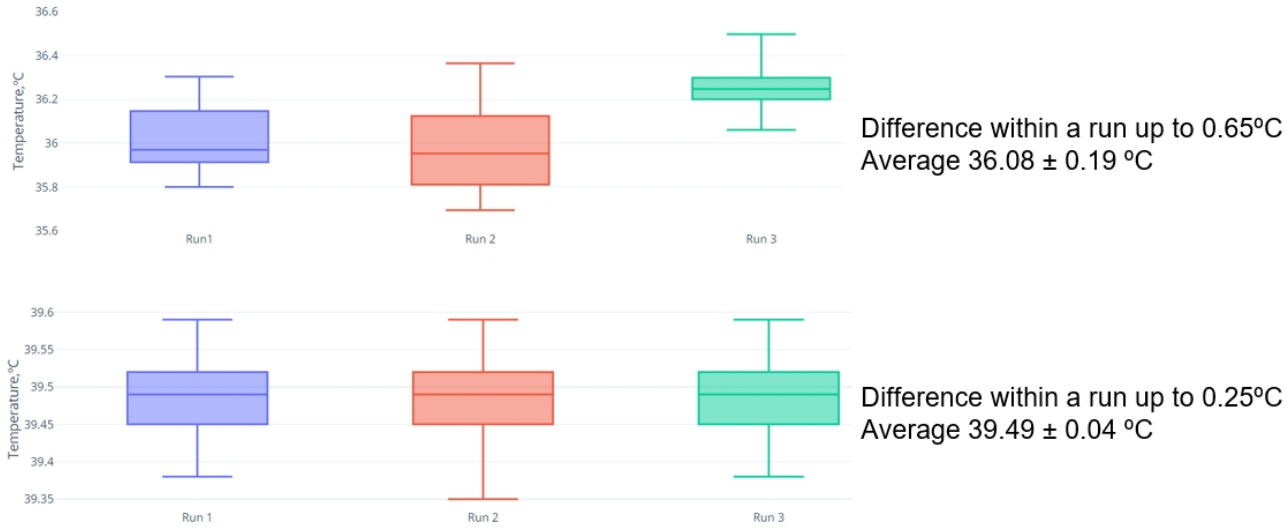

Figure B.8: Temperature control trial results for 3 runs for PDMS on a coverslip chip. Window heater. Top: thermocouple. Bottom: Pt100 sensor.

B.2. Battery performance and portability

Figure B.9: Performance of flow controllers set to constant flow and heating on battery. Reliable performance (no spikes) lasts for an hour, followed by a period with spikes (till 2:20 hours), followed by complete instability of flow.

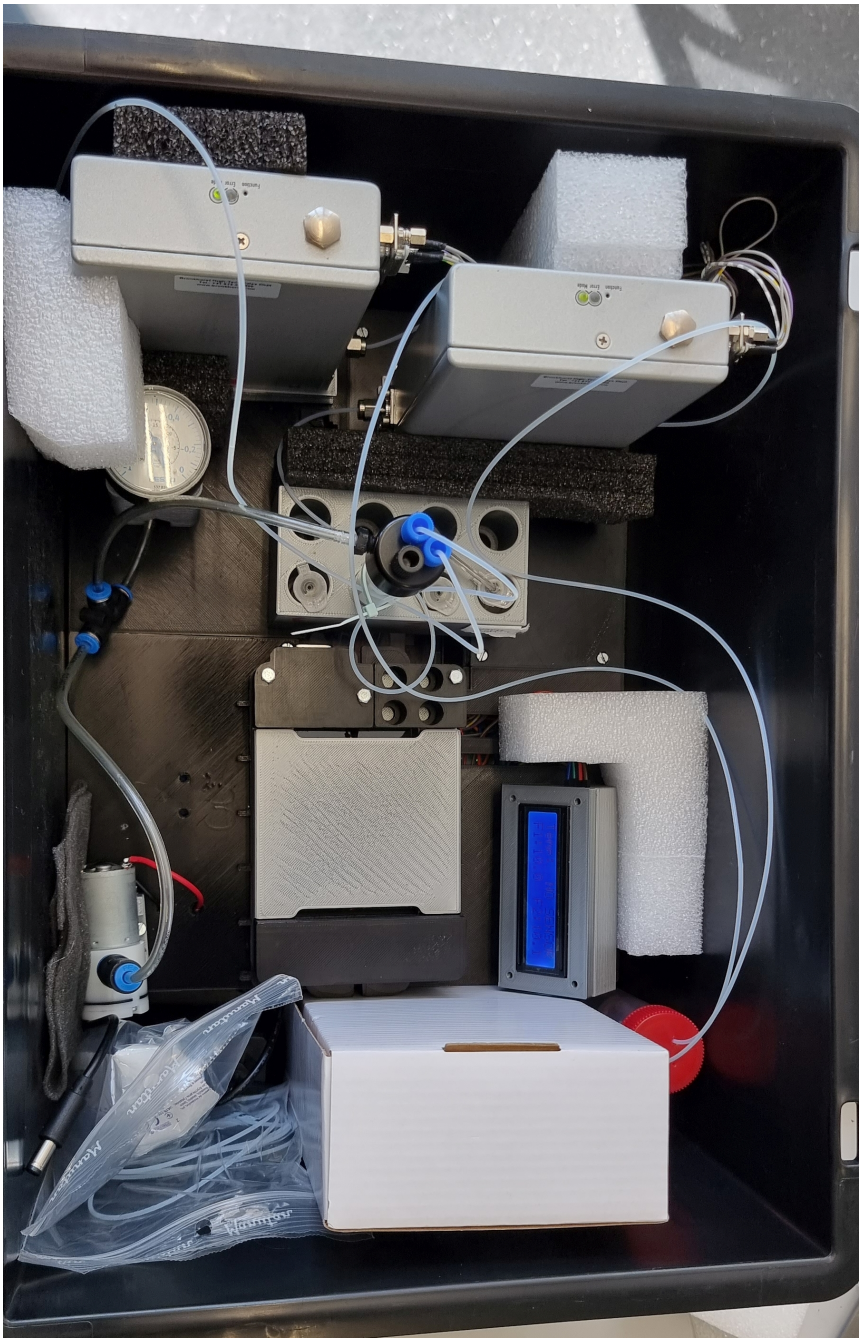

Figure B.10: The exact way how the platform was packed in the box for transportation.

Figure B.11: Platform when transported by bicycle

B.3. Microscopy photos and videos

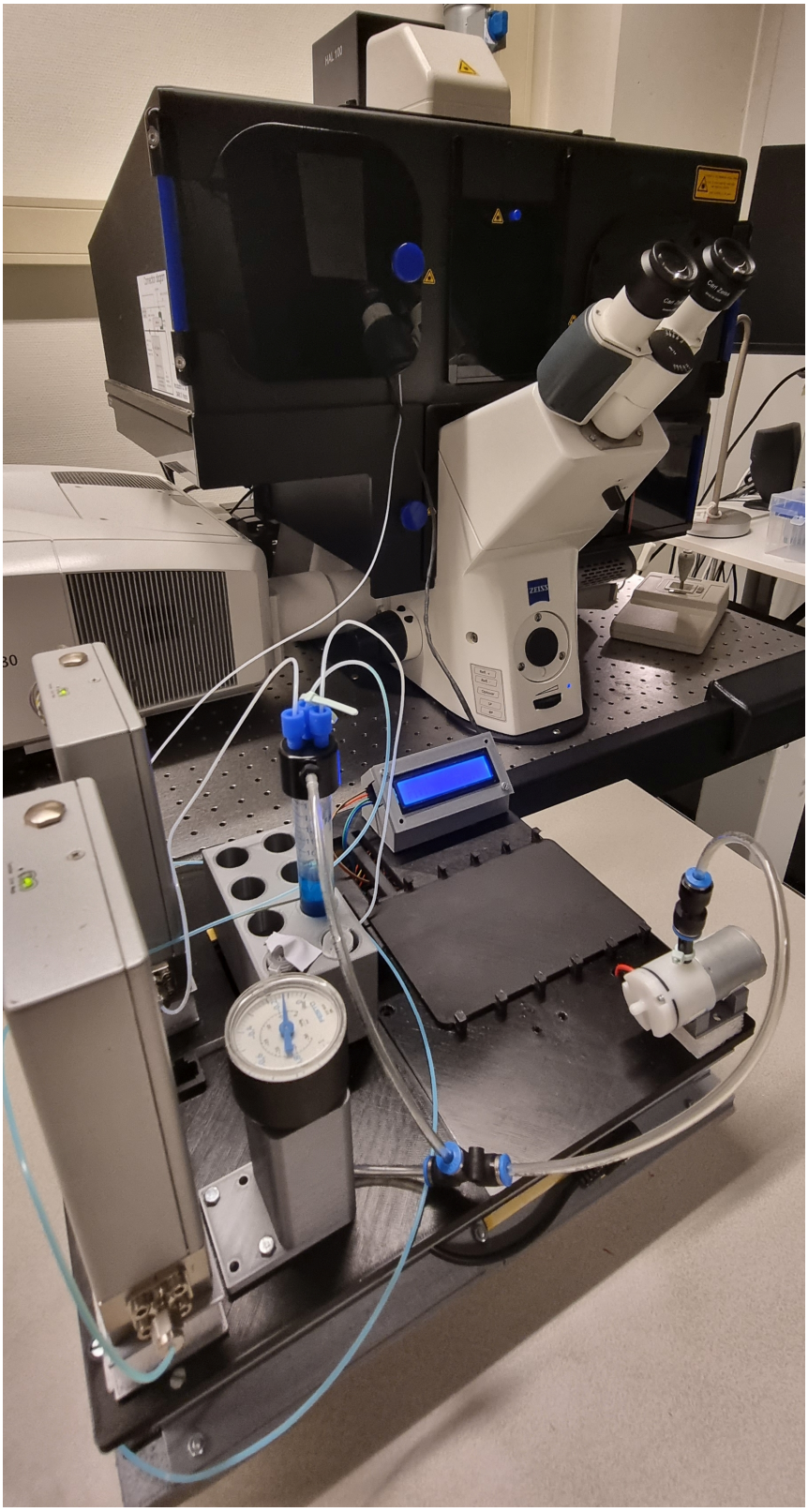

Figure B.12: Platform in operation

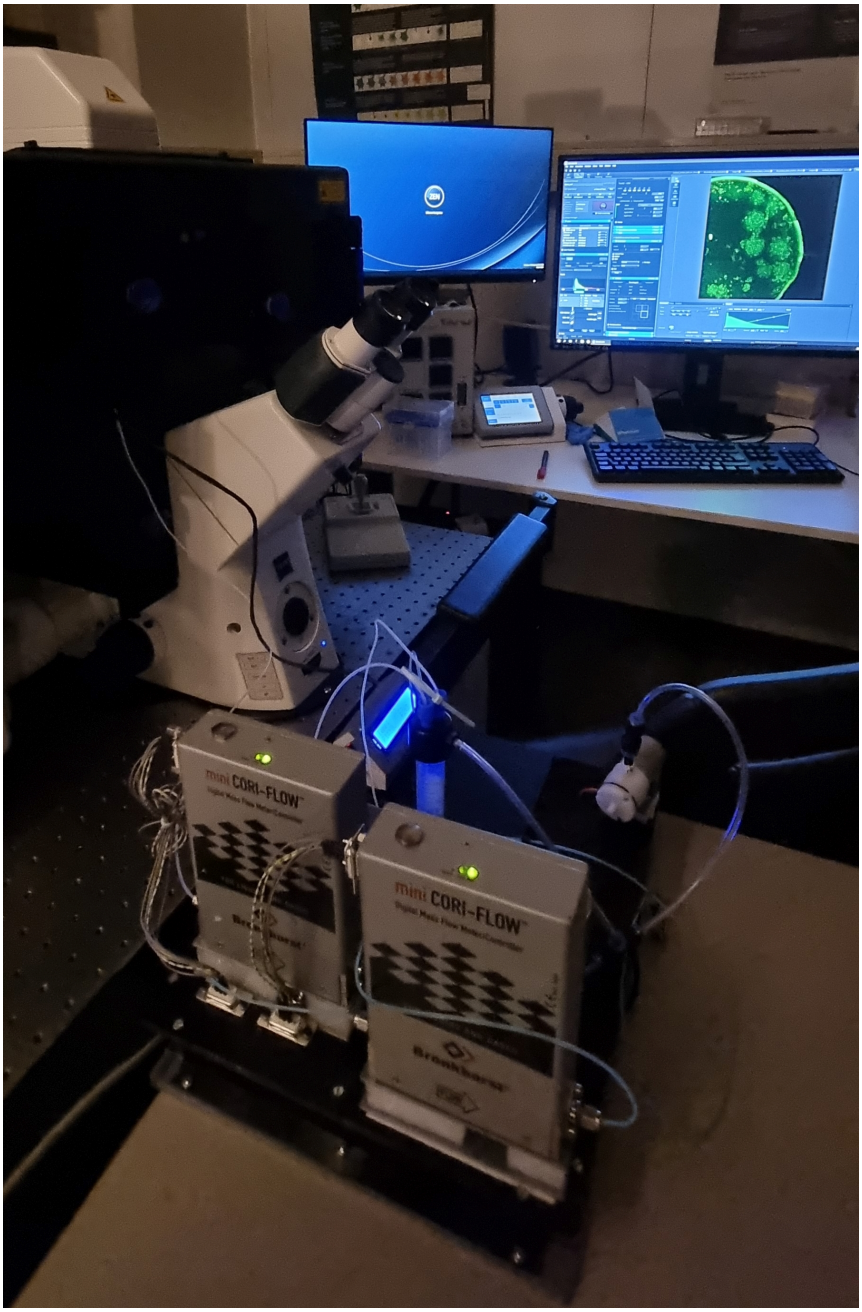

Figure B.13: Platform while doing a time series image under flow and heating

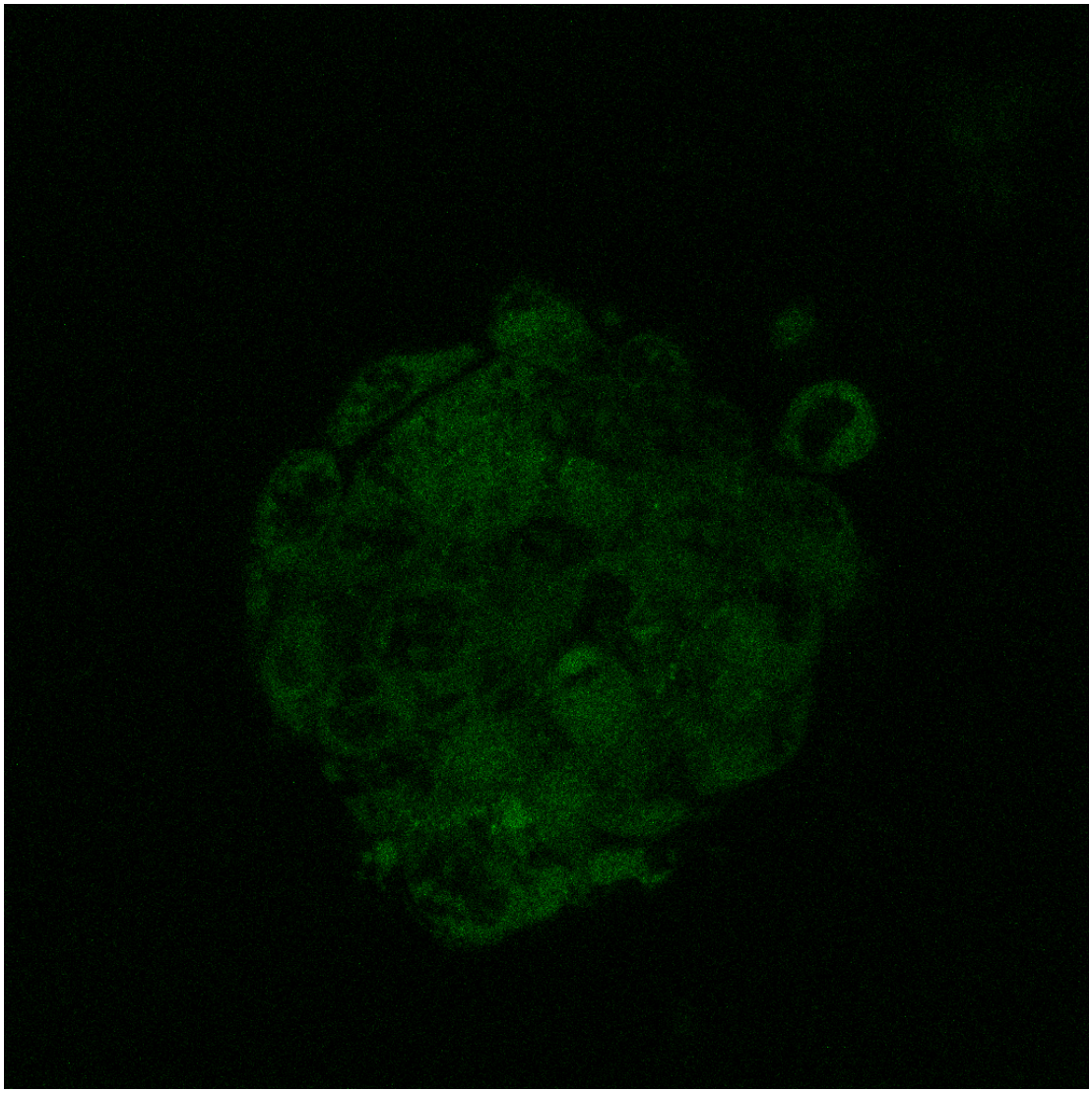

Figure B.14: A spheroid image was obtained with 63x oil objective but the heater had to be removed as the frame was in the way. Single cells and nuclei can be clearly seen.

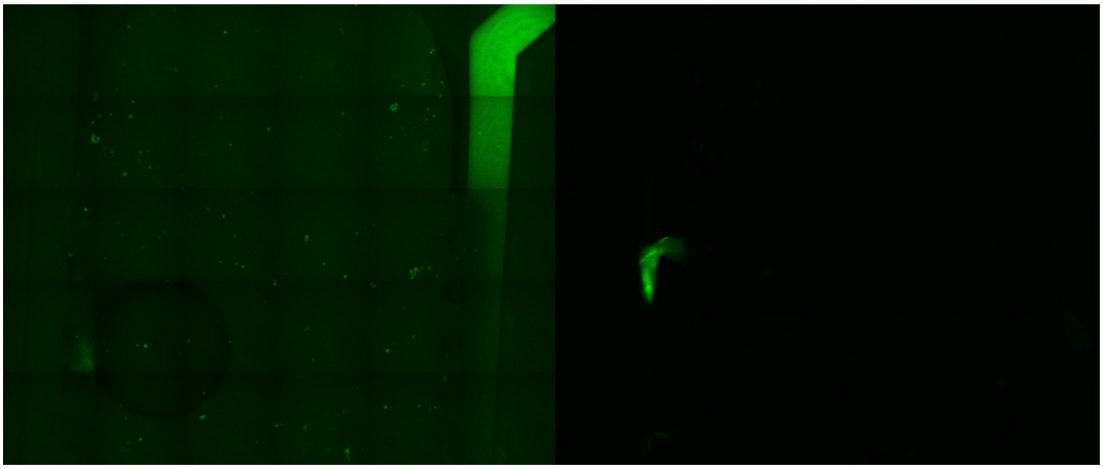

Figure B.15: The effect of ITO glass (with thick ITO layer) on blockage of the green light

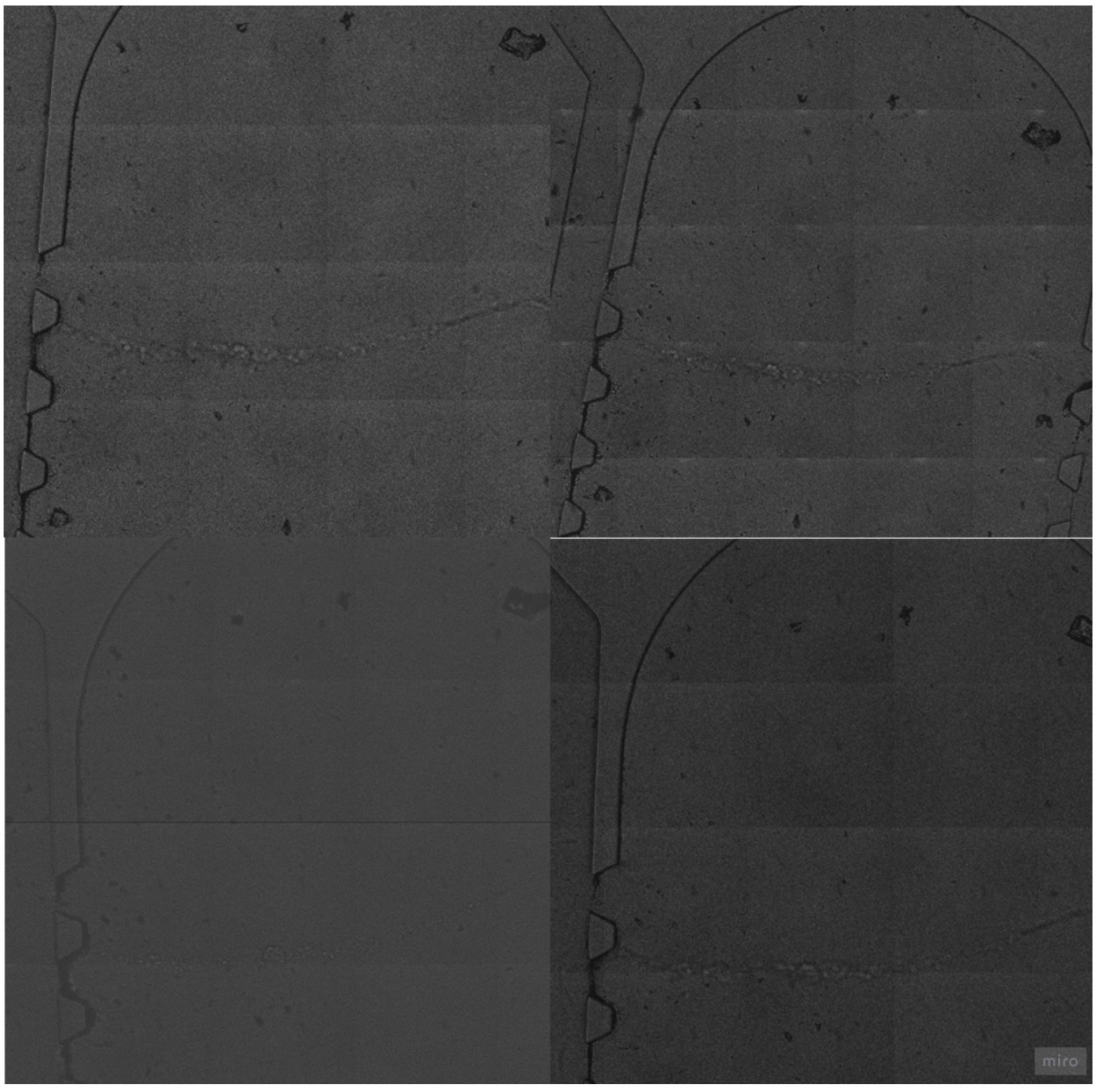

Figure B.16: The deterioration of imaging quality through several layers. All images are on the microscope module with various additional layers mimicking heaters. All images were done with flow. Top Left: Chip on a coverslip. Top Right: Chip on a coverslip + additional coverslip. Bottom Left: Chip on a coverslip + ITO glass (0.7mm thick). Bottom Right: Chip on a coverslip + uncoated slide (1mm thick). It's clear that the ITO glass has the worst effect although it's not the thickest.

B.3.1. Videos

20-minute Confocal tile scan time series with flow and heating enabled: 20 shots with 1-minute intervals, 4 frames per second.

Videos of the same area with heating off and on:

- 20-minute Confocal time series of PDMS chip on a slide with heating disabled: 40 shots with 30-second intervals, 8 frames per second.
- 20-minute Confocal time series of PDMS chip on a slide with heating enabled: 20 shots with 30-second intervals, 8 frames per second.

20-minute Confocal time series of Polymer Ibidi chip with 4.5 μl wells with heating enabled: T-cell invades a spheroid.

Video of Polymer Ibidi chip with 4.5 μl wells installed on the microscope stage: Stage heater with a chip installed on Zeiss Elyra PS1.

C

Arduino code

Some parts of the original platform code were modified or removed. If the components like pressure controller and valves are to be used, please insert the corresponding parts (tasks) from the original code.

```
1    #include <Adafruit_MAX31865.h> //MAX31865 library
2 #define RREF      430.0 // The value of the Rref resistor. Use
     430.0 for PT100 and 4300.0 for PT1000
3 #define RNOMINAL  100.3 // 100.0 for PT100, 1000.0 for PT1000.
     Should be calibrated with icebath! (Vlad) 0.3 for yellow-
     green, 0.31 for purple-blown
4 #define VCC2 36 // Pin 36 as additional 5V
5 #define GND2 38 // Pin 38 as additional GND
6 #define HeatControl 40
7 #include <LiquidCrystal_I2C.h> //LCD library
8 #include <SCoop.h> //Multitask function is used in this program
     , so the library is necessary.
9 //The default settings of the program, including setting up 6
     tasks, the pin code
10 //of switch valves and Arduino ports for transistor switches
     and controllers. It is
11 //not supposed to change the pin codes in this part.//
12 //Multi-task setting
13 defineTask(TaskTest2);
14 defineTask(TaskTest3);
15 defineTask(TaskTest4);
16 defineTask(TaskTest6);
17 defineTask(TaskTest7);
18 defineTask(TaskTest8);
19 //Set pin code of switch valve BCD control, The location of the
      pins can be found by a triangle note on interface.//
20 int Pin1 = 51;
21 int Pin2 = 47;
22 int Pin3 = 45;
23 int Pin4 = 41;
24 int Pin5 = 39;
```

```
25 int Pin7 = 33;
26 int Pin8 = 31;
27 int Pin10 = 27;
28 int Pin11 = 25;
29 int Pin12 = 23;
30 //Default feedback pins of switch valve BCD control. The first
     four pins reflects
31 //the position of motor. Error and Done pins shows use 0/1 to
     show if the motion is
32 //finished successfully. If it has rotated successfully, 1 will
     be shown on serial
33 //chart of Arduino (The last number of 6 numbers in series).//
34 int FB_0;
35 int FB_1;
36 int FB_2;
37 int FB_3;
38 int Error;
39 int Done;
40 //Set pin code of transistor switch. The numbers are the same
     number of Arduino
41 //IO. All are digital IO thus can only output 0/5V to turn off/
     on the transistors.//
42 int AV = 32; //shut-off valve
43 int VP = 30; //vacuum pump
44 int Relay = 24; //relay of vacuum pump
45 int Fan = 53; //Fan control
46 //Pin code of setpoint and readout of controllers. The numbers
     are the same number
47 //of Arduino IO. 'A' means the IO is analog input which can
     readout the analog
48 //signal from controller outputs. Digital IO are used as analog
     output here.
49 //However, the analog output signals are in PWM form thus need
     to be filtered to
50 //pure analog signal.//
51 int cori1in = 5; //setpoint of flow controller 1
52 int cori1out = A1; //readout of flow controller 1
53 int cori2in = 3; //setpoint of flow controller 2
54 int cori2out = A4; //readout of flow controller 2
55 //Analogwrite setting. They are used as intermediate variable
     to show the real
56 //value from controllers.//
57 float val1;
58 float val2;
59 float Val1flow;
60 float Val2flow;
```

```
61 //Three transistor switches and one relay is controlled in this
       section. The
62 //transistor can be triggered by digital signals from Arduino,
     each of them control
63 //vacuum pump(VP), Shut-off valve (AV) and 3-way valve (
     Threeway) respectively. In
64 //the loop part, HIGH means a 5V signal is sent to the
     transistor thus the component
65 //is powered by the outside battery. Otherwise it is turned off
     . The process starts
66 //from up to down in loop part, in each step, a 'sleep' command
       is used to make a
67 //interval between each action. The value behind 'sleep' is in
     unit of miliseconds
68 //thus 'sleep(2000)' means the second action after sleep will
     be 2 seconds after the
69 //previous action.//
70
71 //Code to simplify desired flow rate input
72 float Flowrate1 = 8; //Desired volumetric flow rate for FC1 in
     ul/min
73 float Flowrate2 = 0;//Desired volumetric flow rate for FC2 in
     ul/min
74 float timeflow = 120000; //Time in ms for flow phase of
     intermittent flow (default - 1 minute = 60000 ms)
75 float timepause = 600000; //Duration of pause for intermittent
     flow (default - 10 minutes = 600000 ms)
76 int MaxFlow = 100;
77 float settemp1 = 36.8; //First setting of temperature control
78 float timetemp1 = 50000; //Delay between the start of the
     program and start of the second temperature setting
79 float settemp2 = 37.2; //Second setting of temperature control
80 float timetemp2 = 75000; //Delay between second and third
     setting
81 float settemp3 = 37.2; //Third setting of temperature control
82 float FC1inputfloat = (Flowrate1 + 3.259)/0.2788; // FC1 input
     value (calculation according to the linear approximation from
       the file setpoint_flow_rate_liquid.xlsx)
83 float FC2inputfloat = (Flowrate2 + 3.259)/0.2788; // FC2 input
     value
84 int FC1input = ((int)FC1inputfloat); //Conversion to integer
85 int FC2input = ((int)FC2inputfloat);
86 int FC1inputlow = FC1input; //For constant flow set to equal to
     FC1input, for intermittent set equal to zero
87 int FC2inputlow = FC2input; //For constant flow set to equal to
     FC2input
```

```
88 //Code for I2C 16x2 display an d MAX31865 temperature sensor amplifie
89 LiquidCrystal_I2C lcd(0x27,16,2); //define LCD type
90 Adafruit_MAX31865 thermo = Adafruit_MAX31865(10, 11, 12, 13); //define MAX31865 pins
91
92 void TaskTest2::setup() //Default setting of Components control
93 {
94  pinMode(VP,OUTPUT);
95  pinMode(AV,OUTPUT);
96  pinMode(Relay,OUTPUT);
97 }
98
99 void TaskTest2::loop() //Control of the pumping and valve system
100 {
101 delay(3900); //VP turns on one second before FCs turn on
102  digitalWrite(Relay,LOW); //Connect pump to 5V power
103  delay(100);
104  digitalWrite(VP,HIGH); //Turn on vacuum pump
105  delay(timeflow+3000);
106  if (FC1inputlow == 0 && FC2inputlow == 0) { //Pump will turn off if intermittent flow is enabled (both of FCinputlow equals zero)
107  digitalWrite(VP,LOW);
108  }
109  delay(timepause-2000); //2000ms - difference between delays for VP and FCs, it's substraced from pause time to synchronise delays
110 digitalWrite(VP,HIGH);
111 }
112 //Flow controller of flow path 1 is controlled in this section. Fan is also
113 //controlled here by digital IO of Arduino. The settings of IO1,4,6,7,8,9,10,11,12
114 //are default settings and should not be modified The clock of Arduino is modified
115 //to form a high-frequency PWM. The setpoint from Cori1in pin ranges from 17 to 255.
116 //55 means the desired flow rate in flow path 1 should be the maximum rate while 17
117 //represents the minimum rate in path 1. Please refer to the paper (Section 3.1.1)
118 //and relation diagram for exact value of different fluids. The way to convert the
```

```
119 //relation of DI water to other fluids is: (1)Put desired
      volumetric flow rate and
120 //density of fluid into equation(3) and get desired mass flow
      rate (2)Put the mass
121 //flow rate and density of DI water into equation(3) and get
      equivalent volumetric
122 //flow rate of DI water. (3)Use the relation diagram (liquid OR
       gas) to find the
123 //matched applied voltage. (4)Use equation(4) to get the
      setpoint that needs to be
124 //input into Arduino program, so that a desired volumetric flow
       rate of typical
125 //fluids can be reached.//
126 void TaskTest3::setup() // Default settings of controller 1
      setpoints
127 {
128  TCCR3B = TCCR3B & 0b11111000 | 0x01; //Clock setting of
       Arduino, Increase the frequency of PWM output
129  TCCR2B = TCCR3B & 0b11111000 | 0x01;
130  TCCR4B = TCCR3B & 0b11111000 | 0x01;
131  pinMode(cori1in, OUTPUT);
132  pinMode(Fan, OUTPUT);
133 }
134
135 void TaskTest3::loop() // Setpoint input
136 {
137  analogWrite(1,100);
138 delay(5000);
139  analogWrite(cori1in,FC1input);
140  //digitalWrite(Fan,HIGH); //turn on and turn off the cooling
       fan. Disabled since fan is always on. (Vlad)
141  delay(timeflow);
142  analogWrite(cori1in,FC1inputlow);
143  delay(timepause);
144  analogWrite(4,100);
145
146  analogWrite(6,100);
147
148  analogWrite(7,100);
149
150  analogWrite(8,100);
151
152  analogWrite(9,100);
153
154  analogWrite(10,100);
155
```

```
156  //analogWrite(11,200); No idea why this is needed but when it's on MAX31865 looses the sensor signal (Vlad)
157  //analogWrite(12,100);
158 }
159 //This section controls flow controller of flow path 2. The way to decide the setpoint and program are the same as task3.//
160 void TaskTest4::setup() // Default settings of controller 2 setpoints
161 {
162  TCCR3B = TCCR3B & 0b11111000 | 0x01; //Clock setting of Arduino, Increase the frequency of PWM output
163  TCCR2B = TCCR3B & 0b11111000 | 0x01;
164  TCCR4B = TCCR3B & 0b11111000 | 0x01;
165  pinMode(cori2in, OUTPUT);
166 }
167 void TaskTest4::loop() // Setpoint input
168 {
169  analogWrite(1,100);
170  delay(5000);
171  analogWrite(cori2in,FC2input);
172   delay(timeflow);
173  analogWrite(cori2in,FC2inputlow);
174  delay(timepause);
175  analogWrite(4,100);
176
177  analogWrite(6,100);
178
179  analogWrite(7,100);
180
181  analogWrite(8,100);
182
183  analogWrite(9,100);
184
185  analogWrite(10,100);
186
187  //analogWrite(11,100);
188  //analogWrite(12,100);
189 }
190
191 //The sensed flow rates and pressure level will be displayed by this section. The
192 //graphs can be shown by clicking 'tools' - 'serial plot' so that the graphs of all
193 //values can be shown in a same window. According to applications, several plots can
194 //be deleted by changing them into comments.//
```

```
195 void TaskTest6::setup() //Default settings controller readout
196 {
197  Serial.begin(9600); //Baud rate. Do not change it only if
       necessary.
198  }
199 void TaskTest6::loop() //Readout and print of sensed value
200 {
201  val1 = analogRead(cori1out); //Readout the values from
       controllers
202  val2 = analogRead(cori2out);
203  Val1flow = val1*0.0809+0.0359; //Conversion to volumetric flow
        rate (calculation according to the linear approximation
       from the file setpoint_flow_rate_liquid.xlsx)
204  Val2flow = val2*0.0809+0.0359;
205  Serial.print("X:");
206  Serial.print(Val1flow);
207  Serial.print(",") ;//Plot the value of
208 //flow controller 1
209 //Serial.print("Xset:");
210 //Serial.print(Flowrate1);
211 //Serial.println(",") ;//Plot the set value of
212 //flow controller 1
213  Serial.print("Y:");
214  Serial.print(Val2flow);
215  Serial.print(",");//Plot the value of
216 //flow controller 2
217 //Serial.print("Yset:");
218 //Serial.print(Flowrate2);
219 //Serial.println(",") ;//Plot the set value of
220 //flow controller 2
221 //Serial.println(MaxFlow);
222  delay(400); //Sampling interval. This can be changed according
        to requirements
223 }
224 void TaskTest7::setup() //Settings for MAX31865 and LCD display
225 { Serial.begin(9600);
226   thermo.begin(MAX31865_2WIRE);  // set to 2WIRE or 3 or 4WIRE
       as necessary
227 lcd.init();
228   lcd.backlight();
229   lcd.setCursor(0,0); //First digit stands for colomn (0-15),
       second for row (0-1)
230   lcd.print("Temp: ");
231   lcd.setCursor(0,1);
232   lcd.print("F1:" );
233   lcd.setCursor(9,1);
```

```
234   lcd.print("F2:");
235 }
236 //Calculation of temperature from the resistance. More info can
      be found by googling MAX31865 library.
237 // To find display library info google I2C LCD display
238 void TaskTest7::loop() {
239   uint16_t rtd = thermo.readRTD();
240   //Serial.print("RTDvalue:"); Serial.println(rtd);
241   float ratio = rtd;
242   float temp = thermo.temperature(RNOMINAL, RREF);
243   ratio /= 32768;
244   //Serial.print("Ratio = "); Serial.println(ratio,8);
245   //Serial.print("Resistance = "); Serial.println(RREF*ratio,8)
        ;
246   Serial.print("Temperature:");
247   Serial.print(temp);
248   Serial.println(",");
249 //Serial.print("SetTemp:");
250   //Serial.print(settemp);
251   //Serial.println(",");
252   lcd.setCursor(7,0);
253   if (temp>200 || temp<-50){
254   lcd.print("NO SENSOR");}
255   else
256 {
257   lcd.setCursor(7,0);
258   lcd.print(temp, 1);
259   delay(100);
260 lcd.setCursor(11,0);
261  lcd.print("      ");
262  }
263  lcd.setCursor(3,1);
264  lcd.print(Val1flow, 1); //"1" defines the number of decimals
       for float number
265   lcd.setCursor(12,1);
266  lcd.print(Val2flow, 1);
267   delay(100);
268   lcd.setCursor(6,1);
269   lcd.print("  ");
270   lcd.setCursor(15,1);
271 lcd.print("  ");
272 }
273
274 void TaskTest8::setup() //Settings for MOSFET HEat controller
275 { pinMode(HeatControl,OUTPUT);
276 pinMode(VCC2, OUTPUT);
```

```
277 pinMode(GND2, OUTPUT);
278 }
279
280 float timepassed = 0;
281 float control_interval = 10;
282 //Temperature control code below
283 void TaskTest8::loop(){
284   float temp1 = thermo.temperature(RNOMINAL, RREF);
285  digitalWrite(VCC2, HIGH);
286  digitalWrite(GND2, LOW);
287  digitalWrite(HeatControl,HIGH);
288  if (temp1 <= settemp1 && timepassed<timetemp1){
289   digitalWrite(HeatControl,HIGH);
290  }
291  if (temp1 > settemp1 && timepassed<timetemp1){
292   digitalWrite(HeatControl,LOW);
293   }
294   if (temp1 <= settemp2 && timepassed>=timetemp1 && timepassed<
       timetemp2){
295   digitalWrite(HeatControl,HIGH);
296  }
297  if (temp1 > settemp2 && timepassed>=timetemp1 && timepassed<
      timetemp2){
298   digitalWrite(HeatControl,LOW);
299   }
300   if (temp1 <= settemp3 && timepassed>=timetemp2){
301   digitalWrite(HeatControl,HIGH);
302  }
303  if (temp1 > settemp3 && timepassed>=timetemp2){
304   digitalWrite(HeatControl,LOW);
305   }
306  delay(control_interval);
307  timepassed = timepassed + control_interval;
308 }
309
310 //Necessary code to implement 'multitask' function. Never
      change or delete it.//
311 void setup() {
312  mySCoop.start();
313 }
314 void loop()
315 {
316  yield();
317 }
```